NUMERICAL SIMULATION OF DISPERSION IN GROUNDWATER AQUIFERS

by

Donald Lee Reddell and Daniel K. Sunada

June 1970

HYDROLOGY PAPERS
COLORADO STATE UNIVERSITY
Fort Collins, Colorado

41

NUMERICAL SIMULATION OF DISPERSION IN GROUNDWATER AQUIFERS

by

Donald Lee Reddell

and

Daniel K. Sunada

HYDROLOGY PAPERS

COLORADO STATE UNIVERSITY

FORT COLLINS, COLORADO 80521

June 1970 No. 41

ACKNOWLEDGMENTS

This paper is based primarily on Dr. D. L. Reddell's Ph.D. dissertation entitled, "Dispersion in Ground Water Flow Systems." The work was supported by Colorado Experiment Station Project No. 110, Office of Water Resources Research through the W.R.R. Act of 1964, PL 88-379 and National Science Graduate Traineeship.

TABLE OF CONTENTS

Chapter		Page
Abstract		
I	Introduction	1
	1.1 Description of Problem	1
	1.2 Purposes and Objectives	1
	1.3 Methods of Investigation	2
II	Previous Work Related to This Research	3
	2.1 Theoretical Investigations	3
	2.2 Analytical Solutions	4
	Longitudinal Dispersion	4
	Longitudinal and Lateral Dispersion	5
	2.3 Experimental Results	6
	2.4 Numerical Solutions	7
	Summary	8
III	Presentation of Mathematical Model For Dispersion in Groundwater Aquifers	9
	3.1 General Flow Equation	9
	3.2 Dispersion Equation	9
	3.3 Auxiliary Equations	10
	3.4 Dispersion Coefficients	10
IV	Development of Numerical Model for Dispersion	12
	4.1 Finite Difference Form of Two-Dimensional Flow Equation	12
	4.2 Finite Difference Form of Two-Dimensional Dispersion Equation	12
	4.3 Finite Difference Form of Velocity Equation	14
	4.4 Boundary Conditions	15
	4.5 Description of the Computer Program	15
	4.6 Validity of Computer Simulator	16
V	Results and Interpretations	18
	5.1 Longitudinal Dispersion in Steady, Uniform, One-Dimensional Flow	18
	5.2 Longitudinal and Lateral Dispersion in Steady, Uniform, One-Dimensional Flow	19
	5.3 Numerical Solutions Using the Tensor Concept of Dispersion	21
	Longitudinal Dispersion	21
	Longitudinal and Lateral Dispersion	23
	5.4 Dispersion Along Equilibrium Salt-Water Wedge	27
VI	Summary and Conclusions	30
	6.1 Evaluation of Numerical Simulator	30
	6.2 Suggestions for Future Work	30
	6.3 Observations	31
References		32
Appendix A	Derivation of Fundamental Flow Equation	36
Appendix B	Derivation of Dispersion Equation	39
Appendix C	Development of Finite Difference Equation for the Flow Equation	45

TABLE OF CONTENTS - Continued

		Page
Appendix D	Development of Finite Difference Equation for the Dispersion Equation	48
Appendix E	Stability Analysis for Dispersion Equation.	53
Appendix F	Flow Chart of Program	63
Appendix G	Fortran IV Computer Program	68
Appendix H	List of Symbols Used in this Study.	87

LIST OF FIGURES AND TABLES

Figure		Page
2-1	Schematic column and typical concentration profiles for a slug injection. [After Hoopes and Harleman (1965)]	3
2-2	Schematic sketch of longitudinal dispersion column setup.	5
2-3	Schematic sketch of longitudinal and lateral dispersion column setup.	5
4-1	Grid system used to develop a finite difference equation for the seepage velocity.	14
4-2	Schematic sketch showing relation of seepage velocity at moving point to the seepage velocity calculated at the interface between grids	14
5-1	Comparison of analytical and numerical solution to the longitudinal dispersion problem used by Garder et al. (1964).	18
5-2	Effect of grid size on the error of solution by the method of characteristics.	18
5-3	Comparison of numerical and analytical solutions using different numbers of moving points per grid	19
5-4	Comparison of numerical and analytical solutions using only one moving point per grid.	19
5-5	Comparison of numerical, transient concentration distribution along $x_2=0$ for the two-dimensional dispersion problem with the analytical solution to the one-dimensional dispersion problem.	19
5-6	Comparison of numerical and approximate analytical solution for the one-dimensional flow, two-dimensional dispersion problem at steady state concentration.	20
5-7	Comparison of longitudinal concentration distribution at steady state as calculated numerically and by an approximate analytical solution for the one-dimensional flow, two-dimensional dispersion problem.	20
5-8	Schematic sketch of coordinate axes rotation used for comparing numerical tensor transformation with known analytical solutions.	21
5-9	Comparison of longitudinal concentration distribution calculated with and without tensor transformation for Runs T-1 and T-2.	22
5-10	Comparison of lateral concentration distribution calculated with and without tensor transformation for Runs T-1 and T-2 after 0.46 pore volumes have been injected	22
5-11	Comparison of lateral concentration distribution for Run T-3 after 0.46 pore volumes have been injected.	23
5-12	Comparison of lateral concentration distribution for Runs T-4 and T-5 at steady state.	23

Figure		Page
5-13	Comparison of longitudinal concentration distribution at steady state as calculated numerically using the proposed tensor transformation and by an approximate analytical solution	24
5-14	Comparison of longitudinal concentration distribution at steady state as calculated numerically using no tensor transformation and by an approximate analytical solution.	24
5-15	Comparison of numerical solutions with and without the tensor form of dispersion for steady state concentration at $x_3/\ell_3 = 0.3045$	24
5-16	Comparison of numerical solutions with and without the tensor form of dispersion for steady state concentration at $x_3/\ell_3 = 0.6090$.	24
5-17	Comparison of numerical solutions with and without the tensor form of dispersion for steady state concentration at $x_3/\ell_3 = 0.9570$.	25
5-18	Numerical results for Run T-6 at different time levels.	25
5-19	Numerical results for Run T-4 at different time levels.	25
5-20	Schematic sketch showing the effect of the moving point location on calculating average concentration	26
5-21	Numerical results for Run T-8 at different time levels.	26
5-22	Equilibrium wedge in a confined aquifer	27
5-23	Comparison of fresh water head calculated numerically and by Eq. 5-9 for the salt-water intrusion problem	28
5-24	Comparison of interface location calculated numerically and by Eq. 5-10	29
5-25	Numerical results showing the concentration distribution across the transition zone for various value of 2	29
A-1	Volume element of a porous medium used for developing continuity equation	36
B-1	Volume element of a porous medium used to develop continuity equation for tracer in miscible fluid flow	39
B-2	Tortuous path of fluid element.	40
C-1	Central grid and six adjacent grids with the subscripting used in the finite difference equations	45
D-1	Three-dimensional grid system with subscripting used to develop the finite difference form of the dispersion equation	49

Table		
V-1	Data for computer runs made to verify numerical simulation and tensor transformation of dispersion problem	22

ABSTRACT

A fundamental flow equation for a mixture of miscible fluids was derived by combining the law of conservation of mass, Darcy's law, and an equation of state describing the pressure-volume-temperature-concentration relationship. The result is an equation involving two dependent variables, pressure and concentration.

A relationship for determining concentration was derived by expressing a continuity equation for the dispersed tracer. The problem was formulated on a microscopic basis and averaged over a cross-sectional area of the porous medium to give a macroscopic convective-dispersion equation. The resulting coefficient of dispersion was a second rank tensor.

The two resulting differential equations are solved numerically on the digital computer. An implicit numerical technique was used to solve the flow equation for pressure and the method of characteristics with a tensor transformation was used to solve the convective-dispersion equation. The results from the flow equation were used in solving the convective-dispersion equation and the results from the convective-dispersion equation were then used to resolve the flow equation.

The proposed computer simulator successfully solved the longitudinal dispersion problem and the longitudinal and lateral dispersion problem. Using the tensor transformation, problems of longitudinal and lateral dispersion were successfully solved in a rotated coordinate system.

The computer simulator was used to solve the salt-water intrusion problem. The numerical results for the fresh water head in the aquifer closely matched those obtained analytically. Also, the numerical results for the location of the fresh-salt interface were good except in the region of the wedge toe.

NUMERICAL SIMULATION OF DISPERSION IN GROUNDWATER AQUIFERS

by

Donald Lee Reddell* and Daniel K. Sunada**

Chapter I

INTRODUCTION

1.1 Description of Problem. The rapid growth of the world's population is placing an increasing demand upon fresh water supplies. This has resulted in groundwater becoming an important source of water supply in many regions, and the use of aquifers as operating reservoirs is becoming more common. Efficient use of aquifers as reservoirs will require an understanding of the water quality problems created by sea-water intrusion into coastal aquifers, recharge of surface water into aquifers, underground waste disposal, and infiltration of pollutants from surface sources into aquifers.

Since pollutants, wastes, and recharge waters are normally miscible with the native groundwater, an understanding of the mechanics of miscible fluid displacement is necessary for the analysis of groundwater quality problems. Studies indicate that the mixing of miscible fluids in a porous medium is dependent upon the magnitude and distribution of flow velocities within the porous medium and upon the geometry of the porous structure. This mixing is greater than can be accounted for by molecular diffusion and has been named dispersion by Scheidegger (1954).

The dispersion process can be described by a form of the convective-diffusion equation in which a coefficient of dispersion replaces the standard coefficient of diffusion. Initial efforts at analyzing dispersion used a scalar dispersion coefficient. However, the work of de Josselin de Jong (1958) indicated the dispersion coefficient is not a scalar, and he introduced the use of longitudinal (parallel to flow direction) and lateral (perpendicular to flow direction) dispersion coefficients. Bear (1961a) and Scheidegger (1961) proposed that the dispersion coefficient is a symmetric second order tensor formed from the contraction of a fourth order tensor which depends on the porous medium and a second order tensor which is a function of the flow.

Many basic studies have been conducted to explain the physical laws of the dispersion process. These studies have resulted in analytical solutions to simple flow problems with simple boundary conditions. Also, some approximate solutions have been developed for radial and source-sink flow fields. However, no analytical solutions have been obtained which will be adequate for describing groundwater quality problems on an aquifer wide basis. Moreover, the complexity of the general differential equations describing dispersion is such that it is unlikely that analytical solutions will be developed in the near future.

Because of the inadequate techniques in analytical solutions and the recent advances in numerical and computer technology, an interest in using a computer simulation to describe the dispersion process has developed. Garder et al. (1964) used the method of characteristics (also referred to as "particle in cell" technique) to numerically solve the dispersion equation. However, they did not consider the tensorial nature of the dispersion coefficient for multidimensional flows.

Shamir and Harleman (1966) transformed the cartesian form of the convective-dispersion equation into equipotential and stream function coordinate systems. This technique properly considers the tensorial nature of the dispersion coefficient, but presents problems with unsteady nonuniform flow.

1.2 Purposes and Objectives. The literature indicates very little work toward application of basic dispersion results to field problems. Practical problems involve complex flow geometries in anisotropic and nonhomogeneous media with complicated boundary conditions. A computer simulation of the dispersion process should handle unsteady nonuniform flow problems and, in addition, consider the tensorial nature of the dispersion coefficient.

The objectives of this paper are:

(a) Develop a computer simulation for the mass transport of a fluid miscible with the native groundwater. The theory will be developed for three-dimensional, nonhomogeneous, unsteady flow fields, with density and viscosity variations between the two fluids. However, only two-dimensional flow problems in an isotropic medium using a conservative fluid will be run in the computer simulator.

---

*Ph.D. graduate of Colorado State University, Department of Agricultural Engineering Department, Fort Collins, Colorado, presently Assistant Professor of Agricultural Engineering, Texas A & M, College Station, Texas.

**Associate Professor of Civil Engineering, Colorado State University, Fort Collins, Colorado.

(b) Develop a numerical tensor transformation which considers the tensorial nature of the dispersion coefficient in a cartesian coordinate system.

1.3 Methods of Investigation. The techniques of investigation are directed toward use of the computer as a model simulator. No laboratory experimental techniques are used. The differential equations describing the miscible displacement process are developed and written in finite difference form. An implicit numerical technique is used to solve the flow equation and the method of characteristics with a tensor transformation is used to solve the convective-dispersion equation. The results from the flow equation are used in solving the dispersion equation and the results of the dispersion equation are then used to solve the flow equation again. This procedure has been referred to as a "leap-frog" technique, and will be explained in detail in Chapter IV.

The validity of the computer simulation is tested on some simple problems for which exact or approximate analytical solutions are available. Also, the more complex case of dispersion along an intruded salt-water wedge is considered.

Chapter II

PREVIOUS WORK RELATED TO THIS RESEARCH

Slichter (1905) injected a salt solution into a well and observed the time of arrival at a nearby observation well. He observed that the salt did not arrive at the observation well as a slug, but instead the salt concentration gradually increased with time to some maximum value. Since Slichter's work, many investigations have been made on the flow of miscible fluids in porous media. These investigations are divided into the following four categories for discussion purposes: (2.1) theoretical investigations, (2.2) analytical investigations, (2.3) experimental studies, and (2.4) numerical simulation.

2.1 Theoretical Investigations. The theoretical investigations have been oriented towards developing a basic understanding of the dispersion phenomena. These studies attempt to define the dispersion coefficient in terms of medium properties, fluid properties, and the fluid velocity.

Dispersion and diffusion may be visualized by the injection of a slug of dye into a fluid flowing through a porous medium as shown in Fig. 2-1. The center of the slug will travel along the column axis (r=0) with the average fluid velocity, V_3. As time, t, increases, the slug will increase in size and mix with the surrounding native fluid to form concentration profiles in both the x_3 and r-directions. This variation in concentration, C, is created by both dispersion and diffusion. Diffusion is a direct result of thermal motion of the individual fluid molecules and takes place under the influence of a concentration gradient. Dispersion in porous media is a mechanical or convective mixing process which is the result of individual fluid particles traveling at variable velocities through irregular shaped pores and along tortuous microscopic pathlines.

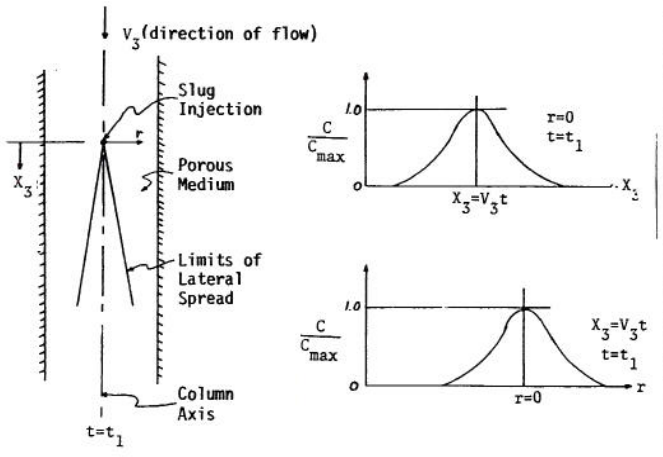

Fig. 2-1 Schematic column and typical concentration profiles for a slug injection. [after Hoopes and Harleman (1965)]

Dispersion results in a variation of concentration similar to that created by diffusion. However, dispersion is the result of convective mixing on a microscopic scale; not of a concentration gradient. Because of the difficulty in describing the boundary conditions for flow through porous media on a microscopic scale, a macroscopic model is used. When using the macroscopic model, dispersion is assumed to be proportional to the concentration gradient. A detailed description of the transition from a microscopic to a macroscopic model is given in Section B-2 of Appendix B.

To investigate the dispersion process, many porous media models have been used. Perhaps one of the simplest models is a bundle of capillaries. Taylor (1953, 1954) investigated the displacement of a fluid from a straight capillary tube of radius, r, by another fluid miscible with the first. His results indicated that the tracer was dispersed relative to a plane moving with velocity, V, exactly as in a Fickian diffusion process, but with a diffusion coefficient,

$$D = \frac{r^2V^2}{48D_d} \quad , \qquad (2\text{-}1)$$

where D_d is the molecular diffusion coefficient. Aris (1956) generalized Taylor's results by considering a bundle of capillary tubes and obtained an effective diffusion coefficient,

$$D = D_d + \tau \frac{r^2V^2}{D_d} \quad , \qquad (2\text{-}2)$$

where τ is a coefficient depending on the shape of the capillary tube's cross-section. Ananthakrishnan et al. (1965) investigated the range of applicability of Eq. 2-2.

Another theoretical approach is to develop a statistical model of the microscopic motion of marked fluid particles and to average these motions to obtain a macroscopic description of dispersion. Scheidegger (1954) neglected molecular diffusion and used the theory of a random walk extended to three dimensions. However, he assumed that the probability for a particle to move a given distance was the same for all directions. This leads to a dispersion coefficient that has the same value in all directions, and has subsequently been proven wrong for the general case.

De Josselin de Jong (1958) also used a statistical approach and was probably the first to develop a model which defined the dispersion coefficient as an anisotropic quantity. His model was constructed of interconnected straight channels oriented at random but uniformly distributed in all directions. The final result was a concentration profile described by a three-dimensional normal distribution in which longitudinal dispersion was greater than transverse dispersion. The concept of longitudinal and transverse dispersion has been verified experimentally [de Josselin de Jong (1958); Bear (1961b)].

Saffman (1959, 1960) used a statistical approach similar to de Josselin de Jong (1958). However, Saffman introduced molecular diffusion into his model and studied the relationship between mechanical dispersion and molecular diffusion. Saffman's first model (1959) assumed dispersion was large compared to molecular diffusion. Saffman's second model (1960) was for the case where molecular diffusion and dispersion are of the same order of magnitude.

Other statistical models have been investigated by Danckwerts (1953), Beran (1955), Rifai et al. (1956), and Day (1956). Scheidegger (1957) developed two theoretical models which yielded,

$$D \sim V \tag{2-3}$$

for one model, and

$$D \sim V^2 \tag{2-4}$$

for the other model. Equation 2-4 represents a model where enough residence time exists in each flow channel for molecular sideways diffusion to cause complete mixing between invading and original fluids. Equation 2-3 represents a model in which no mass is allowed to be transferred from one streamline to another by molecular diffusion. As shall be seen, experimental evidence indicates that Eq. 2-3 comes closer to physical reality. Scheidegger (1960) summarized much of the statistical work done prior to 1960.

Using the results of de Josselin de Jong's work (1958), Bear (1961a) developed an expression for the dispersivity tensor in terms of the average distance traveled by the tracer in the medium. Bear implied that the dispersion coefficient, D_{ij}, was a second rank tensor linear in the components of the velocity. Scheidegger (1961) suggested by induction that:

$$D_{ij} = \varepsilon_{ijmn} \frac{V_m V_n}{V} , \tag{2-5}$$

where ε_{ijmn} is the coefficient of dispersivity, which is a porous medium property, and $V_m V_n / V$ is a tensor which represents the linear influence of velocity. Scheidegger concluded that the coefficient of dispersivity was a fourth rank tensor with 81 components; but due to certain symmetry properties, contains only 36 independent components in the general case of an anisotropic medium. In isotropic media, there are only two dispersivity constants.

Recent work by Poreh (1965), showed from physical and dimensional reasoning that the tensor form of the coefficient of dispersion is

$$\frac{D_{ij}}{D_d} = F_1 \delta_{ij} + F_2 \left(\frac{d}{D_d} \right)^2 V_i V_j , \tag{2-6}$$

where d = pore size parameter, δ_{ij} = kronecker delta, $V_i V_j$ is a tensor representing the linear influence of velocity, and F_1 and F_2 are even functions of Vd/D_d and Vd/ν, the Peclet and Reynolds numbers, respectively. Bear and Bachmat (1967) also showed the dispersion coefficient, D_{ij}, to be a function of the Peclet number.

Several investigators, including Scheidegger (1961) and de Josselin de Jong and Bossen (1961), have suggested that the dispersion of a tracer in fluid flow through saturated homogeneous porous media can be described by the differential equation,

$$\frac{\partial C}{\partial t} = \frac{\partial}{\partial x_i} \left[D_{ij} \frac{\partial C}{\partial x_j} - V_i C \right] , \tag{2-7}$$

where C is the tracer concentration, t is time, V_i is the component of the velocity vector in a cartesian coordinate system, and $x_i (i=1,2,3)$ is the cartesian space coordinates. The double summation convention of tensor notation is implied in the use of Eq. 2-7. Bachmat and Bear (1964) gave the dispersion equation in curvilinear coordinates consisting of streamlines and equipotentials (Φ-Ψ coordinates). Bear and Bachmat (1967) used basic fluid flow equations which are averaged over a representative volume element of porous media to yield the equation of motion and the equation of dispersion.

Perkins and Johnston (1963) gave a good summary of diffusion and dispersion in porous media. A more recent and more detailed summary of the theory of dispersion in porous media was given by Bear et al. (1968, Chapter 11).

2.2 Analytical Solutions. Most dispersion problems have a direct analogy with heat flow. For this reason, a good reference for analytical solutions is Carslaw and Jaeger (1959) or Crank (1956). Some of the more important analytical solutions are discussed below.

Longitudinal Dispersion. A semi-infinite column ($X_3 > 0$) of homogeneous and isotropic porous media with a plane source maintained at $X_3 = 0$ is shown in Fig. 2-2. The flow is maintained at a constant specific discharge, q, in the X_3-direction. For an isotropic media, the axes of the dispersivity tensor is assumed to coincide with the velocity vector. Thus, Eq. 2-7 reduces to

$$\frac{\partial C}{\partial t} = D_L \frac{\partial^2 C}{\partial x_3^2} - V_3 \frac{\partial C}{\partial x_3} , \tag{2-8}$$

where D_L is the longitudinal dispersion coefficient. Initial and boundary conditions are given by,

$$C(0,t) = C_o \quad ; \quad t \geq 0$$

$$C(X_3,0) = 0 \quad ; \quad X_3 \geq 0$$

$$C(\infty,t) = 0 \quad ; \quad t \geq 0 \quad . \qquad (2\text{-}9)$$

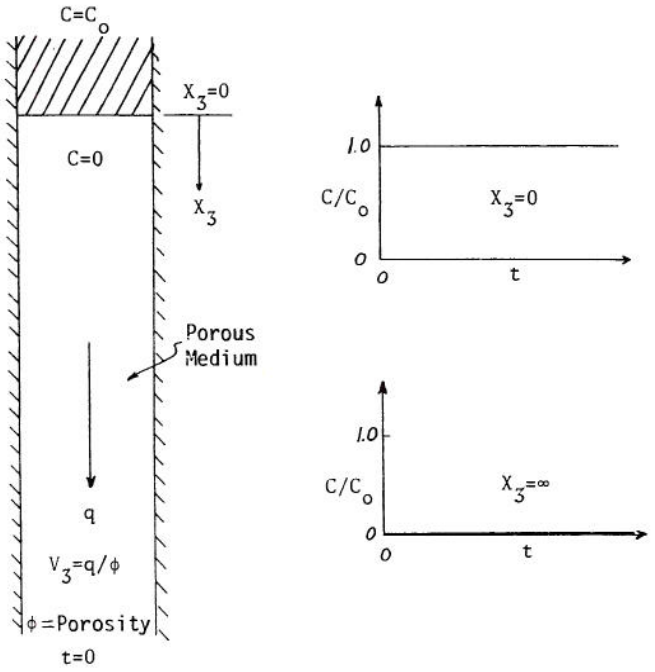

Fig. 2-2 Schematic sketch of longitudinal dispersion column setup

Ogata and Banks (1961) used Laplace transforms to obtain the solution,

$$\frac{C}{C_o} = \frac{1}{2}\left[\operatorname{erfc}\left(\frac{x_3 - V_3 t}{2\sqrt{D_L t}}\right) + \exp\left(\frac{V_3 x_3}{D_L}\right)\operatorname{erfc}\left(\frac{x_3 + V_3 t}{2\sqrt{D_L t}}\right)\right] \quad , \qquad (2\text{-}10)$$

where $\operatorname{erfc}(u) = 1 - \operatorname{erf}(u)$. Ogata and Banks showed that the second term in Eq. 2-10 may be neglected in most cases. For instance, if $D_L < 0.002\, V_3 X_3$ a maximum error of less than three percent is introduced by neglecting the second term. Therefore, unless the region close to the source is considered, an approximate solution to Eqs. 2-8 and 2-9 is

$$\frac{C}{C_o} = \frac{1}{2}\left[\operatorname{erfc}\left(\frac{x_3 - V_3 t}{2\sqrt{D_L t}}\right)\right] \quad . \qquad (2\text{-}11)$$

Ogata (1961, 1964a) gave a solution in integral form to the problem where a slug of radius "a" is injected at $x_3 = 0$. This problem must consider both longitudinal dispersion and transverse dispersion. Using his solutions, Ogata (1964a) developed experimental procedures for determining both D_L and D_T .

In many physical problems, the tracer being used may react with the solid matrix of the porous medium. Depending on the reaction, the tracer may be adsorbed to the matrix or additional tracer may be produced. To handle such cases, a production term dependent on the concentration is added to Eq. 2-8. Using varying functional relationships for the production term, solutions to this problem have been obtained by Ogata (1964b), Banks and Jerasate (1962), Banks and Ali (1964), and Lapidus and Amundson (1952). A closely related problem is that of radioactive decay of a tracer. Bear et al. (1968, p. 347) gave the solution to Eqs. 2-8 and 2-9 where the tracer continuously undergoes radioactive decay. Coats and Smith (1964) investigated the effects of dead-end pore volume on dispersion and gave several solutions to the simple diffusion model characterized by Eq. 2-8.

Longitudinal and Lateral Dispersion. If a rectangular column $(0 \leq x_3 \leq \ell_3 \; , \; 0 \leq x_2 \leq \ell_2)$ is used and a tracer source is maintained over a portion of the input area $(0 \leq x_2 \leq b)$ as shown in Fig. 2-3, then both longitudinal and lateral dispersion will occur. Assuming a homogeneous and isotropic medium with unidirectional flow in the x_3-direction and $\partial C/\partial x_1 = 0$, Eq. 2-7 becomes,

$$\frac{\partial C}{\partial t} = D_L \frac{\partial^2 C}{\partial x_3^2} + D_T \frac{\partial^2 C}{\partial x_2^2} - V_3 \frac{\partial C}{\partial x_3} \quad . \qquad (2\text{-}12)$$

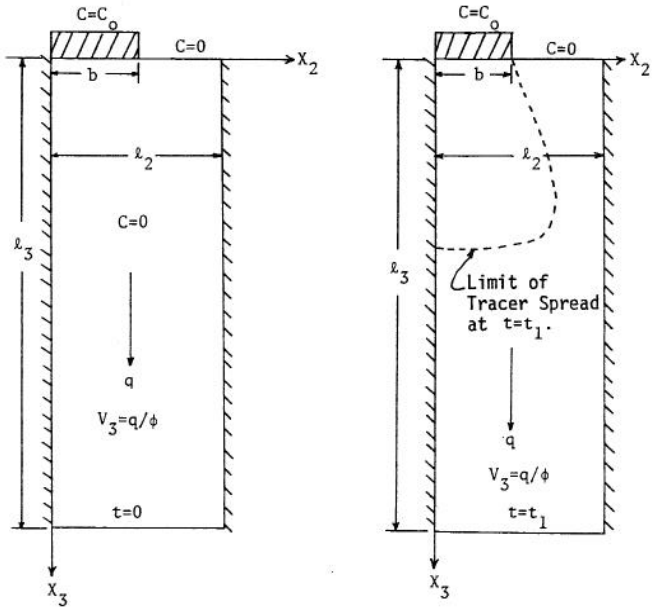

Fig. 2-3 Schematic sketch of longitudinal and lateral dispersion column setup

The initial and boundary conditions are given by:

$$C(x_2,0,t) = C_o \; ; \; 0 \leq x_2 \leq b \; ; \; t \geq 0$$

$$C(x_2,0,t) = 0 \; ; \; b < x_2 < \ell_2 \; ; \; t \geq 0$$

$$\frac{\partial C(0,x_3,t)}{\partial x_2} = 0 \; ; \; t>0$$

$$\frac{\partial C(\ell_2,x_3,t)}{\partial x_2} = 0 \; ; \; t>0$$

$$C(x_2,\infty,t) = \text{Bounded}$$

$$C(x_2,x_3,0) = 0 \; ; \; 0 \leq x_2 \leq \ell_2 \; ; \; x_3 > 0 \quad . \qquad (2\text{-}13)$$

A series solution to Eqs. 2-12 and 2-13 was given by Bruch and Street (1967). Harleman and Rumer (1963) gave the following approximate steady state solution to Eqs. 2-12 and 2-13,

$$\frac{C}{C_o} = \frac{1}{2} \operatorname{erfc}\left[\frac{x_2 - b}{2\sqrt{D_T x_3 / V_3}}\right] \quad . \qquad (2\text{-}14)$$

In their work on waste-water recharge and dispersion, Hoopes and Harleman (1965, 1967a, 1967b) have developed several approximate solutions to the radial dispersion problem. Raimondi et al. (1959) also gave an approximate solution to the radial dispersion problem. Esmail and Kimbler (1967) gave a solution which allows for alternate injection and production.

Dagan (1967) gave an analytical solution for dispersion in a nonhomogeneous porous column. Using the Laplace transform, Shamir and Harleman (1966, 1967) developed analytical solutions for longitudinal and lateral dispersion in layered porous media. Bear and Todd (1960, pp. 27-33) gave some analysis of the unsteady flow problem. Banks and Jerasate (1962) allowed the coefficient of dispersion to vary with time, and solved the problem by introducing a different time scale.

2.3 Experimental Results. Much of the experimental work has attempted to establish relationships so that the dispersion coefficients may be calculated from media and fluid properties. As was pointed out in Section 2.1, theoretical models indicate that the dispersion coefficient is a second rank tensor. Experiments of de Josselin de Jong (1958), Bear (1961b) and Bear and Todd (1960) tend to confirm this concept. Scheidegger's work (1961) indicated that for homogeneous and isotropic media, the dispersion tensor reduces to two independent terms: (1) the longitudinal dispersion coefficient, D_L , and (2) the lateral dispersion coefficient, D_T .

Most of the experimental determinations of the longitudinal dispersion coefficient used Eqs. 2-10 or 2-11 as a basis for analysis. Ebach and White (1958) performed experiments on a wide range of particle sizes, shapes, and Reynolds numbers. They empirically postulated that for Reynolds numbers, $R < 100$,

$$\frac{D_L}{\nu} = \alpha_1 \left(\frac{Vd}{\nu}\right)^{\beta_1} \quad , \qquad (2\text{-}15)$$

where V = fluid velocity, d = particle size of the porous media, and ν = kinematic viscosity. The experimentally determined coefficient α_1 is strongly dependent on the porous medium while β_1 is dependent on flow regime. However, evidence exists (Adam, 1966) that β_1 is also dependent on medium properties. Experimenters have found a large variation in the values of α_1 and β_1 . A large percentage of this variation may be attributed to experimental techniques; especially the different methods for measuring concentration.

Harleman and Rumer (1963) found $\alpha_1 = 0.66$ and $\beta_1 = 1.2$ while Hoopes and Harleman (1965) found $\alpha_1 = 1.70$ and $\beta_1 = 1.2$. Ebach and White (1958) found $\alpha_1 = 1.92$ and $\beta_1 = 1.06$. Experimental results for longitudinal dispersion were given by Banks and Ali (1964), Blackwell (1962), Cairns and Prausnitz (1960), Carberry and Bretton (1958), Simpson (1969), and many others.

Equation 2-15 prompted investigators of lateral dispersion to fit their experimental data to the form,

$$\frac{D_T}{\nu} = \alpha_2 \left(\frac{Vd}{\nu}\right)^{\beta_2} \quad . \qquad (2\text{-}16)$$

Harleman and Rumer (1963) found $\alpha_2 = 0.036$ and $\beta_2 = 0.7$. Hoopes and Harleman (1965) found $\alpha_2 = 0.11$ and $\beta_2 = 0.7$. Lateral dispersion has been investigated by Simpson (1962), Blackwell (1962), Grane and Gardner (1961), van der Poel (1962), and Li and Lai (1966).

Harleman et al. (1963) were able to correlate the longitudinal dispersion coefficient with permeability,

$$\frac{D_L}{\nu} = \alpha_3 \left(\frac{V\sqrt{k}}{\nu}\right)^{\beta_3} \quad , \qquad (2\text{-}17)$$

where k is the permeability with units of L^2 . Harleman et al. found $\alpha_3 = 54$ for spheres and 88 for sand with $\beta_3 = 1.2$ for both media. Hoopes and Harleman (1965) found results similar to Eq. 2-17, with α_3 dependent upon the media. Rumer (1962) investigated longitudinal dispersion and the effects of unsteady flow on the dispersion coefficient. Simpson (1969) investigated the effects of turbulent flow on the longitudinal dispersion coefficient, and Hoopes and Harleman (1967a) showed the dispersion coefficient along streamlines to be the same for both uniform and nonuniform flow at the same velocity.

The effects of molecular diffusion on the above Reynolds number type relationships has been debated in the literature. Relationships such as Eqs. 2-15, 2-16, and 2-17 would appear to be invalid for all ranges of Reynolds numbers. Biggar and Nielsen (1960) gave a very lucid account of the effects of molecular diffusion on dispersion. They proved that molecular

diffusion is very important at small flow velocities, when the medium consists of a natural soil skeleton instead of washed sands or glass beads, and for unsaturated flow. They hypothesized that the presence of dead-end pores (a characteristic of the soil) is highly important in determining the effects of molecular diffusion on the total dispersion process. Coats and Smith (1964) also treated the dead-end pore problem. Bear et al. (1968, pp. 332-335) stated that the dispersion coefficient depends on the flow pattern (e.g., velocity), Peclet number (Vd/D_d), and on some fundamental medium characteristics. A plot of D_L/D_d vs. Vd/D_d is broken up into five regions and characteristics of each region are discussed by Bear.

Adam (1966) used dimensional analysis and experimental results to determine the effects of anisotropic porous media on the dispersion tensor. Adam argued that experimental evidence indicating the dispersion coefficient is nonlinear in velocity (i.e., exponent of velocity is different than one) is incompatible with Eq. 2-3 proposed by Scheidegger (1961) and Bear (1961a). However, List and Brooks (1967) analyzed numerous experimental results and were critical of the velocity power law relationships.

From these various investigations the conclusion is reached that the dispersion coefficient is indeed a tensor of rank two; but an adequate relationship has not been developed for describing the phenomenon over a large range of flow parameters. Much more theoretical work is needed in this area.

A study of dispersion using the concept of similitude has been done by very few people. Raats and Scotter (1968) considered geometrically similar media and sought the conditions for dynamic similarity. Bachmat (1967) investigated the criteria for similitude of the dispersion phenomena in homogeneous and isotropic porous media. Heller (1963) also presented a good discussion on scaling of flows in porous mediums.

Few results from field experiments are available. Harpaz and Bear (1964) presented results of laboratory and field tests on underground storage operations with a single recharging well and with two wells, one recharging and one pumping. Lau et al. (1957) performed some field tests to evaluate various tracers, and found the chloride ion to be the best. Field oriented laboratory experiments have been conducted by Hoopes and Harleman (1965, 1967b) on wastewater recharge and by Rumer and Harleman (1963) on salt-water intrusion along coastal aquifers. Esmail and Kimbler (1967) investigated the effects of gravity segregation and dispersion on the problem of storing fresh water in saline aquifers.

2.4 Numerical Solutions. Because of the difficulty in obtaining analytical solutions to groundwater flow problems, many investigators are now using numerical solutions. Numerical solutions of immiscible flow problems have met with more success than miscible flow problems. Much work remains to be done on developing satisfactory numerical techniques for the dispersion problem.

Many of the reservoir simulation techniques involving immiscible fluids have been developed in the petroleum industry. Douglas, Peaceman, and Rachford (1959) employed an alternating-direction-implicit procedure (ADIP) to solve a two-dimensional, two-phase, incompressible flow model. Blair and Peaceman (1963) extended this to include the effects of compressibility. Larkin (1964) used the alternating-direction-explicit-procedure (ADEP). Quon et al. (1965, 1966) also used ADEP in a reservoir simulator. Coats and Terhune (1966) and Carter (1967) compared the ADIP and ADEP techniques. Bjordammen and Coats (1967) compared alternating direction and successive overrelaxation techniques for the simulation of two- and three-dimensional, two-phase flow reservoirs. Other reservoir simulators have been described by Dougherty and Mitchell (1964), Fagin and Stewart (1966), and Breitenbach, Thurnau, and van Poollen (1968 a, b, and c).

Digital computer simulators in the groundwater field have not been as widely developed as in the petroleum industry. Bittinger et al. (1967), Tyson and Weber (1964), and Chun, Weber, and Mido (1964) have presented some information on reservoir simulation in the groundwater industry. The above mentioned works are just a few of the ones which have been developed in the last few years on reservoir simulation using numerical analysis and digital computers.

The problem of miscible flow has not been treated as extensively numerically as the immiscible flow problem. Peaceman and Rachford (1962) presented a centered-in-time and centered-in-distance equation combined with a "transfer of overshoot" procedure which was demonstrated to work well in one dimension. However, subsequent testing has shown that for multidimensional displacement their method involved a numerical dispersion of the same order of magnitude as the physical dispersion.

Garder, Peaceman and Pozzi (1964) used the method of characteristics to improve the numerical solution to the miscible flow problem, but did not consider the dispersion coefficient as a tensor. Their numerical technique is discussed in detail in Chapter IV.

Stone and Brian (1963) made a thorough analysis of a numerical scheme to solve the one-dimensional dispersion equation. They used three adjacent grids at two time levels, and assigned arbitrary weighting coefficients to the convective and time terms. They then proposed an iterative scheme with three cycles per time step to improve the solution. No consideration was given to the effects of changes in viscosity or density.

Hoopes and Harleman (1965) used an explicit finite difference scheme to obtain a solution for the problem of radial flow from a well. By neglecting lateral dispersion, they also obtained a solution to a two-well problem. The size of the grid spacing and time increment were restricted for the explicit scheme because of a stability criterion. This presented some problems because of large amounts of required computer time.

Shamir and Harleman (1966) used a very ingenious concept in their numerical technique. First they wrote the dispersion equation in terms of the stream function and potential function (i.e., in terms of Φ

and Ψ coordinates). They noted that the velocity is everywhere tangential to the streamlines, and thus their equation was one-dimensional in the convective term. They then used the Stone and Brian (1963) numerical technique for one-dimensional flow and handled the lateral dispersion with an ADIP technique. If the major axis of the dispersion tensor coincides with the velocity vector, then Shamir and Harleman's technique will consider the dispersion coefficient as a tensor. However, their scheme does not consider the effects of density or viscosity changes; nor does it consider unsteady flow except in the few cases where the streamlines do not change position with time.

Nelson (1965) described a computer program for predicting waste transport in groundwater. The program generated permeability information and stream functions using a potential map with a small amount of permeability information. However, he considered a "piston type" flow and neglected dispersion entirely.

Summary. In summary, the following results are important to the present study:

(1) The dispersion coefficient is an anisotropic quantity and must be treated as a second rank tensor.

(2) The dispersion coefficient is linearly related to the components of velocity as given by Eq. 2-5.

(3) The analytical solution to the longitudinal dispersion problem is given by Eq. 2-10.

(4) An approximate steady state solution to the longitudinal and lateral dispersion problem is given by Eq. 2-14.

(5) The longitudinal and lateral dispersion coefficients can be obtained from the empirical relationships given by Eqs. 2-15, 2-16, and 2-17.

(6) Numerical solutions to the problem of miscible displacement in porous media have proven to be difficult. The numerical techniques of Stone and Brian (1963), Garder et al. (1964), and Shamir and Harleman (1966) appear to be the most successful.

Chapter III

PRESENTATION OF MATHEMATICAL MODEL FOR DISPERSION IN GROUNDWATER AQUIFERS

When working with miscible fluid displacement, the conservation of mass for each component present in the system is required. In this study, only two components are considered, a conservative tracer and the native groundwater. Therefore, two equations of mass conservation are required to describe the system considered here. One of these equations will be for the combined masses of both components (i.e., total mass = tracer mass + native groundwater mass). The other equation is for the mass of the tracer.

3.1 General Flow Equation. A fundamental flow equation for the mixture of two miscible fluids is derived by combining the conservation of mass equation for the mixture, Darcy's law, and an equation of state describing the pressure-volume-temperature-concentration relationship. A linear equation relating change in porosity and change in pressure is also used. The result is an equation involving two dependent variables, pressure and tracer concentration. A detailed development of this equation is given in Appendix A. Using shorthand tensor notation, the final equation may be written as:

$$\frac{\partial}{\partial x_i}\left[\frac{\rho \Delta A_i k_{x_i}}{\mu}\left(\frac{\partial P}{\partial x_i} + \rho g \frac{\partial h}{\partial x_i}\right)\right]\Delta x_i =$$

$$= \rho_o \phi_o \Delta\bar{V}(\beta + C_F)\frac{\partial P}{\partial t} + \alpha \phi_o \Delta\bar{V}\frac{\partial C}{\partial t} + \rho_p Q \quad , \qquad (3\text{-}1)$$

where $\Delta x_i (i=1,2,3)$ = dimensions of volume element ---L,

$\Delta A_i (i=1,2,3)$ = cross sectional area of element perpendicular to x_i (i.e., $\Delta A_1 = \Delta x_2 \Delta x_3$) ---$L^2$,

t = time---T,

$\Delta\bar{V} = \Delta x_1 \Delta x_2 \Delta x_3$ = volume of element---L^3,

$x_i (i=1,2,3)$ = Cartesian coordinate system (x_1, x_2, x_3)---L,

ρ = total fluid density---ML^{-3} or FT^2L^{-4},

k_{x_i} = absolute permeability in x_i-direction---L^2,

μ = viscosity of fluid mixture---FTL^{-2},

P = pressure of fluid mixture---FL^{-2},

g = acceleration of gravity---LT^{-2},

h = elevation of volume element above datum---L,

ϕ = porosity---dimensionless,

β = fluid compressibility---L^2F^{-1},

C_F = formation compressibility factor ---L^2F^{-1},

α = proportionality factor relating concentration and density---dimensionless,

C = mass concentration of tracer---ML^{-3} or FT^2L^{-4}.

ρ_p = mass density of produced fluid ---ML^{-3} or FT^2L^{-4}, and

Q = rate of fluid production---L^3T^{-1},

ρ_o = reference value of density---ML^{-3} or FT^2L^{-4},

ϕ_o = reference value of porosity---dimensionless.

To obtain Eq. 3-1 in its present form the following assumptions have been made: (1) Darcy's law is applicable, (2) single phase flow, (3) isothermal flow, (4) a linear relationship between change in porosity and change in pressure, (5) size of volume element does not vary with time, and (6) a linear relationship between density, pressure, and concentration.

The flow of groundwater through an aquifer is used in this study, and the validity of Darcy's law presents no serious obstacles. For problems in the nonlinear flow regime, additional terms involving the gradient of pressure raised to some power would be needed in Eq. 3-1. Should a multiphase problem be considered, then equations of the form of Eq. 3-1 would need to be developed for each phase and the saturation, S, would be different than one. The assumption of isothermal flow eliminates having to consider the density in Eq. 3-1 as a function of temperature, and considering the size of the volume element invariant with time permits the elimination of $\frac{\partial(\Delta\bar{V})}{\partial t}$ from Eq. 3-1. The use of a linear relationship between "change in porosity"-"change in pressure" and density-pressure-concentration is discussed in Section 3.3.

3.2 Dispersion Equation. A convective-dispersion equation may be obtained by combining the conservation of mass equation for the tracer, Fick's law, and an equation of state. A detailed derivation of this equation is given in Appendix B. The general dispersion equation is given by:

$$\frac{\partial}{\partial t}(\phi\Delta\bar{V}C) = \frac{\partial}{\partial X_i}\left[(D_{ij} + D_d T_{ij})\phi\Delta A_i \frac{\partial C}{\partial x_j}\right]\Delta x_i$$

$$- \frac{\partial}{\partial x_i}(CV_i \phi \Delta A_i)\Delta x_i - C_p Q \quad , \qquad (3\text{-}2)$$

where D_{ij} = dispersion coefficient which is a second rank tensor---L^2T^{-1},
D_d = molecular diffusion coefficient---L^2T^{-1},
T_{ij} = porous medium "tortuosity" factor which is also a second rank tensor---dimensionless,
V_i = seepage velocity (flow rate per unit pore area) of fluid mixture in i^{th} direction---LT^{-1},
C_p = concentration of tracer in produced fluid---ML^{-3} or Ft^2L^{-4}, and

all other terms are as described previously.

Assumptions necessary to obtain Eq. 3-2 are: (1) diffusion is described by Fick's law, (2) the convective mixing called dispersion is proportional to the concentration gradient, and (3) single-phase flow exists. The double summation convention of tensors is implied in the use of Eq. 3-2.

The use of Fick's law to describe diffusion means that a dilute solution is being used. In addition, any diffusion due to temperature gradients or velocity gradients is disregarded. Assuming that dispersion is proportional to a concentration gradient is discussed in Appendix B. For multi-phase flow, equations similar to Eq. 3-2 must be written for each phase.

Because of the numerical technique to be used in solving the dispersion equation, an alternate form of Eq. 3-2 is desirable. This is achieved by chaining out the derivatives of concentration as is shown in detail by Eqs. B-31 thru B-40 of Appendix B. The final result is,

$$\frac{\partial C}{\partial t} = \frac{\rho}{\phi \Delta A_i (\rho - \alpha C)} \frac{\partial}{\partial x_i} \left[D^*_{ij} \phi \Delta A_i \frac{\partial C}{\partial x_j} \right] - V_i \frac{\partial C}{\partial x_i} - (C_p - C) \frac{Q}{\phi \Delta \overline{V}} \quad , \tag{3-3}$$

where

$$D^*_{ij} = D_{ij} + D_d T_{ij} \quad . \tag{3-4}$$

The fluid compressibility effects on concentration are neglected in developing Eq. 3-3.

3.3 Auxiliary Equations. Because of the interrelationship among several of the parameters in Eqs. 3-1 and 3-3, the following auxiliary equations are needed in the mathematical model. The components of the seepage velocity for the fluid mixture may be obtained from Darcy's law, and are given by

$$V_i = - \frac{k_{x_i}}{\phi \mu} \left[\frac{\partial P}{\partial x_i} + \rho g \frac{\partial h}{\partial x_i} \right] \; ; \; i=1,2,3 \; . \tag{3-5}$$

The relationship between the porosity of the porous medium and the fluid pressure is assumed to be,

$$\phi = \phi_o \left[1 + C_F (P - P_o) \right] \quad , \tag{3-6}$$

where ϕ_o = original porosity---dimensionless, and
P_o = original fluid pressure---FL^{-2}.

The density of the fluid mixture is assumed to be a linear function of the fluid pressure and tracer concentration,

$$\rho = \rho_o + \beta \rho_o (P - P_o) + \alpha (C - C_o) \quad , \tag{3-7}$$

where ρ_o = original fluid density---ML^{-3} or FT^2L^{-4}, and
C_o = original tracer concentration---ML^{-3} or FT^2L^{-4}.

Also, the viscosity is assumed to be a linear function of the concentration,

$$\mu = \mu_o + \lambda (C - C_o) \quad , \tag{3-8}$$

where μ_o = original viscosity---FTL^{-2}, and
λ = proportionality factor relating concentration and viscosity---dimensionless.

The use of Eqs. 3-6, 3-7, and 3-8 are assumptions. Equation 3-6 has been used in the petroleum industry with success [Breitenbach et. al. (1968b)] . Depending upon the fluids used, relationships other than those given by Eqs. 3-7 and 3-8 may be desirable. For the example problems in this study, salt water and fresh water are used as the two fluids, and the linear relationships of Eqs. 3-7 and 3-8 are believed to be adequate.

3.4 Dispersion Coefficients. Equation 3-3 and the corresponding finite-difference equations of Chapter IV are developed in a general way so that any value may be used for the nine components of the dispersion tensor. However, the use of a functional relationship is desirable which will give the values of all nine components in a systematic manner.

Assuming an isotropic porous medium, the "tortuosity" tensor, T_{ij} , is given by

$$T_{ij} = T \delta_{ij} \quad , \tag{3-9}$$

where T = tortuosity factor---dimensionless, and
δ_{ij} = kronecker delta.

Thus, the nine components of the diffusion tensor are,

$$D_d T_{11} = D_d T_{22} = D_d T_{33} = D_d T \tag{3-10a}$$

and

$$D_d T_{12} = D_d T_{13} = D_d T_{21} = D_d T_{23} = D_d T_{32} = 0 \; . \tag{3-10b}$$

Scheidegger (1961) gave the relationship,

$$D_{ij} = \varepsilon_{ijmn} \frac{V_m V_n}{V} \quad , \tag{3-11}$$

where ε_{ijmn} = the dispersivity of the medium, a fourth rank tensor---L,

V_m, V_n = the components of velocity in the m and n directions, respectively---LT^{-1}, and

V = magnitude of the velocity---LT^{-1}.

For an isotropic media, Scheidegger shows that the dispersivities reduce to only two terms, ε_1 and ε_2, with

$$\varepsilon_{\alpha\alpha\alpha\alpha} = \varepsilon_1$$

$$\varepsilon_{\alpha\alpha\beta\beta} = \varepsilon_2$$

$$\varepsilon_{\alpha\beta\alpha\beta} = 1/2\ (\varepsilon_1 - \varepsilon_2)$$

$$\varepsilon_{\alpha\beta\beta\alpha} = 1/2\ (\varepsilon_1 - \varepsilon_2)$$

all other ε's = 0 . (3-12)

The longitudinal and transverse dispersion coefficients are related to the dispersivities by

$$D_L = \varepsilon_1 V \tag{3-13a}$$

and

$$D_T = \varepsilon_2 V \quad . \tag{3-13b}$$

Expanding Eq. 3-11, introducing Eqs. 3-12 and 3-13, and adding the diffusion tensor given by Eq. 3-10, the following functional relationship for the nine components of the hydrodynamic dispersion coefficient are obtained:

$$D^*_{11} = D_L \frac{V_1 V_1}{V^2} + D_T \frac{V_2 V_2}{V^2} + D_T \frac{V_3 V_3}{V^2} + D_d T \quad ,$$

$$D^*_{22} = D_T \frac{V_1 V_1}{V^2} + D_L \frac{V_2 V_2}{V^2} + D_T \frac{V_3 V_3}{V^2} + D_d T \quad ,$$

$$D^*_{33} = D_T \frac{V_1 V_1}{V^2} + D_T \frac{V_2 V_2}{V^2} + D_L \frac{V_3 V_3}{V^2} + D_d T \quad ,$$

$$D^*_{21} = D^*_{12} = (D_L - D_T) \frac{V_1 V_2}{V^2} \quad ,$$

$$D^*_{31} = D^*_{13} = (D_L - D_T) \frac{V_1 V_3}{V^2} \quad ,$$

$$D^*_{32} = D^*_{23} = (D_L - D_T) \frac{V_2 V_3}{V^2} \quad . \tag{3-14}$$

Other functional relationships for obtaining the components of the hydrodynamic dispersion tensor are given by Bear et al. (1968), Poreh (1965), and List and Brooks (1967).

Chapter IV

DEVELOPMENT OF NUMERICAL MODEL FOR DISPERSION

The computer simulation of the miscible displacement problem will be developed by writing the finite difference form for each of the equations given in Chapter III. Because of limited funds available for analysis, the computer simulator is developed for a two-dimensional vertical flow problem. Finite difference equations and stability criteria for the three-dimensional problem are given in Appendices C, D, and E.

4.1 Finite Difference Form of Two-Dimensional Flow Equation. An implicit, centered-in-space finite difference scheme is used to approximate the time and space derivatives of Eq. 3-1. This scheme is developed in detail in Appendix C for the three-dimensional problem. The two-dimensional finite difference equation has the form

$$\rho^{+}_{x_1} N^{+}_{x_1} p^{t+1}_{i+1,k} + \rho^{-}_{x_1} N^{-}_{x_1} p^{t+1}_{i-1,k} + \rho^{+}_{x_3} N^{+}_{x_3} p^{t+1}_{i,k+1} + \rho^{-}_{x_3} N^{-}_{x_3} p^{t+1}_{i,k-1}$$

$$- \left[\rho^{+}_{x_1} N^{+}_{x_1} + \rho^{-}_{x_1} N^{-}_{x_1} + \rho^{+}_{x_3} N^{+}_{x_3} + \rho^{-}_{x_3} N^{-}_{x_3} + \rho_{i,k} (C_{F_{i,k}} + \beta_{i,k}) / \Delta t \right] p^{t+1}_{i,k}$$

$$= - \frac{\rho_{i,k} (C_{F_{i,k}} + \beta_{i,k})}{\Delta t} p^{t}_{i,k} + \frac{\alpha_{i,k} (C^{t}_{i,k} - C^{t-1}_{i,k})}{\Delta t_o} + \left(\frac{\rho_p Q}{\phi \Delta x_1 \Delta x_3} \right)_{i,k}$$

$$- \left[(\rho^{+}_{x_1})^2 N^{+}_{x_1} g \Delta h^{+}_{x_1} + (\rho^{-}_{x_1})^2 N^{-}_{x_1} g \Delta h^{-}_{x_1} + (\rho^{+}_{x_3})^2 N^{+}_{x_3} g \Delta h^{+}_{x_3} \right.$$

$$\left. + (\rho^{-}_{x_3})^2 N^{-}_{x_3} g \Delta h^{-}_{x_3} \right] \quad . \qquad (4\text{-}1)$$

Here i and k indicate the grid row and grid column respectively, and t indicates time level. The coefficients $\rho^{\pm}_{x_i}$, $N^{\pm}_{x_i}$, and $\Delta h^{\pm}_{x_i}$ are given as Eq. C-7 of Appendix C.

A rectangular grid system is superimposed onto the region of interest, and Eq. 4-1 written for each grid. The dimensions of the grids, Δx_1, and Δx_3, are assumed to be constant over the entire region. Variable dimensional grids may be used, but a change in the coefficients, $N^{\pm}_{x_i}$, is necessary. The coefficients, $\rho^{\pm}_{x_i}$ and $N^{\pm}_{x_i}$, are held constant during each time step. Approximation of the original non-linear equation is obtained by adjusting the values of $\rho^{\pm}_{x_i}$ and $N^{\pm}_{x_i}$ after each computation. If the change in $\rho^{\pm}_{x_i}$ and $N^{\pm}_{x_i}$ is small during each Δt, this procedure will produce acceptable results.

The change in concentration with respect to time on the right hand side of Eq. 4-1 is calculated using the change in concentration from the previous time step, Δt_o. If the change in concentration during each Δt is small, this will also produce acceptable results. If necessary, an iteration between the solution of the flow equation and the dispersion equation can improve this approximation.

If the rectangular grid system has m-rows and n-columns, then there will be mn grids. Since Eq. 4-1 contains unknown pressures from each of the four adjacent grids plus an unknown pressure for the grid in question, the result of writing Eq. 4-1 for all grids is a set of mn simultaneous algebraic equations. This set may be written in matrix form as

$$[A]\ [P] = [rhs] \quad , \qquad (4\text{-}2)$$

where [A] is a mn by mn matrix containing the coefficients of pressure, [P] is a mn column vector containing the unknown pressures, and [rhs] is a mn column vector containing all the factors on the right hand side of Eq. 4-1.

4.2 Finite Difference Form of Two-Dimensional Dispersion Equation. The numerical solution of the multi-dimensional dispersion equation (Eq. 3-3) has been a difficult problem. Therefore, some background material may be helpful in understanding the technique used in this study. If the convective terms and production term of Eq. 3-3 are neglected, the resulting equation is

$$\frac{\partial C}{\partial t} = \frac{\rho}{\phi \Delta A_i (\rho - \alpha C)} \frac{\partial}{\partial x_i} \left[D^{*}_{ij} \phi \Delta A_i \frac{\partial C}{\partial x_j} \right] \quad . \qquad (4\text{-}3)$$

This equation is a second order partial differential equation of parabolic type (heat flow equation) and is of the same form as Eq. 3-1. A dispersion equation of this type could be solved in the same way as the flow equation given in Eqs. 4-1 and 4-2. This particular type of equation has been successfully solved numerically many times.

Now suppose that the dispersion and production terms of Eq. 3-3 are neglected. Then the resulting equation is

$$\frac{\partial C}{\partial t} + V_i \frac{\partial C}{\partial x_i} = 0 \quad , \qquad (4\text{-}4)$$

which is a first order partial differential equation of hyperbolic type and has been treated numerically with some success in one dimension. However, extension to two or more dimensions has proven difficult. Usually one of two things happens: (1) the numerical solution develops oscillations or (2) it becomes smeared by "artificial dispersion" resulting from the numerical process. Thus, when convection and dispersion are considered simultaneously, this "artificial dispersion" may dominate the low physical dispersion which characterizes miscible displacement.

If convection and dispersion are neglected, then a change in concentration can be caused by the production term,

$$\frac{\partial C}{\partial t} + (C_p - C) \frac{Q}{\phi \Delta \bar{V}} = 0 \quad . \qquad (4\text{-}5)$$

Although not immediately obvious, the production term may be written as $[(C_p-C)/\Delta x_i][Q/(\phi \Delta A_i)]$ or $[(C_p-C)/\Delta x_i]V_p$, where V_p is the velocity of the production fluid. This term is analogous to the convective terms of Eq. 4-4, and therefore shall be analyzed in a manner similar to the convective terms. In general, the production term will be a discrete function, and will be introduced through boundary conditions of the problem.

In problems of miscible displacement, the amount of dispersion is usually very small, and this makes the convective-dispersion equation almost of the hyperbolic type shown in Eq. 4-4. Garder et al. (1964) recognized this and developed a numerical technique for solving the convective-dispersion equation based on the method of characteristics. They assume that the dispersion terms are given functions of x_1, x_2, x_3, and t , i.e.,

$$\frac{\rho}{\phi \Delta A_i (\rho - \alpha C)} \frac{\partial}{\partial x_i} \left[D^*_{ij} \phi \Delta A_i \frac{\partial C}{\partial x_j} \right] \equiv f(x_1, x_2, x_3, t) \quad . \qquad (4\text{-}6)$$

Neglecting the production term momentarily, and substituting Eq. 4-6 into Eq. 4-3 gives

$$\frac{\partial C}{\partial t} + V_i \frac{\partial C}{\partial x_i} = f(x_1, x_2, x_3, t) \quad . \qquad (4\text{-}7)$$

Garder et al. (1964) show that a nonhomogeneous equation with the form of Eq. 4-7 has characteristic curves

$$x_1 = x_1(t) \ , \ x_2 = x_2(t) \ , \ x_3 = x_3(t), \text{ and } C = C(t) \quad , \qquad (4\text{-}8)$$

where t is an arbitrary curve parameter which in this case is time. These characteristic curves are the solutions to the ordinary differential equations,

$$\frac{dx_1}{dt} = V_1 \ , \quad \frac{dx_2}{dt} = V_2 \ , \quad \frac{dx_3}{dt} = V_3 \ ,$$

and

$$\frac{dC}{dt} = f(x_1, x_2, x_3, t) \quad . \qquad (4\text{-}9)$$

The concentration, C , is not a constant on these characteristic curves.

The basis of the method of characteristics is that given solutions to Eq. 4-9, a solution to the original partial differential equation (Eq. 4-7) may be produced by following the characteristic curves. The requirement of following the characteristic curves is achieved numerically by introducing a set of moving points in addition to the normal grid system. Each of the moving points is assigned a concentration, which varies with time. At each time interval, the moving points in a two-dimensional system are relocated using a finite difference form given by,

$$x_{1_\ell}^{t+1} = x_{1_\ell}^{t} + \Delta t \, V_{1_\ell}^{t+1} \qquad (4\text{-}10)$$

and

$$x_{3_\ell}^{t+1} = x_{3_\ell}^{t} + \Delta t \, V_{3_\ell}^{t+1} \quad , \qquad (4\text{-}11)$$

where $t+1$ is the new time level, t is the old time level, Δt is the time increment, x_{1_ℓ} and x_{3_ℓ} are the coordinates of the ℓth moving point, while V_{1_ℓ} and V_{3_ℓ} are the velocities of the ℓth moving point in the x_1- and x_3-directions.

Each cell in the grid system is assigned a concentration equal to the average of the concentrations of the moving points located inside the cell at time $t+1$. The concentration of the cell and each moving point inside the cell is then modified for dispersion by solving $dC/dt = f(x_1, x_2, x_3, t)$ using an explicit, centered-in-space finite difference equation. This equation is developed in detail in Appendix D for the three-dimensional problem. The two-dimensional form is

$$\begin{aligned} C_{i,k}^{t+1} = {} & C_{i,k}^{t+\Delta} + E^+_{x_1x_1}(C_{i+1,k}^{t+\Delta} - C_{i,k}^{t+\Delta}) - E^-_{x_1x_1}(C_{i,k}^{t+\Delta} - C_{i-1,k}^{t+\Delta}) \\ & + E^+_{x_3x_3}(C_{i,k+1}^{t+\Delta} - C_{i,k}^{t+\Delta}) - E^-_{x_3x_3}(C_{i,k}^{t+\Delta} - C_{i,k-1}^{t+\Delta}) \\ & + G^+_{x_1x_3}(C_{i,k+1}^{t+\Delta} + C_{i+1,k+1}^{t+\Delta} - C_{i,k-1}^{t+\Delta} - C_{i+1,k-1}^{t+\Delta}) \\ & - G^-_{x_1x_3}(C_{i-1,k+1}^{t+\Delta} + C_{i,k+1}^{t+\Delta} - C_{i,k-1}^{t+\Delta} - C_{i-1,k-1}^{t+\Delta}) \\ & + G^+_{x_3x_1}(C_{i+1,k+1}^{t+\Delta} + C_{i+1,k}^{t+\Delta} - C_{i-1,k+1}^{t+\Delta} - C_{i-1,k}^{t+\Delta}) \\ & - G^-_{x_3x_1}(C_{i+1,k}^{t+\Delta} + C_{i+1,k-1}^{t+\Delta} - C_{i-1,k}^{t+\Delta} - C_{i-1,k-1}^{t+\Delta}) \quad . \qquad (4\text{-}12) \end{aligned}$$

Here i and k indicate grid rows and grid columns respectively, t+1 is the new time level and t+Δ is a time level somewhere between t and t+1. The coefficients $E^{\pm}_{x_i x_i}$ and $G^{\pm}_{x_i x_j}$ are given as Eqs. D-19 of Appendix D.

4.3 Finite Difference Form of Velocity Equation. In the method of characteristics described above, a determination of the seepage velocity is necessary for relocating the moving points during each time step. To accomplish this, a grid and its four adjacent grids are used as shown in Fig. 4-1.

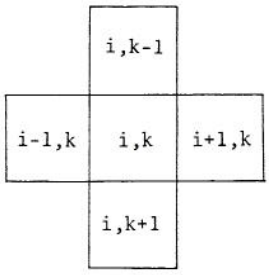

Fig. 4-1 Grid system used to develop a finite difference equation for the seepage velocity.

The flow equation (Eq. 4-2) is solved for the pressures at time level t+1. These pressures are assigned to the centers of each of the grids. Using these pressures and Darcy's law, a value for the seepage velocity at the contact between two grids may be calculated. Thus, a finite difference form of the horizontal seepage velocity at $i+\frac{1}{2},k$ could be written as

$$(V_1)^{t+1}_{i+\frac{1}{2},k} = -\left(\frac{k_{x_1}}{\mu\phi}\right)_{i,k}\left[\left(\frac{P^{t+1}_{i+\frac{1}{2},k}-P^{t+1}_{i,k}}{\Delta x_1/2}\right) + (\rho g)_{i+\frac{1}{2},k}\left(\frac{h_{i+\frac{1}{2},k}-h_{i,k}}{\Delta x_1/2}\right)\right], \quad (4\text{-}13)$$

where all symbols are as previously defined. The horizontal seepage velocity at $i+\frac{1}{2},k$ could also be written as

$$(V_1)^{t+1}_{i+\frac{1}{2},k} = -\left(\frac{k_{x_1}}{\mu\phi}\right)_{i+1,k}\left[\left(\frac{P^{t+1}_{i+1,k}-P^{t+1}_{i+\frac{1}{2},k}}{\Delta x_1/2}\right) + (\rho g)_{i+\frac{1}{2},k}\left(\frac{h_{i+1,k}-h_{i+\frac{1}{2},k}}{\Delta x_1/2}\right)\right]. \quad (4\text{-}14)$$

By continuity, Eqs. 4-13 and 4-14 should give the same value for $(V_1)^{t+1}_{i+\frac{1}{2},k}$. Thus, upon adding the two equations, cancelling like terms, and rearranging, a weighted value of $(V_1)^{t+1}_{i+\frac{1}{2},k}$ is obtained in the form,

$$(V_1)^{t+1}_{i+\frac{1}{2},k} = \frac{-2(k_{x_1})_{i,k}(k_{x_1})_{i+1,k}}{\Delta X_1[(k_{x_1})_{i+1,k}(\phi\mu)_{i,k}+(k_{x_1})_{i,k}(\phi\mu)_{i+1,k}]}\Big[(P^{t+1}_{i+1,k}-P^{t+1}_{i,k})+(\rho g)_{i+\frac{1}{2},k}(h_{i+1,k}-h_{i,k})\Big]. \quad (4\text{-}15)$$

In a similar manner, the vertical seepage velocity, $(V_3)^{t+1}_{i,k+\frac{1}{2}}$, may be written as

$$(V_3)^{t+1}_{i,k+\frac{1}{2}} = \frac{-2(k_{x_3})_{i,k}(k_{x_3})_{i,k+1}}{\Delta X_3[(k_{x_3})_{i,k+1}(\phi\mu)_{i,k}+(k_{x_3})_{i,k}(\phi\mu)_{i,k+1}]}\Big[(P^{t+1}_{i,k+1}-P^{t+1}_{i,k})+(\rho g)_{i,k+\frac{1}{2}}(h_{i,k+1}-h_{i,k})\Big]. \quad (4\text{-}16)$$

Using Eqs. 4-15 and 4-16, the seepage velocities at each interface of a grid is calculated as shown in Fig. 4-2. A seepage velocity must be assigned to

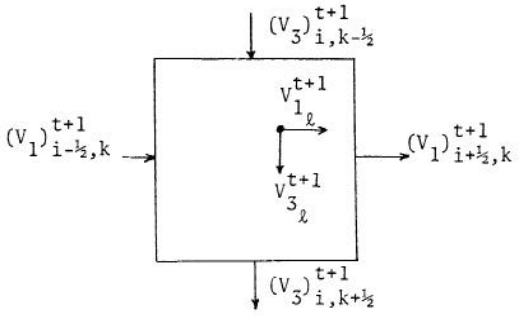

Fig. 4-2 Schematic sketch showing relation of seepage velocity at moving point to the seepage velocity calculated at the interface between grids.

each moving point within the grid based on the value of the seepage velocities at the interfaces. A linear interpolation is used in making this assignment. For instance, the velocity components of the moving point in the grid of Fig. 4-2 are given by,

$$V^{t+1}_{1_\ell} = (V_1)^{t+1}_{i-\frac{1}{2},k} - \frac{x_{1_\ell}-(x_1)_{i-\frac{1}{2},k}}{\Delta x_1}\left[(V_1)^{t+1}_{i-\frac{1}{2},k}-(V_1)^{t+1}_{i+\frac{1}{2},k}\right] \quad (4\text{-}17)$$

and

$$V^{t+1}_{3_\ell} = (V_3)^{t+1}_{i,k-\frac{1}{2}} - \frac{3_\ell-(x_3)_{i,k-\frac{1}{2}}}{\Delta x_3}\left[(V_3)^{t+1}_{i,k-\frac{1}{2}}-(V_3)^{t+1}_{i,k+\frac{1}{2}}\right]. \quad (4\text{-}18)$$

4.4 Boundary Conditions. Appropriate boundary conditions due to geologic and hydrologic influences must be used in conjunction with Eqs. 4-2, 4-10, 4-11, 4-12, 4-17, and 4-18 to obtain a solution. These conditions take the form of (a) no-flow boundaries, (b) hydraulic boundaries at ground surfaces, (c) groundwater underflow boundaries, and (d) known tracer concentrations maintained at certain boundaries.

No-flow boundaries are simulated by assigning a permeability of zero, a longitudinal dispersion coefficient of zero, and a transverse dispersion coefficient of zero to the grids located along the boundary. With such a simulation, the coefficients $N^{\pm}_{x_i}$, $E^{\pm}_{x_i x_i}$, and $G^{\pm}_{x_i x_j}$, as given in Appendix C and Appendix D, are automatically set equal to zero. The one exception that has to be treated separately is the case where grid (i,k) and one of the adjacent grids are both no-flow boundaries (see Fig. 4-1). In this case the coefficients $N^{\pm}_{x_i}$, $E^{\pm}_{x_i x_i}$, and $G^{\pm}_{x_i x_j}$ will become $0/0$ which is indefinite. An "IF" statement in the computer program can effectively take care of this one situation and set the appropriate coefficients equal to zero if this situation should ever occur.

Hydraulic boundaries at the ground surface are most commonly encountered in the form of a direct connection between a groundwater aquifer and a river or lake, and are simulated by programming a time-varying or constant water pressure in the appropriate grids. If the known pressure boundary is encountered in grid (i,k), then the coefficients of the pressures in the adjacent grids are set equal to zero, the coefficient of the pressure in grid (i,k) is set equal to one, and the right hand side of Eq. 4-1 is set equal to the known pressure value. The resulting equation is

$$P^{t+1}_{i,k} = \text{known value.} \qquad (4\text{-}19)$$

In case the known pressure boundary is encountered in one of the grids adjacent to grid (i,k), then the appropriate coefficient $\rho^{\pm}_{x_i} N^{\pm}_{x_i}$ is multiplied by the known pressure and transferred to the right hand side column vector of Eq. 4-2. The corresponding element of the coefficient matrix, $[A]$ is then set equal to zero.

Groundwater underflow boundaries occur when only a portion of an aquifer is being studied. This boundary condition may be simulated in many ways, but perhaps the simplest is to project the pressure gradient and concentration gradient across the boundary and calculate the rate of underflow using these projected gradients.

Boundary conditions for known tracer concentrations must be specified also. These conditions are handled in this simulation by the moving points. As fluid leaves the model, moving points with their corresponding concentration values are removed from the system. As fluid enters the model, moving points with the appropriate boundary concentrations are added to the system.

The boundary conditions described above are the only ones considered in this simulation. Other boundary conditions such as those associated with a leaky aquifer or radioactive decay of a tracer may be encountered. Appropriate additions to the computer program would be required.

4.5 Description of the Computer Program. The computer simulation was programmed in Fortran IV for the CDC6400 Computer at the Colorado State University Computer Center. A flow chart of the program is shown in Appendix F, and a reprint of the program used in solving the salt-water intrusion problem is given in Appendix G.

The MAIN program accepts the input data and governs the sequence of operations to be performed. Subroutine INICON assigns a uniform distribution of "moving" points to each grid along with the initial value of concentration assigned to each point. Subroutine READIN reads in or assigns appropriate values to all physical quantities such as permeability, porosity, viscosity, etc. All of the initial values are then printed out using subroutine INIPRT and subroutine MATROP.

Because of the large amount of computer storage required, auxiliary storage in the form of a scratch tape is used. The locations and concentrations of the moving points are stored in common with the coefficient matrix used in solving the pressure equation. Since the location and concentration of the moving points must not be destroyed, they are written onto the scratch tape each time before the pressure equation is solved and then read back afterwards. This was done by subroutines, WRTAPE and RDTAPE which are systems routines developed at the CSU Computer Center. They allow for reading or writing on the tape while the program continues to execute.

Subroutine MATSOL sets up the coefficient matrix, $[A]$, and the right hand side column vector, $[rhs]$, for solving the pressure equation. This subroutine, as is presently written, may take care of two types of boundary conditions: (1) a constant pressure boundary and (2) a no-flow boundary. Other boundary conditions besides these may easily be added to the program. MATSOL checks the boundary conditions and makes the appropriate changes in $[A]$ and $[rhs]$.

To solve the set of equations set up by MATSOL, the solution of a set of simultaneous equations is required. A general numerical solution should offer several solution techniques such as Gauss elimination, successive overrelaxation (SOR), or iterative alternating direction implicit procedure (ADIPIT). For a review of these techniques, the reader is referred to Breitenbach et al. (1968b).

Gauss elimination is by far the most reliable numerical method one can choose for solving the matrix given by Eq. 4-2. However, the volume of computation required by Gauss elimination for a large matrix can result in large amounts of computer time. In such cases, ADIPIT or SOR may prove to be more efficient with time. For the computer simulator developed herein, Gauss elimination was chosen.

If the matrix, [A] , were written out, the resulting matrix is found to be a band matrix with five diagonals of the form,

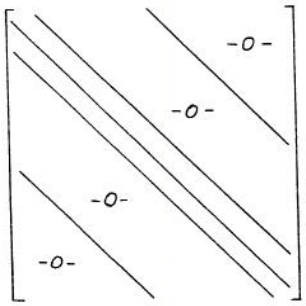

Computer storage is not necessary for the matrix elements above and below the band. Thus, having a minimum band width is desirable. An appropriate choice of the grid numbering pattern can reduce the total width of the band. Another important feature is that the number of rows participating in the upper triangularization for each column is quite limited. Thurnau (1963) developed an algorithm called BANDSOLVE which makes use of these characteristics in solving a five diagonal band matrix.

In this computer simulator, subroutine BSOLVE makes use of the BANDSOLVE algorithm to solve the matrix equation, Eq. 4-2, by Gauss elimination. This subroutine allows for row interchange to combat round-off error. The only problem encountered in using this technique to solve the matrix equation was that of large amounts of computer storage. As an example, a grid network with the dimensions of 10 grids by 25 grids has 250 equations and requires 5250 words of computer storage for BSOLVE. In contrast, a 20 grid by 25 grid network has 500 equations and requires 20,500 words of computer storage for BSOLVE. For large problems, external storage would be necessary on many computers.

After solving for the new pressures, the storage taken up by subroutine BSOLVE is available for other uses. Therefore, the coordinates and concentrations of the moving points are read from the scratch tape and placed in the storage locations previously occupied by BSOLVE.

Subroutine VELOCY calculates the velocities at each grid interface by use of Eqs. 4-15 and 4-16. This routine also calculates the longitudinal and lateral dispersion coefficients using a velocity power relationship of the form of Eqs. 2-15 and 2-16. With values for the dispersion coefficients and velocity components, Eq. 3-14 is used to calculate the components of the dispersion tensor.

Subroutine MOVPT uses the velocities calculated in VELOCY and Eqs. 4-17 and 4-18 to obtain the velocity components of each moving point. Each point is then moved to a new location by use of Eqs. 4-10 and 4-11. A section of this subroutine determines which of the points has moved out of the model. These points are tagged and introduced at an inflow boundary with the appropriate boundary concentration. Of all the subroutines developed for this simulator, MOVPT is probably the least general. At the present time, minor changes in the program must be made when boundary conditions are changed to allow for the proper removal and reintroduction of the moving points. After each point has been moved to a new location, the average concentration of each grid is calculated by arithmetically averaging the concentrations of the "moving points" located in the grid.

With the average concentrations of each grid determined, subroutine DISP uses Eq. 4-12 to determine the change in concentration due to dispersion. The end result is the concentration of each grid at time $t+\Delta t$. To conclude a time step, a mass balance of the system is calculated and appropriate changes in density, viscosity, and porosity are made using Eqs. 3-6, 3-7, and 3-8. A test for print out is made and the program returns to subroutine MATSOL where the pressure equation is resolved and the entire process repeated for the next time step.

4.6 Validity of Computer Simulator. A discussion of the validity of the proposed computer simulator is needed at this point. No rigorous proof of the stability and convergence of the overall simulator is available. Thus, the performance of the program in solving problems will be used as a major test of validity. A discussion of this performance is presented in Chapter V. However, some confidence can be gained by analyzing the individual parts of the simulator for stability and convergence.

The pressure equation is solved using Eq. 4-1 as the finite difference form. This is an implicit, centered-in-space difference scheme with variable coefficients. No general stability criteria for the variable coefficient difference equation has yet been developed. Although not giving a rigorous proof, Richtmyer (1957, p. 72) gave the argument that the stability conditions for the constant coefficient problem must be satisfied at every point in the domain of the difference equation for the variable coefficient difference equation to be stable. Smith (1965) and Richtmyer (1957) both showed that the implicit difference scheme with constant coefficients is unconditionally stable and convergent. Thus, using the heuristic argument of Richtmyer, it may be concluded that Eq. 4-1 is stable for any value of Δx_1, Δx_3, and Δt .

The change in concentration due to dispersion is given by Eq. 4-12, and is an explicit centered-in-space finite difference equation. In general, explicit difference schemes have stability criterion, and Eq. 4-12 is no exception. The stability criterion for a constant coefficient explicit difference form involving $\partial^2 C/\partial x_1^2$, $\partial^2 C/\partial x_2^2$, and $\partial^2 C/\partial x_3^2$ may be found in Smith (1965) or Richtmyer (1957). However, Eq. 4-12 also contains the cross-derivative $\partial^2 C/\partial x_1 \partial x_3$ and a stability analysis of the equation was necessary. The stability analysis was done by a Fourier series approach for both the three-dimensional and two-dimensional problems. This analysis is given in detail in Appendix E. In summary, the stability of Eq. 4-12 is assured if

$$D^*_{11} > 0 \quad , \tag{4-20}$$

$$D^*_{33} > 0 \quad , \tag{4-21}$$

$$4D^*_{11}D^*_{33} > (D^*_{13} + D^*_{31})^2 \quad , \quad . \tag{4-22}$$

and

$$\frac{\omega D^*_{11}\Delta t}{(\Delta x_1)^2} + \frac{\omega D^*_{33}\Delta t}{(\Delta x_3)^2} \leq \frac{1}{2} \quad , \tag{4-23}$$

where D^*_{11}, D^*_{33}, D^*_{13} and D^*_{31} are the components of the dispersion tensor, Δt is the temporal increment, Δx_1 and Δx_3 are the spatial increments and $\omega = \rho/(\rho\text{-}\alpha C)$. The stability of the three-dimensional equation is given as Eq. E-40 of Appendix E.

If Eq. 3-14 is used to obtain D^*_{11} , D^*_{33} , D^*_{13} , and D^*_{31} , then Eqs. 4-20, 4-21, and 4-22 are satisfied automatically. Thus, Eq. 4-23 is the only stability criterion of any importance to the problem being considered here.

A theoretical development of the convergence of the overall "method of characteristics" scheme used to solve the dispersion equation has not been successful. If the stability criterion of Eq. 4-23 is not satisfied, then the numerical solution "blows up ". Some convergence tests made by running problems with known solutions are given in the next chapter.

Chapter V

RESULTS AND INTERPRETATIONS

Because of the difficulty in obtaining theoretical criteria for the validity of the numerical simulator, experience with actual problems is a necessity. The numerical solution of the pressure equation has been done successfully many times, and will not be the subject of detailed review in this study. However, the solution of the dispersion equation by the "method of characteristics" (MOC) has not been so widely studied; especially using the tensor relationships developed in Chapter IV. Therefore, the numerical solution of the dispersion equation is the object of most of the following results and discussion.

5.1 Longitudinal Dispersion in Steady, Uniform, One-Dimensional Flow. If the results of known analytical solutions can be reproduced, a great deal of confidence in the numerical solution can be gained. An analytical solution to the one-dimensional problem with a step input of the tracer as a boundary condition is available. This solution was given as Eq. 2-10. The first test of the MOC will be to see how well it solves the one-dimensional problem.

Garder et al. (1964) showed that accurate solutions of one-dimensional problems can be obtained by the MOC over a wide range of values of the dispersion coefficient, including zero. They also showed that the moving points do not need to be uniformly spaced, and that increasing the number of moving points beyond two points per grid did not significantly improve the accuracy of the solution. A run was made using the data of Garder et al. (1964), and the results are shown in Fig. 5-1.

No theoretical determination of the error has been made for the method of characteristics. For purposes of this study, an estimate of the error between the numerical and analytical solution is given by

$$E(t) = \max_{1 \le i \le n} \left| C_i(t) - C_i^*(t) \right| , \qquad (5\text{-}1)$$

where $E(t)$ is the error at a particular time level, i is the grid number, n is the number of grids being used, $C_i(t)$ is the numerical value of concentration in the ith grid, and $C_i^*(t)$ is the analytical value of concentration for the ith grid. Other measures of error, such as a least squares approach, could be used. However, from a computing standpoint, Eq. 5-1 is the easiest to determine and will give the relative merits of the numerical technique.

To show the effect of grid size on the error, several runs using different values for the spatial increment were made. The results of these runs are summarized in Fig. 5-2. The error for the MOC behaves very strangely, and does not seem to necessarily get smaller with smaller grid size. This erratic behavior of the error is believed to be caused by the method of calculating the average grid concentration and the relative positions of the moving points inside the grid. This problem will be discussed in detail in Section 5.3 of this chapter.

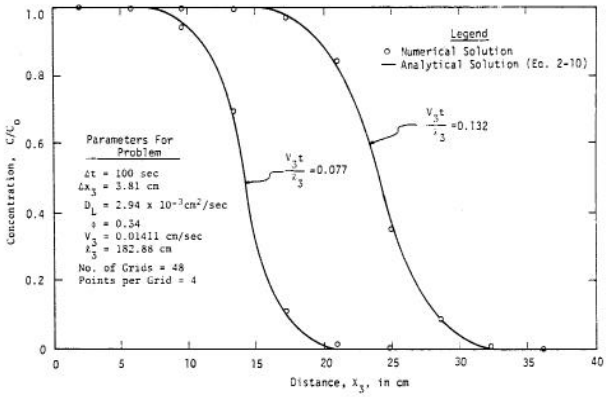

Fig. 5-1 Comparison of analytical and numerical solution to the longitudinal dispersion problem used by Garder et al. (1964).

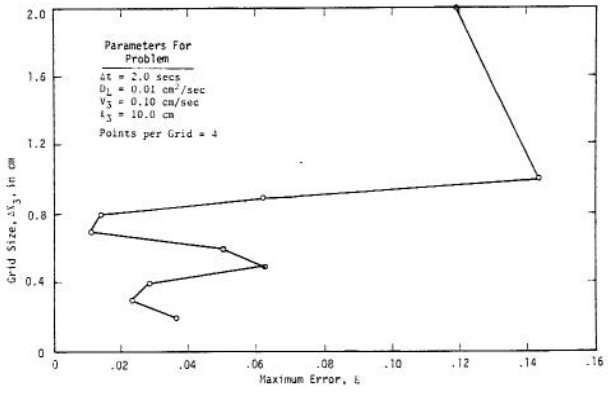

Fig. 5-2 Effect of grid size on the error of solution by the method of characteristics.

Some indication of the nature of the erratic behavior of the error shown in Fig. 5-2 can be obtained by devising a particular grid dimension, velocity, time increment, and moving point location so that even though the moving points have moved they have the same relative positions in the grid at

each time step. Using V_3 = 0.10 cm/sec and Δt = 2 secs, each point will move 0.2 cm each time step. If a grid dimension of 0.4 cm is chosen and two points per grid are used, then the distance between each moving point is 0.2 cm. Thus, at each time step, a moving point just takes the position of the point in front of it at the old time level, and all points are located in the same relative position in every grid. This concept is carried over when 4, 6, 8, or 16 points per grid are used.

The results of runs using the above concept are shown in Fig. 5-3. The fact that the results for 2, 4, 6, 8, and 16 points are the same in Fig. 5-3 is not just graphical. The computer results were the same to all significant figures printed out. These results offer two possible conclusions. The first possible conclusion is that a relationship between the three parameters, velocity, time increment, and distance between moving points, has an effect on the error of solution. The second possible conclusion is that using an arithmetic mean to determine the average concentration of each grid is improper. Some type of weighted average may be more appropriate. These possible conclusions will be explored in detail in the following pages.

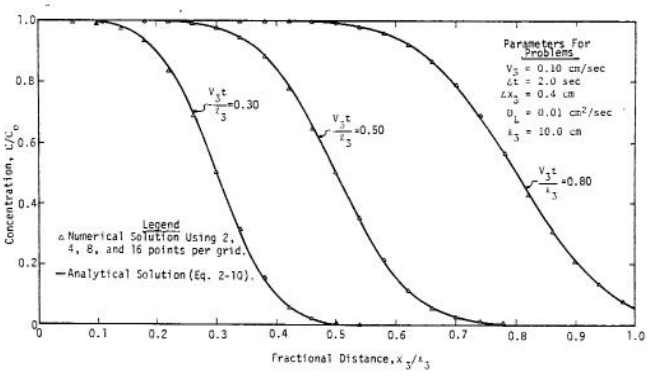

Fig. 5-3 Comparison of numerical and analytical solutions using different numbers of moving points per grid.

The results from using one point per grid (Fig. 5-4) also indicated an interesting phenomenon that was noticeable on other runs. When using one point per grid, there is 0.4 cm between each moving point. Since the points only move 0.2 cm per time step, two time steps are needed for a point to move across a grid. Thus, the concentration of the one point determines the concentration of the grid for two time steps. In effect, the grid concentration is not changed due to convection. Every even time step gives accurate results using one point per grid, while each odd time step will give poor results, with the front lagging behind the actual front as shown in Fig. 5-4. This produces a "jerky" effect in the accuracy of the solution which is undoubtedly some of the reason for the erratic behavior of the error shown in Fig. 5-5. A different method for calculating the average grid concentration appears to be needed.

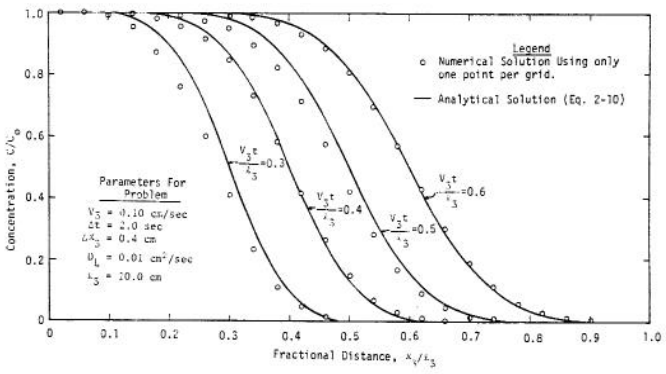

Fig. 5-4 Comparison of numerical and analytical solutions using only one moving point per grid.

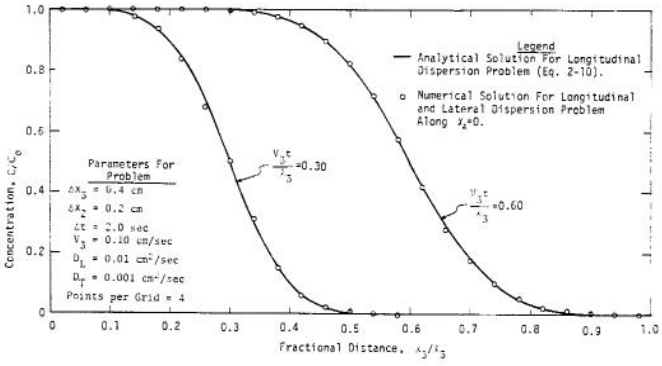

Fig. 5-5 Comparison of numerical, transient concentration distribution along x_2=0 for the two-dimensional dispersion problem with the analytical solution to the one-dimensional dispersion problem.

When sufficient points per grid are used to provide a proper average grid concentration, then the MOC yields good results for the one-dimensional problem.

5.2 Longitudinal and Lateral Dispersion in Steady, Uniform, One-Dimensional Flow. In the previous section, the MOC was shown to be capable of giving good results for the one-dimensional dispersion problem. The extension of this analysis to the slightly more difficult problem of two-dimensional dispersion is the next logical step. A rectangular region, $0 \le x_3 \le \ell_3$ and $0 \le x_2 \le \ell_2$ is considered in which the flow is along the x_3-axis with a steady, uniform seepage velocity, V_3. A fluid of concentration, C_o, is injected over a portion of the input boundary $(0 \le x_2 \le b)$, while the remaining portion of the boundary $(b \le x_2 \le \ell_2)$ is injected with

a fluid of zero concentration. A schematic of this particular problem is shown in the upper right hand corner of Fig. 5-6.

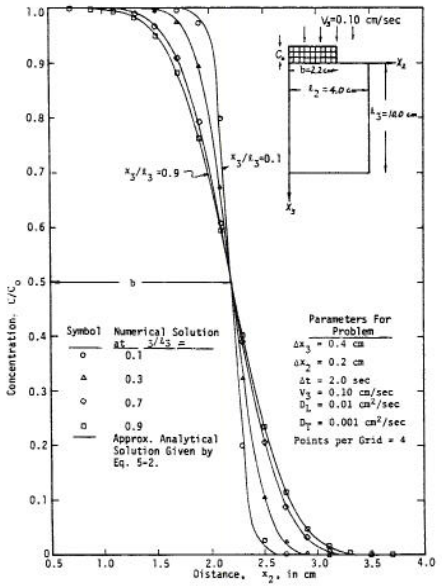

Fig. 5-6 Comparison of numerical and approximate analytical solution for the one-dimensional flow, two-dimensional dispersion problem at steady state concentration.

The differential equation and boundary conditions for this problem were given as Eqs. 2-12 and 2-13. When the input concentration at x_3=0 is maintained for a long time, the concentration distribution will approach a steady state. Harleman and Rumer (1963) neglected the longitudinal dispersion term in the differential equation and solved the steady state problem. Neglecting the longitudinal dispersion is valid because $\partial^2 C/\partial x_3^2$ is very small at steady state. Their approximate solution for the steady state case was

$$\frac{C}{C_o} = \frac{1}{2}\,\mathrm{erfc}\left[\frac{x_2 - b}{2\sqrt{D_T x_3/V_3}}\right] . \qquad (5\text{-}2)$$

The numerical solution of this problem using the MOC was compared with the solution given by Eq. 5-2. Data for this run are: 25 x 20 grids on $0 \le x_3 \le 10$ cm and $0 \le x_2 \le 4$ cm, V_3 = 0.10 cm/sec, D_L = 0.01 cm^2/sec, D_T = 0.001 cm^2/sec, points per grid = 4, Δx_3 = 0.4 cm, Δx_2 = 0.2 cm, b = 2.2 cm, and Δt = 2.0 sec. As was done for the one-dimensional problem, the computer program bypassed the solutions of the pressure equation and velocity equation. Steady state conditions were achieved at about 200 seconds, or after about 100 time steps. The computer time required to solve the dispersion equation for this problem was about 0.55 secs/time step. The step input of concentration was handled numerically by letting C/C_o = 1.0 for $x_2 < b$, C/C_o = 0.5 for x_2 = b, and C/C_o = 0.0 for $x_2 > b$.

The numerical solution provided the transient concentration distribution, but no check of its accuracy was made since Eq. 5-2 is for steady state. However, if D_T is small and b is large, the concentration distribution at x_2 = 0 is not affected by lateral dispersion, and the transient concentration profile along x_2 = 0 should be the same as for the one-dimensional dispersion case. This was found to be true for this run as shown in Fig. 5-5.

The numerical results at steady state (t = 200 secs) are compared with the approximate analytical solution (Eq. 5-2) in Figs. 5-6 and 5-7. The accuracy of the results appear to be quite good except for the area close to x_3 = 0. This should be expected since the assumption of $\partial^2 C/\partial x_3^2$ = 0 in the analytical solution is not valid in this area. Some of this discrepancy may also be the result of the very steep concentration profile in the x_2-direction for the area close to x_3 = 0. Although not tried, smaller grid dimensions in the x_2-direction might improve the results. Figure 5-7 gives the longitudinal concentration distribution at steady state for various values of x_2. The small curvature of the lines in Fig. 5-7 compared with the curvature shown in Fig. 5-6 lends support to the assumption that $\partial^2 C/\partial x_3^2 \approx 0$ at steady state.

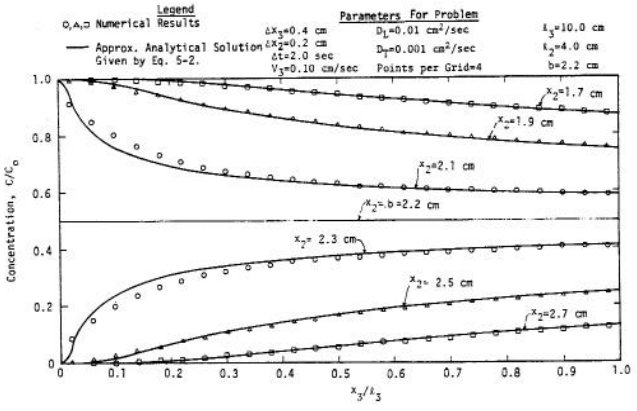

Fig. 5-7 Comparison of longitudinal concentration distribution at steady state as calculated numerically and by an approximate analytical solution for the one-dimensional flow, two-dimensional dispersion problem.

The MOC appears to be capable of solving problems of longitudinal and lateral dispersion with as much ease as it did longitudinal dispersion alone. No problems with "overshoot" occurred and no numerical smearing was noticed.

5.3 Numerical Solutions Using the Tensor Concept of Dispersion. One of the primary objectives of this work is to consider the dispersion coefficient as a tensor and evaluate the importance of using the tensor concept. To be perfectly rigorous, the dispersion coefficient was treated as a tensor in the previous two sections. However, in those instances the axes of the dispersion tensor was oriented parallel to the coordinate axes x_1, x_2, and x_3. This resulted in the coefficients D^*_{21}, D^*_{12}, D^*_{31}, D^*_{13}, D^*_{32}, and D^*_{23} all being zero, and $D^*_{11} = D_L$, $D^*_{33} = D_T$. Thus, the previous analysis was reduced to working with longitudinal and lateral dispersion.

In an isotropic medium, experimental results indicate that the dispersion tensor is oriented so that longitudinal dispersion is parallel to the velocity vector and lateral dispersion is perpendicular to the velocity vector. Thus, if the velocity vector is oriented at some angle to the coordinate axes, then the dispersion tensor is also at some angle to the coordinate axes. In the original paper by Garder et al. (1964), it was assumed that the velocity vector was essentially parallel to the x_1-axis. However, in most complex groundwater flow situations the velocity vector will not be parallel to the coordinate axes, but will be constantly changing direction at different locations in the system.

The general dispersion equation (Eq. 3-3) and the tensor transformation equations (Eq. 3-14) were derived and written in finite difference form so that assuming the velocity vector parallel to one of the coordinate axis is not necessary. Thus, any type of complex flow system may be analyzed using the proposed numerical simulator.

No analytical solutions are available for a multidimensional flow problem involving the proposed tensor transformations. To check the numerical simulation, the problems described in Sections 5.1 and 5.2 were made two-dimensional by orienting the coordinate axes at some angle to the flow vector. Solving these problems in the rotated coordinate system forces the use of the tensor transformation and numerical scheme. However, the physics of the problem have not been changed, and the resulting answers should be the same as those obtained in Sections 5.1 and 5.2.

After some preliminary calculations, the coordinate axes were rotated so that an angle of 45° existed between the velocity vector and the coordinate axes. The derivation of the stability criteria in Appendix E influenced the decision for using 45°. This is because at increments of $\pi/4$, $3\pi/4$, $5\pi/4$, and $7\pi/4$ the off diagonal tensor components D^*_{12}, D^*_{21}, D^*_{31}, D^*_{13}, D^*_{23} and D^*_{32} are at a maximum. Thus, the maximum influence of the tensor transformation would occur when the angle between the velocity vector and the coordinate axes was given by $n\pi/4 (n=1,3,5,7...)$. Figure 5-8 is a schematic sketch of the proposed numerical scheme.

The one detail about the proposed scheme for testing the numerical tensor transformation that may provide trouble is the boundary conditions. As seen in Fig. 5-8, the straight boundaries of the original

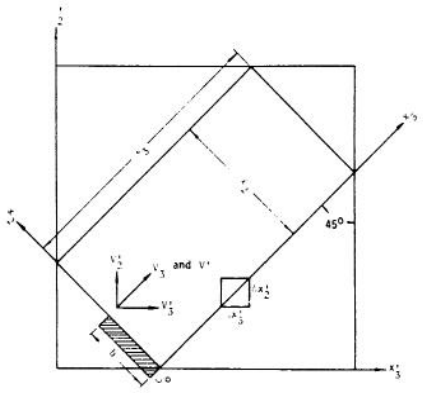

Fig. 5-8 Schematic sketch of coordinate axes rotation used for comparing numerical tensor transformation with known analytical solutions.

column will be approximated by a series of rectangles or squares in the rotated column. As $\Delta x'_2$ and $\Delta x'_3$ become very small, a better approximation of the boundary conditions can be obtained. In the computer runs, the results along the boundary grids were not as accurate as they should be. However, moving away from the boundary only a small distance, the results were found to be consistent with the analytical solutions.

Longitudinal Dispersion. The first computer runs using the tensor transformation were made for the longitudinal dispersion problem discussed in Section 5.1. Three different runs were made, and the data for these runs are shown in Table V-1 as runs number T-1, T-2, and T-3. As can be seen from the data, lateral as well as longitudinal dispersion was allowed to take place. However, a fluid of concentration $C/C_o = 1.0$ was injected across the entire interface $0 \leq x_2 \leq \ell_2$. This should result in $\partial C/\partial x_2 = 0$, and elimination of lateral dispersion. Thus, an effective test of the numerical approximation for $\partial C/\partial x'_2$ and $\partial C/\partial x'_2 \partial x'_3$ is provided.

The computer time required to solve this problem was approximately 0.50 sec/time step for the 20 x 20 grid network and approximately 1.25 sec/time step for the 38 x 38 grid network. This is the time required to solve only the dispersion equation since the solutions of the pressure equation and velocity equation were bypassed for these runs. Thus, increasing the number of grids by a factor of 3.6 resulted in increasing the computer time by a factor of 2.5

The results for Run T-1, in which Eq. 3-14 was used for the tensor transformation, are shown in Fig. 5-9. For comparison, the analytical solution determined from Eq. 2-10 is given. As can be seen, the results are quite good. No problems with "overshoot" occurred for this case. For $x_3/\ell_3 > 0.9$, some error is noticeable on the 0.92 pore volume injected curve. This is because the boundary condition of the analytical solution has been violated. The analytical solution is for a semi-infinite column; not a finite column. Thus, the end effects of the column became noticeable.

TABLE V-1 Data for computer runs made to verify numerical simulation and tensor transformation of dispersion problem

Run	Δt (sec)	$\Delta x'_3$ (cm)	$\Delta x'_2$ (cm)	V'_3 (cm/sec)	V'_2 (cm/sec)	V' (cm/sec)	No. of Points per Grid	Tensor Transformation used
T-1	1.5	0.2	0.2	.071	.071	0.10	2	yes
T-2	1.5	0.2	0.2	.071	.071	0.10	2	no
T-3	2.0	0.4	0.4	.071	.071	0.10	2	yes
T-4	2.0	0.4	0.4	.071	.071	0.10	4	yes
T-5	1.5	0.2	0.2	.071	.071	0.10	2	yes
T-6	1.5	0.2	0.2	.071	.071	0.10	2	yes
T-7	1.5	0.2	0.2	.071	.071	0.10	2	no
T-8	1.5	0.2	0.2	.071	.071	0.10	2	yes

TABLE V-1. Continued.

Run	No. of Grids in x'_3-Direction	No. of Grids in x'_2-Direction	D_L (cm^2/sec)	D_T (cm^2/sec)	ℓ_3 (cm)	ℓ_2 (cm)	b (cm)
T-1	38	38	0.01	0.003	6.509	4.245	4.245
T-2	38	38	0.01	0.003	6.509	4.245	4.245
T-3	20	20	0.01	0.001	5.66	5.66	5.66
T-4	20	20	0.01	0.001	7.358	3.962	1.981
T-5	38	38	0.01	0.001	6.509	4.245	2.122
T-6	38	38	0.01	0.003	6.509	4.245	2.122
T-7	38	38	0.01	0.003	6.509	4.245	2.122
T-8	38	38	0.01	0.003	6.509	4.245	2.122

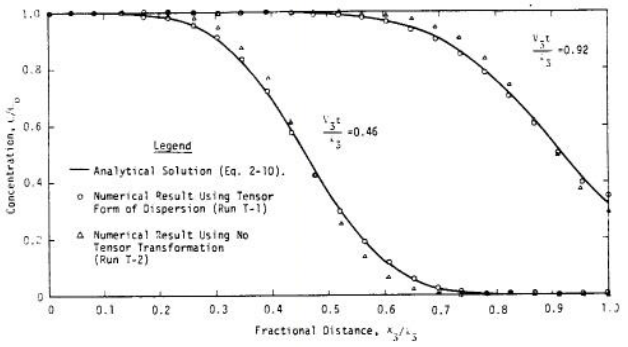

Fig. 5-9 Comparison of longitudinal concentration distribution calculated with and without tensor transformation for Runs T-1 and T-2.

Also shown on Fig. 5-9 are the results of Run T-2 in which the tensor transformation was not used. For this case, $D^*_{11} = D_L$, $D^*_{22} = D_T$, and $D^*_{12} = D^*_{21} = 0$. This means that the dispersion tensor was assumed to be oriented parallel to the rotated coordinate axes rather than the velocity vector. The results of Run T-2 indicate that by not using the tensor transformation, an error results in the numerical solution. The run without the tensor transformation gives a steeper concentration distribution curve than the analytical solution. Although not tried, the use of a larger value for D_L should move the curve for Run T-2 nearer the analytical solution.

Although the error created by disregarding the tensor transformation is discernible, this is the maximum error that will occur. As the coordinate axes are rotated from the present 45° to either 0° or 90°, the two solutions given by Run T-1 and Run T-2 will gradually approach each other. Thus, in many practical problems, the error in determining the dispersion coefficient will probably result in greater errors than that created by neglecting the tensor transformation. However, the tensor transformation required very little more computer time, and did result in a more accurate solution.

Figure 5-10 shows the lateral concentration distribution for Runs T-1 and T-2 after injecting 0.46 pore volumes of fluid. The data along $x_2/\ell_2 = 0.5$ correspond to those shown in Fig. 5-9 for $V_3t/\ell_3 = 0.46$. Again, the numerical result using the tensor transformation are more accurate than those without the transformation. As was surmised earlier, approximating the straight boundary of the column with a square grid (see Fig. 5-8) has resulted in a larger error along the boundary. The numerical results for any value of x_3/ℓ_3 were generally the same to three decimal places for $0.3 \leq x_2/\ell_2 \leq 0.7$.

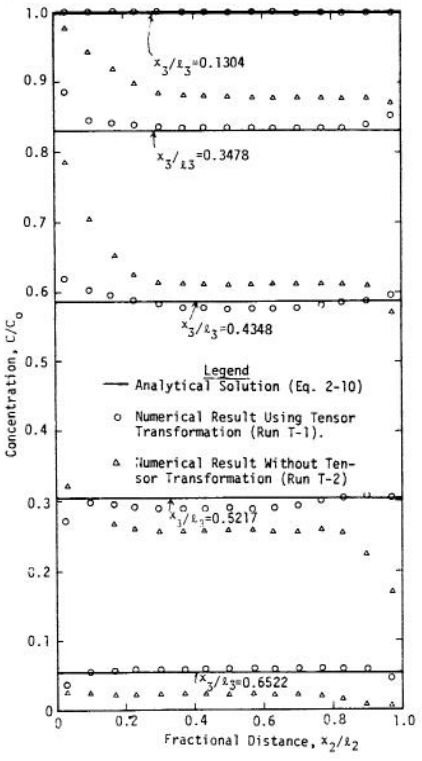

Fig. 5-10 Comparison of lateral concentration distribution calculated with and without tensor transformation for Runs T-1 and T-2 after 0.46 pore volumes have been injected.

The no-flow boundary condition in Run T-1 was approximated numerically by setting the dispersion coefficients equal to zero for all grids along the boundary. Another way to treat the no-flow boundary is to use a reflective boundary condition. Run T-3 was made with a reflective boundary condition along $x_2/\ell_2 = 0$ and a boundary condition with the dispersion coefficients equal to zero along $x_2/\ell_2 = 1.0$. As can be seen in Fig. 5-11, the use of the reflective boundary condition apparently reduces the amount of error. The reflective boundary condition improves the results because the finite difference equation for the cross derivative $\partial^2 C/\partial x_3 \partial x_2$ involves using a "nine-star" grid pattern (see Fig. D-1, Appendix D) instead of the usual "five-star" grid pattern. This means that the derivative of concentration in the boundary grid has an influence further into the media. This influence is more adequately accounted for by the reflective boundary condition.

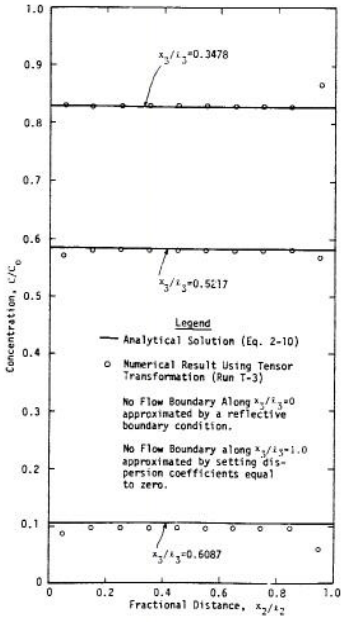

Fig. 5-11 Comparison of lateral concentration distribution for Run T-3 after 0.46 pore volumes have been injected.

Longitudinal and Lateral Dispersion. With the set up shown in Fig. 5-8, the longitudinal and lateral dispersion problem discussed in Section 5.2 was solved in the rotated coordinate system using the tensor transformation relationships. In these runs, fluid with a concentration of $C/C_o = 1.0$ was injected over the interval $0 \leq x_2 \leq b$, and fluid with a concentration of $C/C_o = 0.0$ was injected over the interval $b \leq x_2 \leq \ell_2$. Runs T-4, T-5, T-6, T-7, and T-8 were made to study the effects of the tensor transformation when both longitudinal and lateral dispersion take place. The data for these runs are given in Table V-1.

The first run in this series (Run T-4) was made with $\Delta x_3'$ and $\Delta x_2'$ equal to 0.4 cm. The results from this run yielded more error than was tolerable. An example of this error is shown in Fig. 5-12 after 2.3 pore volumes had been injected. This was assumed to be approximately at steady state. Since the results of Run T-4 are smooth and display no anomalies, the error was presumed to be the result of using large spatial dimensions in the region of the steep concentration profile along $x_2 = b$.

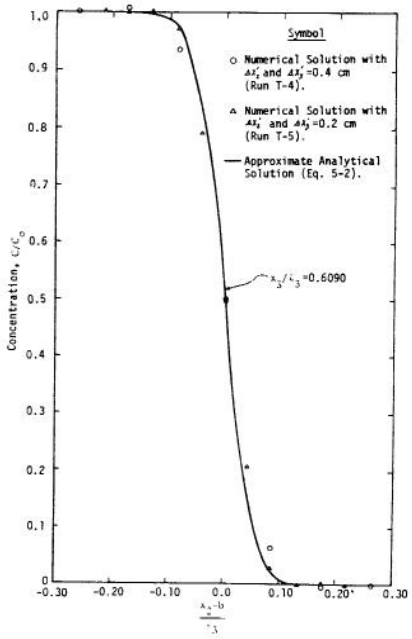

Fig. 5-12 Comparison of lateral concentration distribution for Runs T-4 and T-5 at steady state.

To check this hypothesis, Run T-5 was made using x_3' and x_2' equal to 0.2 cm. The results were much better as shown in Fig. 5-12, but are still not accurate enough. The spatial dimensions could have been decreased more, and a more accurate solution would probably have been obtained. However, Run T-5 required the use of a 38 x 38 grid system or a 40 x 40 grid system when the boundary grids are included. This is 1600 grids and 3200 moving points. The computer program for this problem required about 25,200 words of computer storage. This was near the available computer storage, and decreasing the spatial dimensions further was not attempted.

Since the very sharp concentration front along $x_2 = b$ appears to be causing the problem, then increasing the width of the dispersed zone might help. With this in mind, Run T-6 was made with $D_T = 0.003$ cm^2/sec instead of $D_T = 0.001$ cm^2/sec. The results of this run are shown in Fig. 5-13, and they are much improved. Except for the area near the inflow boundary $(x_3/\ell_3 < 0.3)$ where the analytical solution is not good, the results compare favorably with the approximate analytical solution given by Eq. 5-2.

Run T-7 was then made using the same data as Run T-6, except the tensor transformation equations

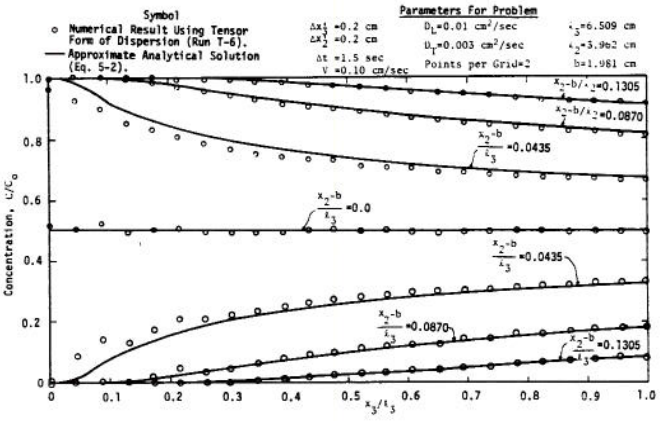

Fig. 5-13 Comparison of longitudinal concentration distribution at steady state as calculated numerically using the proposed tensor transformation and by an approximate analytical solution.

were not used. These results are shown in Fig. 5-14, and do not match the analytical solution. Figs. 5-15, 5-16, and 5-17 give a comparison of the lateral concentration distributions for Runs T-6 and T-7 at various values of x_3/ℓ_3. Run T-7, using no tensor transformation, shows a flatter concentration distribution than the analytical solution.

Figures 5-15, 5-16, and 5-17 do not show any "overshoot" or "undershoot". However, "overshoot" and "undershoot" did occur; but was generally restricted to the third or fourth decimal place. This small significance resulted in no noticeable "overshoot" in the graphical presentation. The use of the "nine-star" grid pattern to estimate the cross-derivative $\partial^2 C/\partial x_2 \partial x_3$ is believed to be the source of this small amount of "overshoot". However, the magnitude of the "overshoot" (10^{-3} to 10^{-4}) is much smaller than the overall error (10^{-2}), and is not considered to be a major detriment to the numerical scheme.

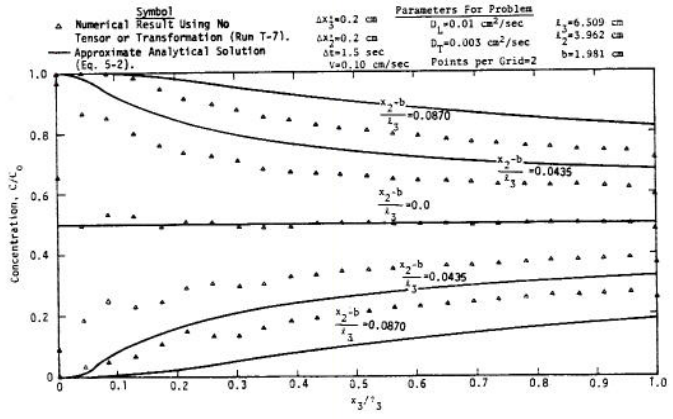

Fig. 5-14 Comparison of longitudinal concentration distribution at steady state as calculated numerically using no tensor transformation and by an approximate analytical solution.

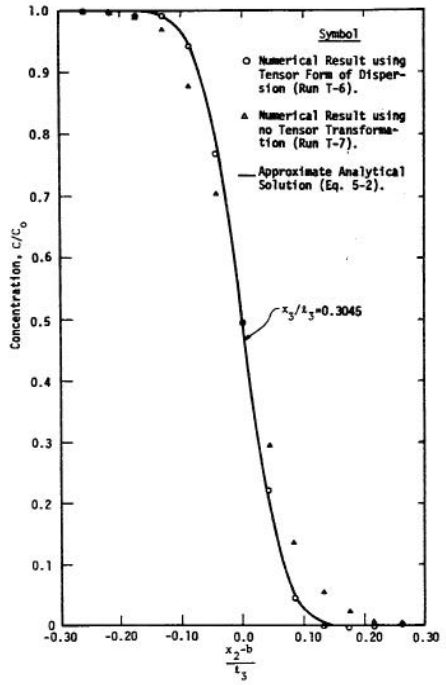

Fig. 5-15 Comparison of numerical solutions with and without the tensor form of dispersion for steady state concentration at $x_3/\ell_3 = 0.3045$.

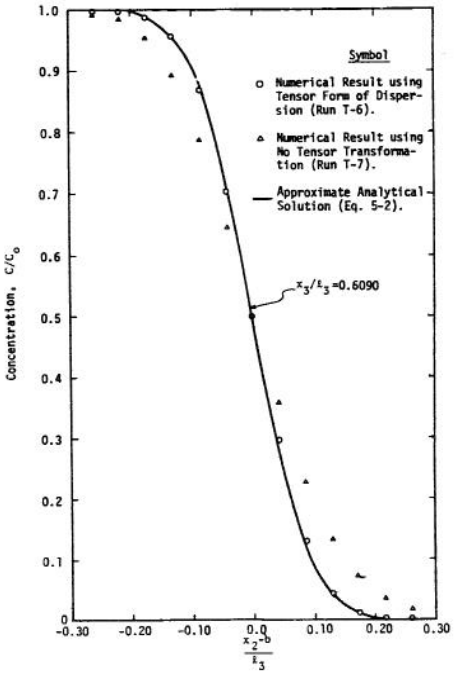

Fig. 5-16 Comparison of numerical solutions with and without the tensor form of dispersion for steady state concentration at $x_3/\ell_3 = 0.6090$.

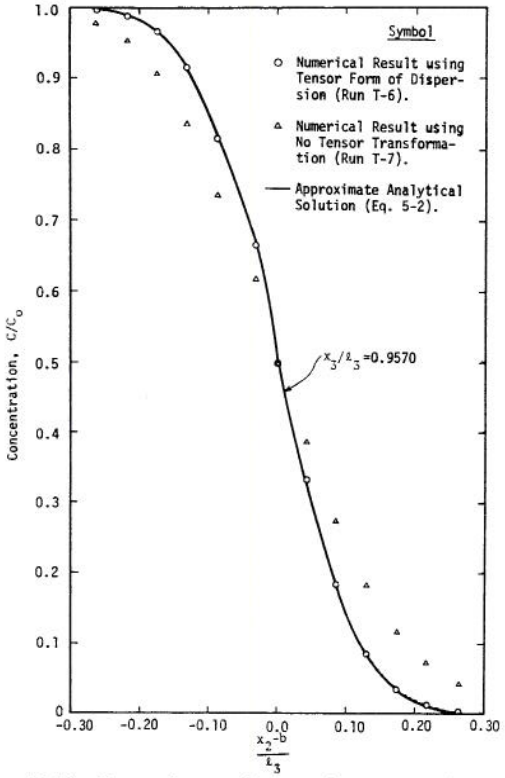

Fig. 5-17 Comparison of numerical solutions with and without the tensor form of dispersion for steady state concentration at $x_3/\ell_3 = 0.9570$.

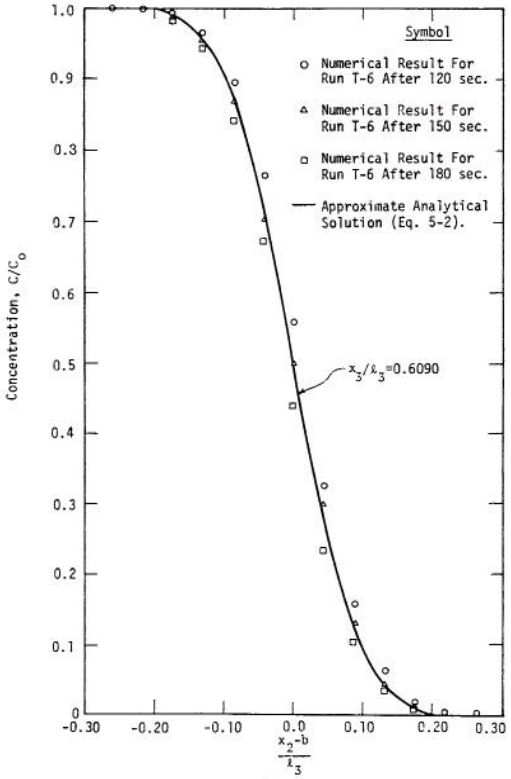

Fig. 5-18 Numerical results for Run T-6 at different time levels.

A more serious obstacle to the success of the numerical scheme appears to be the moving points. In Section 5.1, a lag in the concentration profile for longitudinal dispersion was noticed when the same points remained inside a grid throughout a time step. This resulted in a "jerky" movement of the concentration front as was shown in Fig. 5-4 for the case of one point per grid. In other words, the accuracy of the numerical scheme appears to be dependent upon the time increment selected for a given grid size.

The problem with the "jerky" frontal movement was also noticeable in the two-dimensional dispersion problem where two points per grid were used. The results for Run T-6 shown in Figs. 5-13, 5-15, 5-16, and 5-17 are after injecting for 150 seconds and are quite good. However, Fig. 5-18 shows the results for Run T-6 at 120 seconds and at 180 seconds. These results are obviously not as good as those for 150 seconds. Thus, the accuracy of the numerical solution apparently depends on which time level is chosen to print out the results. The results for Run T-4, in which four points per grid were used, did not show this apparent accuracy dependence on time. As is seen in Fig. 5-19, the results of Run T-4 are approximately the same for t = 120 seconds, t = 150 seconds, and t = 180 seconds.

A conclusion which might be deduced from the above observations is that the number of points per grid does have an effect on the accuracy of the results. However, the use of hand calculations to move the points from location to location indicated that the relative position of the moving points in a particular grid at a given time level influences the results more than the number of points. Figures 5-20a, b, and c illustrate an example of this hypothesis.

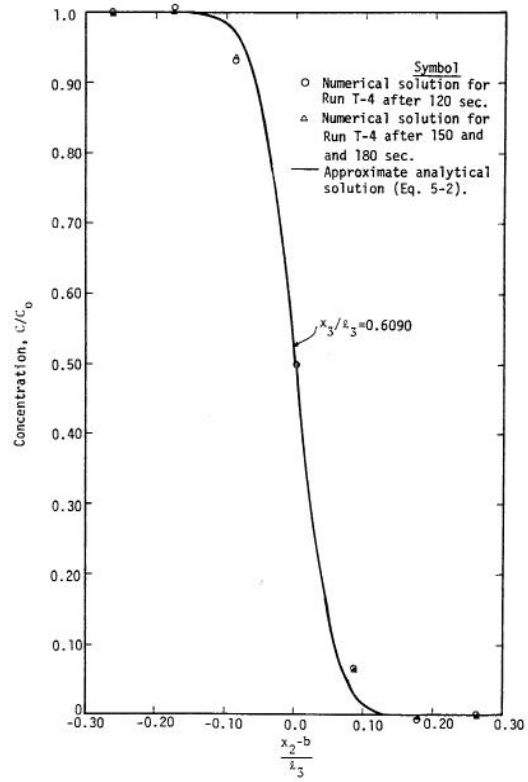

Fig. 5-19 Numerical results for Run T-4 at different time levels.

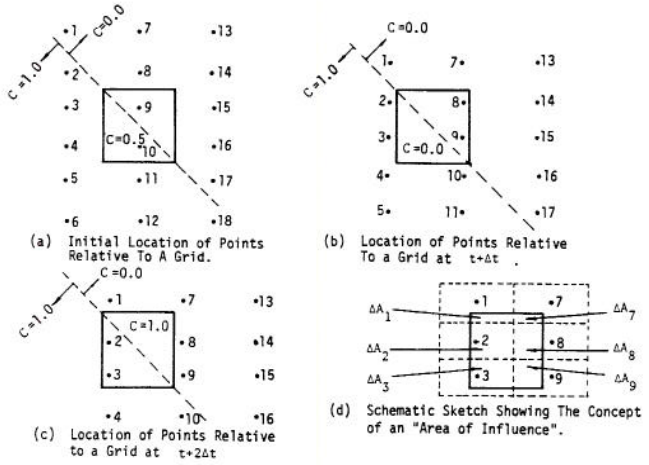

(a) Initial Location of Points Relative To A Grid.

(b) Location of Points Relative To a Grid at $t+\Delta t$.

(c) Location of Points Relative to a Grid at $t+2\Delta t$

(d) Schematic Sketch Showing The Concept of an "Area of Influence".

Fig. 5-20 Schematic sketch showing the effect of the moving point location on calculating average concentration.

In Fig. 5-20a, two points are centrally located in the grid, and points in the adjacent grids are located as shown. All points above the diagonal are assigned a concentration of zero, and all points below the diagonal are assigned a concentration of one. No dispersion is allowed to take place. Under this setup, the average concentration assigned to the grid would be $(1.0 + 0.0)/2 = 0.5$.

Now suppose that the velocity vector is oriented parallel to the diagonal, and that the magnitude of the velocity and time increment are such that at the next time step the points are located in the grid as shown in Fig. 5-20b. Even though two points are still in the grid they are positioned along the right side of the grid and both are above the diagonal. For this case, the average concentration assigned to the grid is $(0.0 + 0.0)/2 = 0.0$. Thus, by going from one time step to the next, the concentration has changed from 0.5 to 0.0.

To carry the case to an even further extreme, suppose the magnitude of the velocity and time increment are such that at the next time step the points are located as shown in Fig. 5-20c. The two points in this instance are located very close to the left side of the grid and are below the diagonal. Thus, the average grid concentration is $(1.0 + 1.0)/2 = 1.0$.

Three completely different answers were obtained at three different time levels depending on how the points were positioned in the grid. Obviously all three answers cannot be right. The correct answer is, of course, 0.5 which was given by the point locations in Fig. 5-20a. The phenomenon depicted in Figs. 5-20a, b, and c is exactly the phenomenon encountered in Run T-6 in which distorted values were obtained at certain time levels and accurate results were given at other time levels.

The phenomenon discussed above could be reduced to a tolerable level by increasing the number of moving points per grid. This is indicated by the fact that Run T-4 with four points per grid did not show an accuracy dependence on time. However, perhaps the key to the problem is not increasing the number of points, but determining the average concentration by another method. A proper weighted averaging scheme will help things considerably.

Run T-8 was made with all data exactly like Run T-6 except that area was used as a weighting factor. The average concentration was calculated by

$$C = \frac{1}{\Delta x_2' \Delta x_3'} \sum_{i=1}^{n} C_i \Delta A_i \quad , \qquad (5\text{-}3)$$

where C is the average concentration, $\Delta x_2'$ and $\Delta x_3'$ are the spatial dimensions of the grid, C_i is the concentration of the ith moving point, ΔA_i is the "area of influence" of the ith moving point, and $\sum_{i=1}^{n} \Delta A_i = \Delta x_2' \Delta x_3'$. The concept of an "area of influence" is schematically shown in Fig. 5-20d. Using such a concept, points 1, 7, 8, and 9 will have some influence on the average grid concentration while the influence of points 1 and 2 has been diminished. The results for Run T-8 using the weighted average are shown in Fig. 5-21 after 120 seconds, 150 seconds, and 180 seconds. These results are much improved over those of Run T-6 shown in Fig. 5-18.

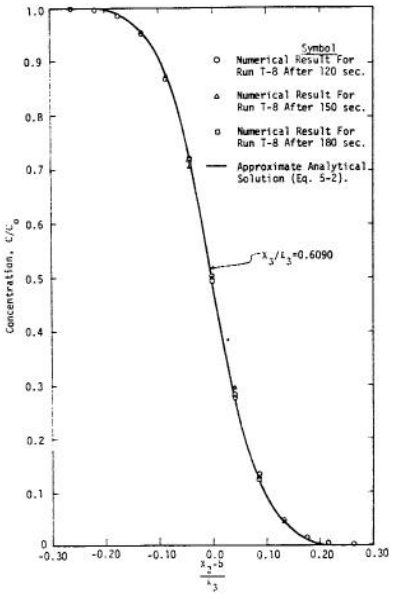

Fig. 5-21 Numerical results for Run T-8 at different time levels.

The conclusion that must be reached here is that the method of calculating the average grid concentration is an important factor in the numerical scheme. If some type of weighted average is not used, then a sufficient number of moving points must be used to guarantee a reasonable estimate of the average. Although Garder et al. (1964) concluded that two points per grid gave sufficient accuracy, the results obtained in this study indicate the number of points per grid may need to be greater than two. The exact number needed is unknown, and would appear to be

dependent on the nature of the problem being considered.

If an adequate scheme for weighting the concentration can be developed, then a smaller number of points per grid may be used. Using an "area of influence" as a weighting function gave good results for the problem considered here where a uniform, steady velocity field was used. The numerical problems encountered in determining an "area of influence" for each point in a nonuniform, unsteady flow field appear to be numerous. Other weighting schemes, besides area, which could easily be calculated for the nonuniform, unsteady case might prove to be adequate. This problem is left to future thought and research.

5.4 Dispersion Along Equilibrium Salt-Water Wedge. In Sections 5.1, 5.2, and 5.3, the numerical simulation of the dispersion equation and the tensor transformation of the dispersion coefficient was compared with known analytical solutions. However, the total simulator using both the dispersion equation and the flow equation have not been used. A problem which seems favorable to this type of analysis is the salt-water intrusion problem. Rumer and Harleman (1963) used a laboratory model of a two-dimensional confined aquifer to investigate convection and dispersion along a salt-water wedge. Columbus (1965) used a Hele-Shaw model to investigate sea-water intrusion in an unconfined model neglecting dispersion. Because Rumer and Harleman's (1963) data contained information on the value of the dispersion coefficients, a computer run was made using the data from one of their laboratory runs.

The equilibrium salt-water wedge, when subjected to the steady flow of fresh water to the ocean, will develop a transition zone. Using Darcy's law and the Dupuit-Forchheimer approximation, the specific discharge of fresh water per unit width of ocean front, $\tilde{q}$, can be written as

$$\tilde{q} = Ky \frac{dh^*}{dx_1} \quad , \tag{5-4}$$

in which K = hydraulic conductivity, y is the distance between the top of the aquifer and the wedge interface, and h^* is the piezometric head (Fig. 5-22). The medium is assumed to be homogeneous, isotropic, and no mixing occurs at the interface.

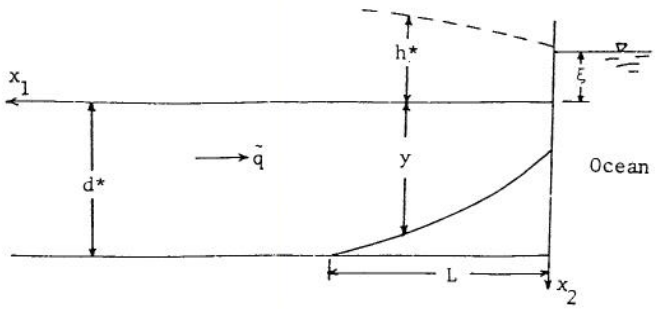

Fig. 5-22 Equilibrium wedge in a confined aquifer.

The condition of equal pressures in the salt-water and the fresh water at each point along the interface yields

$$y = \frac{\rho_f}{\Delta\rho} h^* - \frac{\rho_s}{\Delta\rho} \xi \quad , \tag{5-5}$$

where ρ_f and ρ_s are the densities of fresh and salt-water, respectively, and $\Delta\rho = \rho_s - \rho_f$. Substituting Eq. 5-5 into Eq. 5-4 gives

$$(h^* - \frac{\rho_s}{\rho_f} \xi) dh^* = \frac{\tilde{q} \frac{\Delta\rho}{\rho_f}}{K} dx_1 \quad . \tag{5-6}$$

Integrating and solving for h^* ,

$$h^* = \sqrt{\frac{2\tilde{q} \frac{\Delta\rho}{\rho_f}}{K} x_1 + B} + \frac{\rho_s}{\rho_f} \xi \quad . \tag{5-7}$$

The constant of integration, B , can be obtained by using the value of h^* at $x_1=0$. Henry (1959) showed that the outcrop opening (y at $x_1=0$) was given by,

$$y_{(x_1=0)} = \frac{0.741\ \tilde{q}}{K\ \Delta\rho/\rho_f} \quad . \tag{5-8}$$

Substituting Eq. 5-8 into Eq. 5-5 gives

$$h^*_{(x_1=0)} = \frac{0.741\ \tilde{q}}{K} + \frac{\rho_s}{\rho_f} \xi \quad . \tag{5-9}$$

Using Eq. 5-9 in Eq. 5-7, gives $B = (0.741\tilde{q}/K)^2$. Thus, the piezometric head is given by,

$$h^* = \sqrt{\frac{2\tilde{q} \frac{\Delta\rho}{\rho_f}}{K} x_1 + \left(\frac{0.741\ \tilde{q}}{K}\right)^2} + \frac{\rho_s}{\rho_f} \xi \quad . \tag{5-10}$$

Substituting Eq. 5-10 in Eq. 5-5, gives the equation for the interface,

$$y = \sqrt{\frac{2\tilde{q}}{K \frac{\Delta\rho}{\rho_f}} x_1 + \left(\frac{0.741\tilde{q}}{K \frac{\Delta\rho}{\rho_f}}\right)^2} \quad . \tag{5-11}$$

Although the static interface between fresh and salt water will be subjected to dispersion, Rumer and Harleman (1963) showed that the position of the mean isoclor ($C = 0.5$) is adequately predicted by Eq. 5-11.

Rumer and Harleman (1963) gave the following information for their Run No. N-2: $\tilde{q}=0.0733$ cm^2/sec,

$\Delta\rho/\rho_f = 0.006$, K = 0.835 cm/sec, porous medium = plastic spheres, and median grain diameter = 0.965 mm. A computer run was made using Rumer and Harleman's information, plus some additional data required by the numerical simulator. The data used in the computer run are: $\Delta x_1 = 6.0$ cm, $\Delta x_2 = 6.0$ cm, $\Delta t =$ 500 sec, $k = 9.885 \times 10^{-6}$ cm^2, $\phi = 0.39$, $\rho_f = 1.000$, $\rho_s = 1.006$, $\Delta\rho = 0.006$, $\mu = .0116$ poise, fluid compressibility = 0.0, rock compressibility = 0.0, $\lambda = 0.0$, $\alpha = 0.006$, grid dimensions = 12 x 27, depth of aquifer = 60 cm, length of aquifer = 156 cm, $\xi = 33$ cm, $\tilde{q} = 0.0736$ cm^2/sec, moving points per grid = 2, and the acceleration of gravity = 980 cm/sec^2. In addition to these data, the dispersion coefficients were assumed to be given by

$$\frac{D_L\rho}{\mu} = 0.66\left(\frac{V\, d_{50}\rho}{\mu}\right)^{1.2} \qquad (5\text{-}12)$$

and

$$\frac{D_T\rho}{\mu} = 0.036\left(\frac{V\, d_{50}\rho}{\mu}\right)^{0.7} . \qquad (5\text{-}13)$$

The reason for using Eqs. 5-12 and 5-13 is that Harleman and Rumer (1963) determined these relationships for the same medium (plastic spheres) used by Rumer and Harleman (1963) in their study of sea-water intrusion.

The computer run was made for 60 time steps or about 8.33 hours. Whether this was long enough for the wedge to reach equilibrium is unknown. The concentrations were not changing very rapidly, and the toe of the wedge was moving very slowly. Therefore, the wedge was assumed to be in equilibrium. The computer time required for solving both the flow equation and dispersion equation for this 12 x 27 grid network was about 3.4 sec per time step.

Fluid enters the model at $x_1 = 156$ cm and leaves the model at $x_1 = 0$. No fluid flows across $x_2 = 0$ and $x_2 = 60$ cm. Thus, the boundary conditions are given by

$$\frac{\partial P}{\partial x_2} + \rho g \frac{\partial h}{\partial x_2} = 0 \quad \text{at} \quad x_2 = 0 \quad \text{and} \quad x_2 = 60 \text{ cm}, \qquad (5\text{-}14)$$

$$P(0,x_2) = P(0,0) - \rho_s g[h(0,x_2) - h(0,0)] \quad \text{at} \quad x_1 = 0 , \qquad (5\text{-}15)$$

and

$$P(156,x_2) = P(156,0) - \rho_f g[h(0,x_2) - h(0,0)] \quad \text{at} \quad x_1 = 156 \text{ cm} \qquad (5\text{-}16)$$

$P(0,0)$ is assumed to arbitrary and was taken to be 29,576.40 cynes/cm^2 for this run. $P(156,0)$ was maintained at the necessary level to cause a fresh-water flow of $\tilde{q} = 0.0733$ cm^2/sec.

The boundary conditions given by Eqs. 5-14 and 5-16 are believed to be adequate. However, the boundary condition given by Eq. 5-15 is subject to some suspicion. The actual physical boundary condition where the fresh water discharges into the ocean is very difficult to describe numerically. The computer run indicated that some recirculation of fluid took place along this boundary. If the simulator should be used to study the salt-water intrusion problem in detail, additional work on describing this boundary condition will be necessary.

A comparison of the fresh-water head calculated numerically and by Eq. 5-10 is shown in Fig. 5-23. The comparison shows that the numerical results and those by Eq. 5-10 are very close except for the region close to the ocean front. This would be the region affected most by the use of the Dupuit-Forchheimer assumptions. Also this region is probably affected by the boundary condition given in Eq. 5-15.

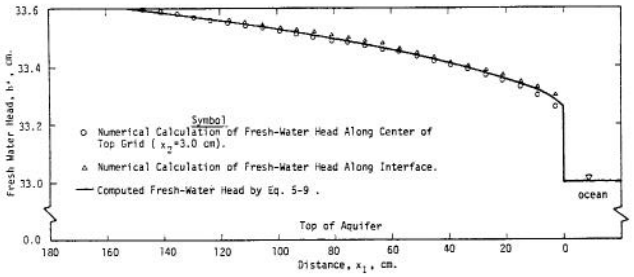

Fig. 5-23 Comparison of fresh-water head calculated numerically and by Eq. 5-9 for the salt-water intrusion problem.

Figure 5-24 shows a comparison of the mean concentration line $(C/C_o=0.50)$ calculated numerically and the interface location obtained from Eq. 5-11. These results are good except in the vicinity of the wedge toe. Several factors may be contributing to this error. First, the numerical results may not be completely at a steady state. However, the 60 time steps computed required 205 seconds of computer time. The concentration changes taking place were slow enough so that large amounts of computer time would be required to carry the solution to a real steady state. The present grant for computer usage would not allow such large amounts of computer time. Thus, runs of longer duration were not made.

Another factor which proved a limitation on this problem can be seen in Fig. 5-25. The concentration profiles are extremely steep. In fact, the profile is so steep that the grid concentrations obtained from the computer were generally either $C/C_o=1.0$ or $C/C_o=0.0$. Very few grids had a value for C/C_o between these two extremes. Thus, a large amount of interpolation was required to determine the line $C/C_o=0.5$. To alleviate this problem, smaller spatial dimensions are needed which will require more computer storage. This will necessitate making changes in the program for more extensive use of auxiliary storage (i.e., tape).

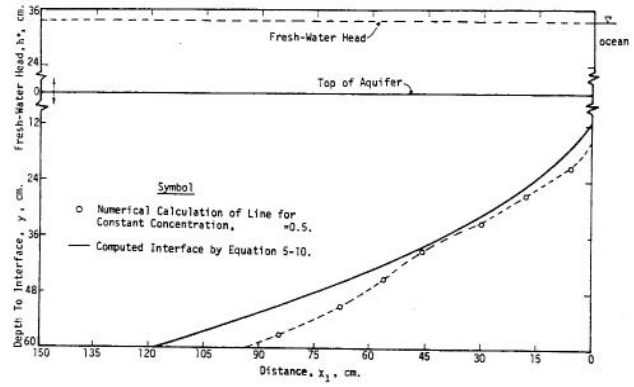

Fig. 5-24 Comparison of interface location calculated numerically and by Eq. 5-10.

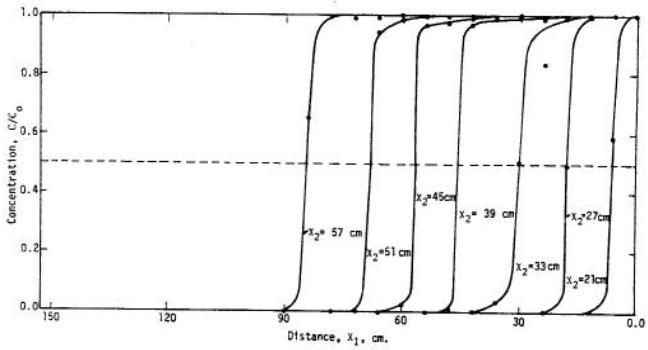

Fig. 5-25 Numerical results showing the concentration distribution across the transition zone for various values of x_2 .

Another problem is that of having the moving points heavily weighted to one side of the grid. This problem was discussed in Section 5.3, and the use of a weighted average using the "area of influence" as a weighting factor proved successful. However, the unsteady, nonuniform flow field encountered in the salt-water wedge makes the determination of an "area of influence" difficult. Using more moving points per grid than the two used in this run would probably help this problem.

The computer program indicates that a small amount of salt-water flow (approximately 0.008 cm /sec) occurred in the salt-water wedge. This would have the effect of moving the wedge toe toward the ocean; although not by enough to account for all the discrepancy shown in Fig. 5-24.

Another factor which might have effected the location of the interface is the boundary condition given by Eq. 5-15 to approximate the ocean front. The computer results indicated that some recirculation of fluid was occurring along the two grids adjacent to the ocean.

To investigate all of the above effects on the numerical solution would require additional computer funding. Such funds are not presently available. This should be made the object of some future research proposal.

Chapter VI

SUMMARY AND CONCLUSIONS

A three-dimensional fundamental flow equation for a mixture of miscible fluids flowing through a groundwater aquifer was derived. Also, a three-dimensional convective-dispersion equation describing the movement of a tracer miscible with the groundwater was derived. Finite difference forms of these two equations were developed, but because of insufficient computer funds the three-dimensional equations were never used.

A computer program using the two-dimensional finite difference equations was developed and tested with success on problems with known analytical solutions. Assuming an isotropic medium, a tensor transformation for the dispersion process was tested extensively. Because the numerical simulation of the tensor transformation involves the cross-derivatives of concentration, new stability criterion were developed for the explicit finite difference scheme used to solve for dispersion.

6.1 Evaluation of Numerical Simulator. The results of this work will allow the study of numerous miscible displacement problems in complex groundwater flow fields. The numerical simulator can be used for steady or unsteady flow, homogeneous or nonhomogeneous aquifers, isotropic or anisotropic media, constant densities or varying densities, and constant viscosities or varying viscosities. The use of the proposed simulator has resulted in the following:

a. The one-dimensional flow problem with longitudinal dispersion can be handled without any difficulty, and excellent results were obtained. No "overshoot" or numerical smearing was noticeable.

b. The one-dimensional flow problem with both longitudinal and lateral dispersion can be handled satisfactorily. No "overshoot" or numerical smearing were observed. Small spatial dimensions are required along a sharp concentration front to adequately describe the front.

c. Working with a rotated coordinate system, the proposed numerical simulation for the tensor transformation of the dispersion process was successful. The use of the "nine-star" finite-difference pattern to describe $\partial^2 C/\partial X_1 \partial X_2$ was sufficient except along no-flow boundaries. The use of a reflective boundary condition instead of setting the dispersion coefficient equal to zero helped alleviate this problem.

d. Garder et al. (1964) concluded that the method of characteristics numerical scheme for dispersion would give good answers for as few as two points per grid. The results of this work indicate that the points per grid may need to be greater than two. The exact number needed is unknown, and would appear to be dependent on the nature of the problem being considered.

e. The method of calculating the average grid concentration proved to be an important factor in the numerical scheme. If an arithmetic average of the points located in a grid at a particular time level is used, then more points than two per grid may be necessary to obtain an adequate average. A weighted average using the "area of influence" for each point was proposed and proven effective for a steady, uniform flow field. Calculation of an "area of influence" is difficult for an unsteady, nonuniform flow field.

f. The numerical simulator was used to solve the salt-water intrusion problem. The numerical results for the fresh water head in the aquifer matched closely those obtained analytically. The numerical results for the location of the fresh-salt interface were good except in the region of the wedge toe. Insufficient funds prevented exploring the effects of smaller spatial dimensions and a larger number of grids.

The efficiency of the numerical scheme would seem to make it useful as a practical tool. However, large amounts of computer time will be required because the numerical solution must be carried out from the initial condition to the required time by increments of Δt. Most practical problems will also require the use of large amounts of computer storage. Thus, the present program will need to be modified so that more extensive use of external computer storage can be made.

6.2 Suggestions for Future Work. Subjects not covered, or not covered adequately, in this study are:

a. The investigation of a weighting technique, other than the "area of influence," which could be used to determine the average grid concentration for an unsteady, nonuniform flow field.

b. A method whereby the pressure equation is solved for larger spatial and temporal increments than the dispersion equation.

c. The effect of smaller spatial increments, more points per grid, and different boundary conditions on the salt-water intrusion problem.

d. A study of dispersion in layered and nonhomogeneous porous media.

e. A study of dispersion in anisotropic media. Some method of determining the principle axes of the dispersion tensor would be required. After this is determined, the solution would be much the same as that already presented.

f. The simulator should be used to solve an actual field problem.

6.3 Observations. The results of this work would indicate that hydrodynamic dispersion in a homogeneous and isotropic media is a valid and reproducible phenomenon. However, the actual significance of the dispersion process may be questioned because of the smallness of the dispersed zone when compared to the overall model dimensions. The conclusion that dispersion is not worth worrying about except for the most noxious pollutants and radioisotopes would seem to be warranted.

However, field tests at Berkeley by Lau, et al. (1957, 1958) showed that the dispersion constants resulting from a pumping test were from 20 to 30 meters compared to less than 1 mm in the laboratory. This is a change of 3 orders of magnitude. Other field work in transport phenomena indicates that the dispersed zone is significant in real aquifers. An obvious conclusion is that mixing processes not involved in laboratory models and homogeneous and isotropic media are present in aquifers. This extra mixing process would appear to be the result of nonhomogeneous and anisotropic media which characterize real aquifers.

The reason for the above observations are that the results of this study show a significant, but not overwhelming, difference between solutions with and without the tensor transformation. Many people may easily conclude that using the tensor transformation is not worth the effort. If the real aquifer magnifies the error between solutions with and without the tensor transformation as much as it does the dispersed zone, then a significant error may occur in the solution of field problems.

This work is a first step in developing a numerical solution for miscible displacement which makes use of the tensorial nature of the dispersion process. Until work in real aquifers indicates otherwise, the numerical simulator should maintain the capability of treating the dispersion process as a tensor. The work on this project needs to continue with a study of the dispersion process in a nonhomogeneous aquifer.

REFERENCES

Adam, J. R., 1966, Dispersion in anisotropic porous media. Ph.D. Dissertation, Department of Civil Engineering, Michigan State University, East Lansing, Michigan, 88 p.

Ananthakrishnan, V., W. N. Gill, and A. J. Barduhn, 1965, Laminar dispersion in capillaries: part 1, mathematical analysis. American Institute of Chemical Engineers Journal, Vol. 11, pp. 1063-1072.

Aris, R., 1956, On the dispersion of a solute in a fluid flowing through a tube. Proceedings, Royal Society of London, Series A, Vol. 235, pp. 67-77.

Bachmat, Y., 1967, On the similitude of dispersion phenomena in homogeneous and isotropic porous mediums. Water Resources Research, Vol. 3, No. 4, 4th quarter 1967, pp. 1079-1083.

Bachmat, Y. and Jacob Bear, 1964, The general equations of hydrodynamic dispersion in homogeneous, isotropic porous mediums. Journal of Geophysical Research, Vol. 69, No. 12, June 15, 1964, pp. 2561-2567.

Banks, R. B. and I. Ali, 1964, Dispersion and adsorption in porous media flow. Proceedings, American Society of Civil Engineers (Hydraulics Division), Vol. 90, HY5, Paper No. 4022, September 1964, pp. 13-31.

Banks, R. B. and S. Jerasate, 1962, Dispersion in unsteady porous media flow. Proceedings, American Society of Civil Engineers (Hydraulics Division), Vol. 88, HY3, Paper No. 3109, May 1962, pp. 1-21.

Bear, Jacob, 1961a, On the tensor form of dispersion in porous media. Journal of Geophysical Research, Vol. 66, No. 4, April 1961, pp. 1185-1198.

Bear, Jacob, 1961b, Some experiments in dispersion. Journal of Geophysical Research, Vol. 66, No. 8, August 1961, pp. 2455-2467.

Bear, Jacob and Y. Bachmat, 1967, A generalized theory on hydrodynamic dispersion in porous media. International Association of Scientific Hydrology, Publication No. 72, Symposium of Hafia, Marcn 1967, pp. 7-16.

Bear, Jacob and D. K. Todd, 1960, The transition zone between fresh and salt waters in coastal aquifers. Contribution No. 29, Water Resources Center, University of California at Berkeley, September 1960, 156 p.

Bear, Jacob, D. Zaslavsky, and S. Irmay, 1968, Physical principles of water percolation and seepage. United Nations Educational, Scientific and Cultural Organization, Vol. XXIX in the Series on Arid Zone Research, New York, 1968, 465 p.

Beran, M. J., 1955, Dispersion of soluble matter in slowly moving fluids. Ph.D. Dissertation, Division of Applied Science, Harvard University, Cambridge, Massachusetts, 1955, 92 p.

Biggar, J. W. and D. R. Nielsen, 1960, Diffusion effects in miscible displacement occurring in saturated and unsaturated porous materials. Journal of Geophysical Research, Vol. 65, No. 9, September 1960, pp. 2887-2895.

Bird, R. B., W. E. Stewart and E. N. Lightfoot, 1960, Transport phenomena. John Wiley and Sons, Inc., New York, 1960, 780 p.

Bittinger, M. W., H. R. Duke, and R. A. Longenbaugh, 1967, Mathematical simulations for better aquifer management. International Association of Scientific Hydrology, Publication No. 72, Symposium of Haifa, March 1967, pp. 509-519.

Bjordammen, J. and K. H. Coats, 1967, Comparison of alternating direction and successive over-relaxation techniques in simulation of two- and three-dimensional, two-phase flow in reservoirs. Society of Petroleum Engineers of AIME, Preprint No. SPE 1880, Houston Meeting, October 1-4, 1967.

Blackwell, R. J., 1962, Laboratory studies of microscopic dispersion phenomena. Society of Petroleum Engineers Journal, Vol. 2, No. 1, March 1962, pp. 1-8.

Blair, P. M. and D. W. Peaceman, 1963, An experimental verification of a two-dimensional technique for computing performance of gas-drive reservoirs. Society of Petroleum Engineers Journal, Vol. 3, No. 1, March 1963, pp. 19-27.

Breitenbach, E. A., D. H. Thurnau, and H. K. van Poollen, 1968a, Immiscible fluid flow simulator. Society of Petroleum Engineers of AIME, Preprint No. SPE 2019, Dallas Meeting, April 22-23, 1968.

Breitenbach, E. A., D. H. Thurnau and H. K. van Poollen, 1968b, The fluid flow simulation equations. Society of Petroleum Engineers of AIME. Preprint SPE 2020, Dallas Meeting, April 22-23, 1968.

Breitenbach, E. A., D. H. Thurnau and H. K. van Poollen, 1968c, Solution of the immiscible fluid flow simulation equations. Society of Petroleum Engineers of AIME, Preprint SPE 2021, Dallas Meeting, April 22-23, 1968.

Bruch, J. C. and R. L. Street, 1967, Two-dimensional dispersion. Proceedings, American Society of Civil Engineers (Sanitary Engineering Division), Vol. 93, SA6, Paper No. 5636, December 1967, pp. 17-39.

Cairns, E. J. and J. M. Prausnitz, 1960, Longitudinal mixing in packed beds. Chemical Engineering Science, Vol. 12, No. 1, 1960, pp. 20-34.

Carberry, J. J. and R. H. Bretton, 1958, Axial dispersion of mass in flow through fixed beds. American Institute of Chemical Engineers Journal, Vol. 4, No. 3, September 1958, pp. 367-375.

Carslaw, H. S. and J. C. Jaeger, 1959, Conduction of heat in solids. Oxford University Press, London, 2nd edition, 1959, 510 p.

Carter, R. D., 1967, Comparison of alternating direction explicit and implicit procedures in two-dimensional flow calculations--discussion. Society of Petroleum Engineers Journal, Vol. 7, No. 1, March 1967.

Chun, R. Y. D., E. M. Weber, and Kiyoshi Mido, 1964, Computers--tools for sound management of groundwater basins. International Association of Scientific Hydrology, Publication No. 64, General Assembly of Berkeley, pp. 424-437.

Coats, K. H. and B. D. Smith, 1964, Dead-end pore volume and dispersion in porous media. Society of Petroleum Engineers Journal, Vol. 4, No. 1, March 1964, pp. 73-84.

Coats, K. H. and M. H. Terhune, 1966, Comparison of alternating direction explicit and implicit procedures in two-dimensional flow calculations. Society of Petroleum Engineers Journal, Vol. 6, No. 4, December 1966, pp. 350-362.

Columbus, Nathan, 1965, Viscous model study of sea water intrusion in water table aquifers. Water Resources Research, Vol. 1, No. 2, 2nd Quarter 1965, pp. 313-323.

Crank, J., 1956, The mathematics of diffusion. Oxford University Press, London, 1956, 347 p.

Dagan, G., 1967, Hydrodynamic dispersion in a nonhomogeneous porous column. Journal of Geophysical Research, Vol. 72, No. 16, August 15, 1967, pp. 4075-4080.

Danckwerts, P. V., 1953, Continuous flow systems; distribution of residence times. Chemical Engineering Science, Vol. 2, No. 1, February 1953, pp. 1-13.

Day, P. R., 1956, Dispersion of a moving salt-water boundary advancing through saturated sand. Transactions, American Geophysical Union, Vol. 37, pp. 595-601.

de Josselin de Jong, G., 1958, Longitudinal and transverse diffusion in granular deposits. Transactions, American Geophysical Union, Vol. 39, No. 1, February 1958, pp. 67-74.

de Josselin de Jong, G. and M. J. Bossen, 1961, Tensor form of dispersion in porous media--discussion. Journal of Geophysical Research, Vol. 66, No. 10, October 1961, pp. 3623-3624.

Dougherty, E. L. and H. C. Mitchell, 1964, Simulation of oil reservoirs on a digital computer. Computers in the Mineral Industries, Part 2, Stanford University, pp. 787-822.

Douglas, J., Jr., D. W. Peaceman and H. H. Rachford, Jr., 1959, A method for calculating multidimensional immiscible displacement. Transactions, AIME, Vol. 216, pp. 297-308.

Ebach, E. A. and R. R. White, 1958, Mixing of fluids flowing through beds of packed solids. American Institute of Chemical Engineers Journal, Vol. 4, No. 2, June 1958, pp. 161-169.

Esmail, O. J. and O. K. Kimbler, 1967, Investigation of the technical feasibility of storing fresh water in saline aquifers. Water Resources Research, Vol. 3, No. 3, 3rd Quarter 1967, pp. 683-695.

Fagin, R. G. and C. H. Stewart, Jr., 1966, A new approach to the two-dimensional multiphase reservoir simulator. Society of Petroleum Engineers Journal, Vol. 6, No. 2, June 1966, pp. 175-182.

Garder, A. O., D. W. Peaceman and A. L. Pozzi, Jr., 1964, Numerical calculation of multidimensional miscible displacement by the method of characteristics. Society of Petroleum Engineers Journal, Vol. 4, No. 1, March 1964, pp. 26-36.

Grane, F. E. and G. H. F. Gardner, 1961, Measurements of transverse dispersion in granular media. Journal of Chemical and Engineering Data, Vol. 6, No. 2, April 1961, pp. 283-287.

Harleman, D. R. F. and R. R. Rumer, Jr., 1963, Longitudinal and lateral dispersion in an isotropic porous medium. Journal of Fluid Mechanics, Vol. 16, Part 3, July 1963, pp. 385-394.

Harleman, D. R. F., P. F. Mehlhorn and R. R. Rumer, Jr., 1963, Dispersion-permeability correlation in porous media. Proceedings, American Society of Civil Engineers (Hydraulics Division), Vol. 89, HY2, Paper No. 3459, March 1963, pp. 67-85.

Harpaz, Y. and Jacob Bear, 1964, Investigations on mixing of waters in underground storage operations. International Association of Scientific Hydrology, Publication No. 64, General Assembly of Berkeley, pp. 132-153.

Heller, J. P., 1963, The interpretation of model experiments for the displacement of fluids through porous media. American Institute of Chemical Engineers Journal, Vol. 9, No. 4, pp. 452-459.

Henry, H. R., 1959, Salt intrusion into fresh-water aquifers. Journal of Geophysical Research, Vol. 64, No. 11, November 1959, pp. 1911-1920.

REFERENCES - Continued

Hoopes, J. A. and D. R. F. Harleman, 1965, Waste water recharge and dispersion in porous media. Technical Report No. 75, Hydrodynamics Laboratory, Massachusetts Institute of Technology, Cambridge, Massachusetts, June 1965, 166 p.

Hoopes, J. A. and D. R. F. Harleman, 1967a, Dispersion in radial flow from a recharge well. Journal of Geophysical Research, Vol. 72, No. 14, July 15, 1967, pp. 3595-3607.

Hoopes, J. A. and D. R. F. Harleman, 1967b, Wastewater recharge and dispersion in porous media. Proceedings, American Society of Civil Engineers (Hydraulics Division), Vol. 93, HY5, September 1967, pp. 51-71.

Kells, L. M., 1950, Analytic geometry and calculus. Prentice-Hall, Inc., New York, p. 78.

Lapidus, L. and N. R. Amundson, 1952, Mathematics of adsorption in beds, VI: The effect of longitudinal diffusion in ion exchange and chromatographic columns. Journal of Physical Chemistry, Vol. 56, pp. 984-988.

Larkin, B. K., 1964, Some stable explicit difference approximations to the diffusion equation. Mathematics of Computation, Vol. 18, No. 86, pp. 196-202.

Lau, L. K., W. J. Kaufman, and D. K. Todd, 1957, Studies of dispersion in a radial flow system. Progress Report No. 3, Canal Seepage Research, Sanitary Engineering Research Laboratory, University of California at Berkeley, July 1957, 44 p.

Lau, L. K., W. J. Kaufman, G. T. Orlob, and D. K. Todd, 1958, Studies of flow dispersion in porous media. Progress Report No. 4, Canal Seepage Research, Sanitary Engineering Research Laboratory, University of California at Berkeley, July 1958, 67 p.

Li, W. H. and F. H. Lai, 1966, Experiments on lateral dispersion in porous media. Proceedings, American Society of Civil Engineers (Hydraulics Division), Vol. 92, HY6, November 1966, pp. 141-149.

List, E. J. and N. H. Brooks, 1967, Lateral dispersion in saturated porous media. Journal of Geophysical Research, Vol. 72, No. 10, May 15, 1967, pp. 2531-2541.

Nelson, R. W., 1965, A sequence for predicting waste transport by ground water. Battelle-Northwest Laboratory, Report No. BNWL-63, Richland, Washington, April 15, 1965.

O'Brien, G. G., M. A. Hyman and S. Kaplan, 1951, A study of the numerical solution of partial differential equations. Journal of Mathematics and Physics, Vol. 29, pp. 223-251.

Ogata, A., 1961, Transverse diffusion in saturated isotropic granular media. Professional Paper 411-B, U.S. Geological Survey, U.S. Govt. Printing Office, Washington, D.C., 8 p.

Ogata, A., 1964a, The spread of a dye stream in an isotropic granular medium. Professional Paper 411-G, U.S. Geological Survey, U.S. Govt. Printing Office, Washington, D. C., 11 p.

Ogata, A., 1964b, Mathematics of dispersion with linear adsorption isotherm. Professional Paper 411-H, U.S. Geological Survey, U.S. Govt. Printing Office, Washington, D. C., 9 p.

Ogata, A. and R. B. Banks, 1961, A solution of the differential equation of longitudinal dispersion in porous media. Professional Paper 411-A, U.S. Geological Survey, U.S. Govt. Printing Office, Washington, D. C., 7 p.

Peaceman, D. W. and H. H. Rachford, Jr., 1962, Numerical calculation of multidimensional miscible displacement. Society of Petroleum Engineers Journal, Vol. 2, No. 4, December 1962, pp. 327-339.

Perkins, T. K. and O. C. Johnston, 1963, A review of diffusion and dispersion in porous media. Society of Petroleum Engineers Journal, Vol. 3, No. 1, March 1963, pp. 70-84.

Poreh, Michael, 1965, The dispersivity tensor in isotropic and axisymmetric mediums. Journal of Geophysical Research, Vol. 70, No. 16, August 15, 1965, pp. 3909-3913.

Quon, D., P. M. Dranchuk, S. R. Allada and P. K. Leung, 1965, A stable, explicit computationally efficient method for solving two-dimensional mathematical models of petroleum reservoirs. Journal of Canadian Petroleum Technology, Vol. 4, No. 2, p. 530.

Quon, D., P. M. Dranchuk, S. R. Allada and P. K. Leung, 1966, Application of the alternating direction explicit procedure to two-dimensional natural gas reservoirs. Society of Petroleum Engineers Journal, Vol. 6, No. 2, June 1966, pp. 137-142.

Raats, P. A. C. and D. R. Scotter, 1968, Dynamically similar motion of two miscible constituents in porous mediums. Water Resources Research, Vol. 4, No. 3, June 1968, pp. 561-568.

Raimondi, P., G. H. F. Gardner, and C. B. Petrick, 1959, Effect of pore structure and molecular diffusion on the mixing of miscible liquids flowing in porous media. American Institute of Chemical Engineers-Society of Petroleum Engineers, Joint Symposium, Part II, Preprint 43, San Francisco, December 6-9, 1959.

REFERENCES - Continued

Richtmeyer, R. D., 1957, Difference methods for initial value problems. Interscience Publishers, Inc., New York, 1st edition, 189 p.

Rifai, M. N. E., W. J. Kaufman and D. K. Todd, 1956, Dispersion phenomena in laminar flow through porous media. Report No. 3, I.E.R. Series 90, Sanitary Engineering Research Laboratory, Univeristy of California at Berkeley, July 1956, 157 p.

Rumer, R. R., 1962, Longitudinal dispersion in steady and unsteady flow. Proceedings, American Society of Civil Engineers (Hydraulics Division), Vol. 88, HY4, Paper No. 3202, July 1962, pp. 147-172.

Rumer, R. R. and D. R. F. Harleman, 1963, Intruded salt-water wedge in porous media. Proceedings, American Society of Civil Engineers (Hydraulics Division), Vol. 89, HY6, Paper No. 3707, November 1963, pp. 193-220.

Saffman, P. G., 1959, A theory of dispersion in a porous medium. Journal of Fluid Mechanics, Vol. 6, Part 3, pp. 321-349.

Saffman, P. G., 1960, Dispersion due to molecular diffusion and macroscopic mixing in flow through a network of capillaries. Journal of Fluid Mechanics, Vol. 7, Part 2, pp. 194-208.

Scheidegger, A. E., 1954, Statistical hydrodynamics in porous media. Journal of Applied Physics, Vol. 25, No. 8, August 1954, pp. 994-1001.

Scheidegger, A. E., 1957, On the theory of flow of miscible phases in porous media. International Association of Scientific Hydrology, Publication No. 44, General Assembly of Toronto, Vol. 2, pp. 236-242.

Scheidegger, A. E., 1960, The physics of flow through porous media. McMillan Company, New York, 313 p.

Scheidegger, A. E., 1961, General theory of dispersion in porous media. Journal of Geophysical Research, Vol. 66, No. 10, October 1961, pp. 3273-3278.

Shamir, U. Y. and D. R. F. Harleman, 1966, Numerical and analytical solutions of dispersion problems in homogeneous and layered aquifers. Technical Report No. 89, Hydrodynamics Laboratory, Massachusetts Institute of Technology, Cambridge, Massachusetts, May 1966, 206 p.

Shamir, U. Y. and D. R. F. Harleman, 1967, Dispersion in layered porous media. Proceedings, American Society of Civil Engineers (Hydraulics Division), Vol. 93, HY5, Paper No. 5455, September 1967, pp. 237-260.

Simpson, E. S., 1962, Transverse dispersion in liquid flow through porous media. Professional Paper 411-C, U.S. Geological Survey, U.S. Govt. Printing Office, Washington, D. C., 30 p.

Simpson, Harold D., 1969, Laminar and turbulent dispersion of miscible fluids in porous media. M.S. Thesis, Department of Civil Engineering, Colorado State University, Fort Collins, Colorado, June 1969, 46 p.

Slichter, C. S., 1905, Field measurements of the rate of movement of underground waters. Water Supply and Irrigation Paper No. 140, U.S. Geological Survey, U.S. Govt. Printing Office, Washington, D. C., 122 p.

Smith, G. O., 1965, Numerical solution of partial differential equations. Oxford University Press, New York and London, 179 p.

Stone, H. L. and P. L. T. Brian, 1963, Numerical solution of convective transport problems. American Institute of Chemical Engineers Journal, Vol. 9, No. 5, September 1963, pp. 681-688.

Taylor, Angus E., 1955, Advanced Calculus. Gin and Company, New York, 1955, 786 p.

Taylor, G. I., 1953, Dispersion of soluble matter in solvent flowing slowly through a tube. Proceedings, Royal Society of London, Series A, Vol. 219, pp. 186-203.

Taylor, G. I., 1954, The dispersion of matter in turbulent flow through a pipe. Proceedings, Royal Society of London, Series A, Vol. 223, pp. 446-468.

Thurnau, D. H., 1963, Algorithm 195, Bandsolve. Communications of the Association for Computing Machinery, Vol. 6, No. 8, p. 441.

Tyson, H. N., Jr. and E. M. Weber, 1964, Groundwater management for the nation's future-computer simulation of groundwater basins. Proceedings, American Society of Civil Engineers (Hydraulics Division), Vol. 90, Paper No. 3973, July 1964, pp. 59-77.

van der Poel, C., 1962, Effect of lateral diffusivity on miscible displacement in horizontal reservoirs. Society of Petroleum Engineers Journal, Vol. 2, No. 4, December 1962, pp. 317-326.

Wylie, C. R., Jr., 1966, Advanced engineering mathematics, McGraw-Hill Book Company, New York, 3rd edition, 813 p.

APPENDIX A

DERIVATION OF THE FUNDAMENTAL FLOW EQUATION

A fundamental flow equation for a displacement process involving miscible fluids can be derived by combining the law of conservation of mass, Darcy's law, and an equation of state describing the pressure-volume-temperature-concentration relationship. The result is an equation involving two dependent variables, pressure and concentration.

A.1 Continuity Equation. An important relationship in fluid flow is the principle of conservation of mass. This principle is a statement of material balance with respect to a volume element fixed in space, and may be simply stated as:

(Rate of Mass Inflow) - (Rate of Mass Outflow) =

(Rate of Change of Mass Inside Volume Element) .

Applying this principle to the volume element shown in Fig. A-1 results in

$$M_{x_1-\Delta x_1/2} - M_{x_1+\Delta x_1/2} + M_{x_2-\Delta x_2/2} - M_{x_2+\Delta x_2/2} + M_{x_3-\Delta x_3/2} - M_{x_3+\Delta x_3/2} = \frac{\partial M_{VE}}{\partial t} + M_p \quad , \qquad \text{(A-1)}$$

where $M_{x_1-\Delta x_1/2}$, $M_{x_2-\Delta x_2/2}$, $M_{x_3-\Delta x_3/2}$ =

rate of mass inflow across faces $x_1-\Delta x_1/2$, $x_2-\Delta x_2/2$, and $x_3-\Delta x_3/2$ respectively,

$M_{x_1+\Delta x_1/2}$, $M_{x_2+\Delta x_2/2}$, $M_{x_3+\Delta x_3/2}$ =

rate of mass outflow across faces $x_1+\Delta x_1/2$, $x_2+\Delta x_2/2$, and $x_3+\Delta x_3/2$ respectively,

M_{VE} = mass contained inside the volume element, and

M_p = a mass source or sink term which is positive when a sink and negative when a source.

Applying a Taylor series expansion about the point (x_1, x_2, x_3) of Fig. A-1 gives:

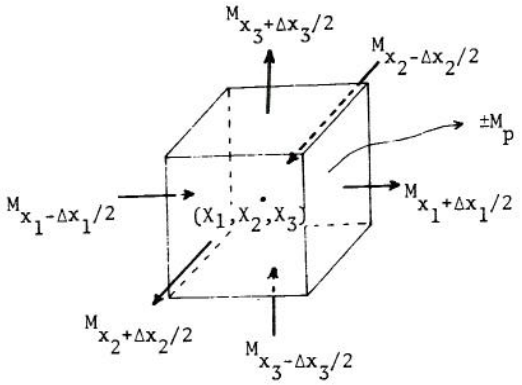

Fig. A-1 Volume element of a porous medium used for developing continuity equation.

$$M_{x_1-\Delta x_1/2} = M_{x_1} - \frac{\partial M_{x_1}}{\partial x_1}\frac{\Delta x_1}{2} + \frac{1}{2!}\frac{\partial^2 M_{x_1}}{\partial x_1^2}\left(\frac{\Delta x_1}{2}\right)^2 - \cdots ,$$

$$M_{x_2-\Delta x_2/2} = M_{x_2} - \frac{\partial M_{x_2}}{\partial x_2}\frac{\Delta x_2}{2} + \frac{1}{2!}\frac{\partial^2 M_{x_2}}{\partial x_2^2}\left(\frac{\Delta x_2}{2}\right)^2 - \cdots ,$$

$$M_{x_3-\Delta x_3/2} = M_{x_3} - \frac{\partial M_{x_3}}{\partial x_3}\frac{\Delta x_3}{2} + \frac{1}{2!}\frac{\partial^2 M_{x_3}}{\partial x_3^2}\left(\frac{\Delta x_3}{2}\right)^2 - \cdots ,$$

$$M_{x_1+\Delta x_1/2} = M_{x_1} + \frac{\partial M_{x_1}}{\partial x_1}\frac{\Delta x_1}{2} + \frac{1}{2!}\frac{\partial^2 M_{x_1}}{\partial x_1^2}\left(\frac{\Delta x_1}{2}\right)^2 + \cdots ,$$

$$M_{x_2+\Delta x_2/2} = M_{x_2} + \frac{\partial M_{x_2}}{\partial x_2}\frac{\Delta x_2}{2} + \frac{1}{2!}\frac{\partial^2 M_{x_2}}{\partial x_2^2}\left(\frac{\Delta x_2}{2}\right)^2 + \cdots ,$$

$$M_{x_3+\Delta x_3/2} = M_{x_3} + \frac{\partial M_{x_3}}{\partial x_3}\frac{\Delta x_3}{2} + \frac{1}{2!}\frac{\partial^2 M_{x_3}}{\partial x_3^2}\left(\frac{\Delta x_3}{2}\right) + \cdots . \qquad \text{(A-2)}$$

Neglecting second order terms and higher, the following relationships are obtained from Eq. A-2:

$$M_{x_1-\Delta x_1/2} - M_{x_1+\Delta x_1/2} = -\frac{\partial M_{x_1}}{\partial x_1}\Delta x_1 \quad ,$$

$$M_{x_2-\Delta x_2/2} - M_{x_2+\Delta x_2/2} = -\frac{\partial M_{x_1}}{\partial x_2}\Delta x_2 \quad ,$$

$$M_{x_3-\Delta x_3/2} - M_{x_3+\Delta x_3/2} = -\frac{\partial M_{x_3}}{\partial x_3}\Delta x_3 \quad . \qquad \text{(A-3)}$$

Substituting Eq. A-3 into Eq. A-1 gives:

$$\frac{\partial M_{x_1}}{\partial x_1}\Delta x_1 + \frac{\partial M_{x_2}}{\partial x_2}\Delta x_2 + \frac{\partial M_{x_3}}{\partial x_3}\Delta x_3 = -\frac{\partial M_{VE}}{\partial t} - M_p \quad . \qquad \text{(A-4)}$$

Each one of the mass flow rate components may be expressed in terms of the fluid density, the dimensions of the volume element, and the volume flux. Thus,

$$M_{x_1} = \rho q_1 \Delta x_2 \Delta x_3 \quad , \qquad \text{(A-5a)}$$

$$M_{x_2} = \rho q_2 \Delta x_1 \Delta x_3 \quad , \qquad \text{(A-5b)}$$

$$M_{x_3} = \rho q_3 \Delta x_1 \Delta x_2 \quad , \qquad \text{(A-5c)}$$

$$M_{VE} = \rho \phi S \Delta x_1 \Delta x_2 \Delta x_3 \quad , \qquad \text{(A-5d)}$$

and

$$M_p = \rho_p Q \quad , \qquad \text{(A-5e)}$$

where ρ = mass density of the solution,

q_1, q_2, q_3 = components of the volume flux in the x_1-, x_2-, and x_3-directions,

ϕ = porosity of the medium,

S = saturation of fluid,

Q = production term with units of L^3T^{-1}, and

ρ_p = mass density of production fluid.

Substituting Eq. A-5 into Eq. A-4 gives:

$$\frac{\partial}{\partial x_1}(\rho q_1 \Delta x_2 \Delta x_3)\Delta x_1 + \frac{\partial}{\partial x_2}(\rho q_2 \Delta x_1 \Delta x_3)\Delta x_2 + \frac{\partial}{\partial x_3}(\rho q_3 \Delta x_1 \Delta x_2)\Delta x_3 = -\frac{\partial}{\partial t}(\rho \phi S \Delta x_1 \Delta x_2 \Delta x_3) - \rho_p Q \quad . \qquad \text{(A-6)}$$

A.2 Fundamental Flow Equation. To develop the flow equation, an expression for the volume flux terms is required. Darcy's law is assumed to be applicable for this flow situation and the axes of the cartesian coordinate system (x_1, x_2, x_3) are assumed to coincide with the axes of the permeability tensor. Thus, the volume flux terms are given by:

$$q_1 = -\frac{k_{x_1} k_r}{\mu}\left(\frac{\partial P}{\partial x_1} + \rho g \frac{\partial h}{\partial x_1}\right) \quad ,$$

$$q_2 = -\frac{k_{x_2} k_r}{\mu}\left(\frac{\partial P}{\partial x_2} + \rho g \frac{\partial h}{\partial x_2}\right) \quad ,$$

$$q_3 = -\frac{k_{x_3} k_r}{\mu}\left(\frac{\partial P}{\partial x_3} + \rho g \frac{\partial h}{\partial x_3}\right) \quad , \qquad \text{(A-7)}$$

where $k_{x_1}, k_{x_2}, k_{x_3}$ = absolute permeability in the x_1-, x_2-, and x_3-directions, respectively,

k_r = relative permeability to fluid,

μ = viscosity of fluid at reservoir conditions,

P = fluid pressure,

g = acceleration of gravity, and

h = the elevation of the volume element above an arbitrary datum which is perpendicular to the direction of gravity.

After substituting Eq. A-7 into Eq. A-6, the results are

$$\frac{\partial}{\partial x_1}\left[\frac{\rho k_{x_1} k_r}{\mu}\left(\frac{\partial P}{\partial x_1} + \rho g \frac{\partial h}{\partial x_1}\right)\Delta x_2 \Delta x_3\right]\Delta x_1 + \frac{\partial}{\partial x_2}\left[\frac{\rho k_{x_2} k_r}{\mu}\left(\frac{\partial P}{\partial x_2} + \rho g \frac{\partial h}{\partial x_2}\right)\Delta x_1 \Delta x_3\right]\Delta x_2 + \frac{\partial}{\partial x_3}\left[\frac{\rho k_{x_3} k_r}{\mu}\left(\frac{\partial P}{\partial x_3} + \rho g \frac{\partial h}{\partial x_3}\right)\Delta x_1 \Delta x_2\right]\Delta x_3 = \frac{\partial}{\partial t}(\rho \phi S \Delta x_1 \Delta x_2 \Delta x_3) + \rho_p Q \quad . \qquad \text{(A-8)}$$

Multi-phase flow requires the development of an equation similar to Eq. A-8 for each phase being considered. Such equations have been developed for three-phase flow by Breitenbach et al. (1968b). The derivation being developed here is to be used in a single-phase flow simulator in which $S \equiv 1$ and $k_r \equiv 1$. Thus, Eq. A-8 reduces to

$$\frac{\partial}{\partial x_1}\left[\frac{\rho k_{x_1}}{\mu}\left(\frac{\partial P}{\partial x_1} + \rho g \frac{\partial h}{\partial x_1}\right)\Delta x_2 \Delta x_3\right]\Delta x_1 + \frac{\partial}{\partial x_2}\left[\frac{\rho k_{x_2}}{\mu}\left(\frac{\partial P}{\partial x_2} + \rho g \frac{\partial h}{\partial x_2}\right)\Delta x_1 \Delta x_3\right]\Delta x_2 + \frac{\partial}{\partial x_3}\left[\frac{\rho k_{x_3}}{\mu}\left(\frac{\partial P}{\partial x_3} + \rho g \frac{\partial h}{\partial x_3}\right)\Delta x_1 \Delta x_2\right]\Delta x_3 = \frac{\partial}{\partial t}(\rho \phi \Delta x_1 \Delta x_2 \Delta x_3) + \rho_p Q \quad . \qquad \text{(A-9)}$$

The right hand side of Eq. A-9 contains the porosity, ϕ, which is assumed to be a linear function of pressure given by

$$\phi = \phi_o[1 + C_F(P-P_o)] \quad , \tag{A-10}$$

where C_F is the formation compressibility factor, ϕ_o is the original value of porosity, and P_o is the original value of pressure. The density, ρ, varies with x_1, x_2, x_3, and t, and is dependent upon pressure, P, concentration, C, and temperature, T. Assuming isothermal conditions, the effects of temperature may be neglected and an equation of state of the following form is assumed:

$$\rho = \rho_o + \beta\rho_o(P-P_o) + \alpha(C-C_o) \quad , \tag{A-11}$$

where β is the fluid compressibility, α is a proportionality factor relating concentration and density, and the subscript (o) refers to the original value of the variable.

Differentiating Eq. A-10 with respect to t gives

$$\frac{\partial\phi}{\partial t} = C_F\phi_o \frac{\partial P}{\partial t} \quad . \tag{A-12}$$

Likewise, differentiating Eq. A-11 with respect to t gives

$$\frac{\partial\rho}{\partial t} = \beta\rho_o \frac{\partial P}{\partial t} + \alpha \frac{\partial C}{\partial t} \quad . \tag{A-13}$$

Expanding the right hand side of Eq. A-9, introducing Eqs. A-12 and A-13, and assuming that the size of the volume element $(\Delta\overline{V} = \Delta x_1\Delta x_2\Delta x_3)$ does not change with time gives

$$\text{rhs} = \Delta x_1\Delta x_2\Delta x_3(\rho\phi_o C_F + \rho_o\phi\beta) \frac{\partial P}{\partial t} + \alpha\phi\Delta x_1\Delta x_2\Delta x_3 \frac{\partial C}{\partial t} \quad . \tag{A-14}$$

Substituting Eq. A-10 and A-11 into Eq. A-14 gives

$$\text{rhs} = \rho_o\phi_o\Delta x_1\Delta x_2\Delta x_3\left[C_F + 2C_F\beta(P-P_o) + \beta + C_F\frac{\alpha(C-C_o)}{\rho_o}\right]\frac{\partial P}{\partial t} + \alpha\phi_o\Delta x_1\Delta x_2\Delta x_3\left[1 + C_F(P-P_o)\frac{\partial C}{\partial t}\right] \quad . \tag{A-15}$$

Since C_F and β are of the same order of magnitude (10^{-6} in most cases), then $2C_F\beta(P-P_o) << 10^{-6}$ for small pressure changes and can be neglected. For small concentration changes, $C_F\alpha(C-C_o) << 10^{-6}$. Also, the term $C_F(P-P_o) << 1$ for small pressure changes. Thus, for small pressure and concentration changes, Eq. A-15 may be approximated by

$$\text{rhs} = \rho_o\phi_o\Delta x_1\Delta x_2\Delta x_3(C_F+\beta)\frac{\partial P}{\partial t} + \alpha\phi_o\Delta x_1\Delta x_2\Delta x_3 \frac{\partial C}{\partial t} \quad . \tag{A-16}$$

Substituting Eq. A-16 into Eq. A-9 and using shorthand tensor notation gives

$$\frac{\partial}{\partial x_i}\left[\frac{\rho\Delta A_i k x_i}{\mu}\left(\frac{\partial P}{\partial x_i} + \rho g \frac{\partial h}{\partial x_i}\right)\right]\Delta x_i = \rho_o\phi_o\Delta\overline{V}(\beta+C_F)\frac{\partial P}{\partial t} + \alpha\phi_o\Delta\overline{V}\frac{\partial C}{\partial t} + \rho_p Q \quad . \tag{A-17}$$

where $i = 1,2,3$ is a cartesian coordinate system (x_1,x_2,x_3),

ΔA_i = cross sectional area perpendicular to flux q_i, and

$\Delta\overline{V}$ = volume of volume element, $\Delta x_1\ \Delta x_2\ \Delta x_3$.

Equation A-17 is the fundamental flow equation for the saturated flow of a solution containing a miscible tracer, and will be referred to as the flow equation.

APPENDIX B

DERIVATION OF THE DISPERSION EQUATION

To solve the flow equation (Eq. A-17), a relationship for determining the concentration C is needed. This relationship may be obtained by expressing a continuity equation for the dispersing tracer. The problem is formulated on a microscopic basis and then averaged over a cross-sectional area of the porous medium to give the desired macroscopic equation of dispersion.

Two different size elements, a fluid element and a representative volume element, are used in this analysis. A fluid element with very small dimensions is used inside the pores of the porous medium for the microscopic analysis. A representative volume element of the porous medium is defined as the smallest volume around a point such that adding an infinitesimal volume has a negligible effect on the values of medium properties such as porosity. The representative volume element is used in the macroscopic analysis and contains both medium and fluid.

B.1 Continuity Equation for the Tracer. The continuity equation for the tracer is given as:

(Rate of Mass Inflow of Tracer) -

(Rate of Mass Outflow of Tracer) =

(Rate of Change of Tracer Mass Inside Volume Element).

When applied to a representative volume element of porous media with the dimensions of Δx_1, Δx_2, and Δx_3, as shown in Fig. B-1, the results are:

$$(M_t)_{x_1-\Delta x_1/2} - (M_t)_{x_1+\Delta x_1/2} + (M_t)_{x_2-\Delta x_2/2} - (M_t)_{x_2+\Delta x_2/2} + (M_t)_{x_3-\Delta x_3/2} - (M_t)_{x_3+\Delta x_3/2} = \frac{\partial M_{tVE}}{\partial t} + M_{tp} \quad , \qquad \text{(B-1)}$$

where $(M_t)_{x_1-\Delta x_1/2}$, $(M_t)_{x_2-\Delta x_2/2}$, $(M_t)_{x_2-\Delta x_3/2}$ =

Rate of mass inflow of tracer across faces $x_1-\Delta x_1/2$, $x_2-\Delta x_2/2$, and $x_3-\Delta x_3/2$ respectively,

$(M_t)_{x_1+\Delta x_1/2}$, $(M_t)_{x_2+\Delta x_2/2}$, $(M_t)_{x_3+\Delta x_3/2}$ =

Rate of mass outflow of tracer across faces $x_1+\Delta x_1/2$, $x_2+\Delta x_2/2$, and $x_3+\Delta x_3/2$ respectively,

M_{tVE} = Mass of tracer contained inside the volume element, and

M_{tp} = Mass source or sink term for the tracer which is positive when a sink and negative when a source.

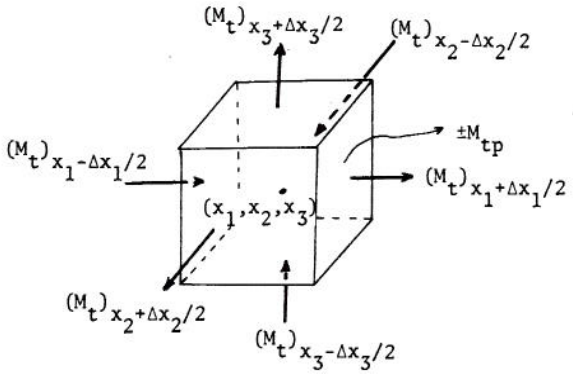

Fig. B-1 Volume element of a porous medium used to develop continuity equation for tracer in miscible fluid flow.

Expanding each one of the mass flow rate terms in a Taylor series about the point (x_1, x_2, x_3) gives

$$(M_t)_{x_1-\Delta x_1/2} = (M_t)_{x_1} - \frac{\partial}{\partial x_1}(M_t)_{x_1}\frac{\Delta x_1}{2} + \frac{1}{2!}\frac{\partial^2 (M_t)_{x_1}}{\partial x_1^2}\left(\frac{\Delta x_1}{2}\right)^2 - \cdots ,$$

$$(M_t)_{x_2-\Delta x_2/2} = (M_t)_{x_2} - \frac{\partial}{\partial x_2}(M_t)_{x_2}\frac{\Delta x_2}{2} + \frac{1}{2!}\frac{\partial^2 (M_t)_{x_2}}{\partial x_2^2}\left(\frac{\Delta x_2}{2}\right)^2 - \cdots ,$$

$$(M_t)_{x_3-\Delta x_3/2} = (M_t)_{x_3} - \frac{\partial}{\partial x_3}(M_t)_{x_3}\frac{\Delta x_3}{2} + \frac{1}{2!}\frac{\partial^2 (M_t)_{x_3}}{\partial x_3^2}\left(\frac{\Delta x_3}{2}\right)^2 - \cdots ,$$

$$(M_t)_{x_1+\Delta x_1/2} = (M_t)_{x_1} + \frac{\partial}{\partial x_1}(M_t)_{x_1}\frac{\Delta x_1}{2} + \frac{1}{2!}\frac{\partial^2 (M_t)_{x_1}}{\partial x_1^2}\left(\frac{\Delta x_1}{2}\right)^2 + \ldots ,$$

$$(M_t)_{x_2+\Delta x_2/2} = (M_t)_{x_2} + \frac{\partial}{\partial x_2}(M_t)_{x_2}\frac{\Delta x_2}{2} + \frac{1}{2!}\frac{\partial^2 (M_t)_{x_2}}{\partial x_2^2}\left(\frac{\Delta x_1}{2}\right)^2 + \ldots ,$$

and

$$(M_t)_{x_3+\Delta x_3/2} = (M_t)_{x_3} + \frac{\partial}{\partial x_3}(M_t)_{x_3}\frac{\Delta x_3}{2} + \frac{1}{2!}\frac{\partial^2 (M_t)_{x_3}}{\partial x_2^2}\left(\frac{\Delta x_3}{2}\right)^2 + \ldots . \qquad \text{(B-2)}$$

The tracer mass flow rates may be expressed in terms of the tracer mass flux, the dimensions of the volume element, and the porous medium properties, i.e.,

$$(M_t)_{x_1} = J_1^*\phi S\Delta x_2\Delta x_3 , \qquad \text{(B-3a)}$$

$$(M_t)_{x_2} = J_2^*\phi S\Delta x_1\Delta x_3 , \qquad \text{(B-3b)}$$

$$(M_t)_{x_3} = J_3^*\phi S\Delta x_1\Delta x_2 , \qquad \text{(B-3c)}$$

$$M_{tVE} = \phi S\Delta x_1\Delta x_2\Delta x_3 C , \qquad \text{(B-3d)}$$

and

$$M_{tP} = C_p Q , \qquad \text{(B-3e)}$$

where C = average tracer concentration in the volume element, mass of tracer per volume of solution,

J^*_1, J^*_2, J^*_3 = macroscopic tracer mass flux components in x_1-, x_2-, and x_3-directions respectively,

ϕ = porosity,

S = saturation of phase containing tracer,

Q = production term with units of L^3T^{-1}, and

C_p = tracer concentration of production fluid.

In Eq. B-3, the mass flux components, J_1^*, J_2^*, and J_3^*, are defined as the mass flow rate per unit pore area. The reason for choosing a flux per unit pore area is because the microscopic fluid elements will be averaged over a cross-section of the volume element to yield J_1^*, J_2^*, and J_3^*. Since fluid elements only exist in the pores, the result is a flux in terms of the pore area rather than gross area.

Substituting Eqs. B-3 and B-2 into Eq. B-1, neglecting the second order terms in Eq. B-2, and using tensor notation gives

$$\frac{\partial}{\partial x_i}(J_i^*\phi S\Delta A_i)\Delta x_i = -\frac{\partial}{\partial t}(\phi S\Delta x_1\Delta x_2\Delta x_3 C) - C_p Q , \qquad \text{(B-4)}$$

where $i = 1, 2, 3$ corresponds to x_1, x_2, and x_3 coordinates, and

ΔA_i = cross-sectional area perpendicular to mass flux component, J_i^*.

B.2 Determining the Tracer Mass Flux Components, J_i^*. To accomplish this portion of the derivation, the microscopic mass flux equations are developed and then averaged over a cross-sectional area of the representative volume element to give a statistically meaningful macroscopic mass flux equation.

Microscopic Analysis. For a fluid element inside a pore of the porous medium, the diffusive mass flux of the tracer with respect to the volumetric velocity, $\hat{V}$, is given by Fick's first law (Bird, Stewart and Lightfoot, 1960):

$$\vec{J} = \hat{C}(\vec{\hat{V}_t} - \vec{\hat{V}}) = -D_d \operatorname{grad} \hat{C} , \qquad \text{(B-5)}$$

where $\vec{J}$ = diffusive mass flux of the tracer,

$\hat{C}$ = concentration of tracer in fluid element,

$\vec{\hat{V}}_t$ = velocity of the tracer in fluid element with respect to a fixed coordinate system,

$\vec{\hat{V}}$ = volumetric velocity of fluid element, and

D_d = coefficient of molecular diffusion.

A fluid element in a porous media must follow a tortuous path as it moves through the pores. Let a tortuous path of length $d\sigma$ be depicted as shown in Fig. B-2. The diffusive mass flux term may be written as

$$\vec{J} = -D_d\frac{d\hat{C}}{d\sigma} . \qquad \text{(B-6)}$$

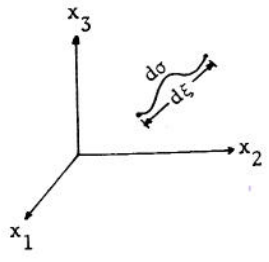

Fig. B-2 Tortuous path of fluid element.

The determination of $\vec{J}$ as a function of the difference in concentration between the ends of the tortuous path and the direct distance between the ends is desirable. Thus, Eq. B-6 may be expressed as

$$\vec{J} = - D_d \frac{d\hat{C}}{d\xi} \frac{d\xi}{d\sigma} \quad . \tag{B-7}$$

The diffusive mass flux, $\vec{J}$, does not have to be in the direction of $dC/d\xi$ because the tortuous path varies in direction from point to point. Projecting $\vec{J}$ as given in Eq. B-7 onto the ξ-direction (the axis of the tortuous path) results in

$$J_\xi = |\vec{J}| \cdot |1\xi| \cos\theta \quad , \tag{B-8}$$

where $|\vec{J}|$ = magnitude of $\vec{J}$,

$|1\vec{\xi}|$ = magnitude of unit vector in ξ-direction,

θ = angle between $\vec{J}$ and $1\vec{\xi}$, and

$\cos\theta = d\xi/d\sigma$.

Substituting Eq. B-7 into Eq. B-8 gives

$$J_\xi = - D_d \left(\frac{d\xi}{d\sigma}\right)^2 \frac{d\hat{C}}{d\xi} \quad . \tag{B-9}$$

The components of J_ξ in the $x_i (i=1,2,3)$ coordinate system are given by

$$J_i = |J_\xi| \cdot |1\vec{x}_i| \cos\theta \quad , \tag{B-10}$$

where $|J_\xi|$ = magnitude of J_ξ,

$|1x_i|$ = magnitude of unit vector in x_i-direction,

θ = angle between J_ξ and $1\vec{x}_i$, and

$\cos\theta = dx_i/d\xi$.

Substituting Eq. B-9 into Eq. B-10 yields

$$J_i = - D_d \left(\frac{d\xi}{d\sigma}\right)^2 \frac{dx_i}{d\xi} \frac{d\hat{C}}{d\xi} \quad . \tag{B-11}$$

By the definition of a total derivative,

$$\frac{d\hat{C}}{d\xi} = \frac{\partial\hat{C}}{\partial x_1} \frac{dx_1}{d\xi} + \frac{\partial\hat{C}}{\partial x_2} \frac{dx_2}{d\xi} + \frac{\partial\hat{C}}{\partial x_3} \frac{dx_3}{d\xi} \quad . \tag{B-12}$$

Equations B-11 and B-12 combine to give

$$J_i = - D_d \left(\frac{d\xi}{d\sigma}\right)^2 \frac{dx_i}{d\xi} \frac{dx_j}{d\xi} \frac{\partial\hat{C}}{\partial x_j} \quad , \tag{B-13}$$

where the double summation convention of tensor notation has been invoked. The term $(d\xi/d\sigma)^2 (dx_i/d\xi) (dx_j/d\xi)$ is analogous to the reciprocal of a term commonly referred to as tortuosity, and is a tensor of rank two which "deflects" or "twists" the gradient of concentration to form a new vector oriented in a different direction. By definition, let

$$\hat{T}_{ij} \equiv \left(\frac{d\xi}{d\sigma}\right)^2 \frac{dx_i}{d\xi} \frac{dx_j}{d\xi} \quad . \tag{B-14}$$

Substituting Eqs. B-13 and B-14 into Eq. B-5, the following form of Fick's law for describing diffusion on a microscopic scale in a porous medium is obtained:

$$\hat{C} \hat{V}_{t_i} = \hat{C} \hat{V}_i - D_d \hat{T}_{ij} \frac{\hat{C}}{x_j} \quad . \tag{B-15}$$

Macroscopic Analysis. The objective here is to obtain a relationship for the components, J_i^*, of the tracer mass flux vector corresponding to the representative volume element shown in Fig. B-1. Equation B-15 gives the tracer mass flux for a fluid element in a pore of the representative volume element. Since the cross-sectional area, ΔA_i, of the representative volume element is perpendicular to the tracer mass flux component, J_i^*, the total mass flowing thru this cross section is just the sum from all the fluid elements located in ΔA_i, i.e.,

$$(\text{Total tracer mass})_i = \int_{(\phi S \Delta A_i)} \hat{C} \hat{V}_i \, dA_i - \int_{(\phi S \Delta A_i)} D_d \hat{T}_{ij} \frac{\partial\hat{C}}{\partial x_j} \, dA_i \quad , \tag{B-16}$$

where dA_i = the area of the fluid element parallel to ΔA_i. The tracer mass flux, J_i^*, for the representative volume element may be expressed as

$$J_i^* = \frac{(\text{Total tracer mass})_i}{\phi S \Delta A_i} \quad , \tag{B-17}$$

where $\phi S \Delta A_i$ is the total pore area through which the fluid moves. Substituting Eq. B-16 into Eq. B-17 gives

$$J_i^* = \frac{1}{\phi S \Delta A_i} \left[\int_{(\phi S \Delta A_i)} \hat{C} \hat{V}_i dA_i - \int_{(\phi S \Delta A_i)} D_d \hat{T}_{ij} \frac{\partial\hat{C}}{\partial x_j} \, dA_i \right] \quad . \tag{B-18}$$

To evaluate the terms of Eq. B-18, the following definitions are made:

$$\begin{aligned} \hat{C} &= C + \mathring{C} \\ \hat{V}_i &= V_i + \mathring{V}_i \\ \hat{T}_{ij} &= T_{ij} + \mathring{T}_{ij} \end{aligned} \quad , \tag{B-19}$$

in which $\hat{C}$, $\hat{V}_i$, and $\hat{T}_{ij}$ are the actual values of the variable at a point; C, V_i, and T_{ij}

are the averaged values of the variables over the cross-sectional area, ΔA_i ; and $\overset{\circ}{C}$, $\overset{\circ}{V}_i$, and $\overset{\circ}{T}_{ij}$ represent the deviations of the variables at a point from the cross-sectional averages. By definition, the spatial average of the variables $\overset{\circ}{C}$, $\overset{\circ}{V}_i$, and $\overset{\circ}{T}_{ij}$ over the cross-sectional area, ΔA_i , is zero (i.e., $\overline{\overset{\circ}{C}} = \overline{\overset{\circ}{V}_i} = \overline{\overset{\circ}{T}_{ij}} = 0$) . Using Eq. B-19 in Eq. B-18 gives

$$J_i^* = \frac{1}{\phi S \Delta A_i} \left[\int_{(\phi S \Delta A_i)} (C+\overset{\circ}{C})(V_i+\overset{\circ}{V}_i) dA_i - \int_{(\phi S \Delta A_i)} D_d (T_{ij}+\overset{\circ}{T}_{ij}) \frac{\partial (C+\overset{\circ}{C})}{\partial x_j} dA_i \right] . \quad \text{(B-20)}$$

Expanding terms in Eq. B-20 gives

$$J_i^* = \frac{1}{\phi S \Delta A_i} \left[\int_{(\phi S \Delta A_i)} CV_i dA_i + \int_{(\phi S \Delta A_i)} C\overset{\circ}{V}_i dA_i + \int_{(\phi S \Delta A_i)} V_i \overset{\circ}{C} dA_i + \int_{(\phi S \Delta A_i)} \overset{\circ}{C}\overset{\circ}{V}_i dA_i - \int_{(\phi S \Delta A_i)} D_d T_{ij} \frac{\partial C}{\partial x_j} dA_i - \int_{(\phi S \Delta A_i)} D_d T_{ij} \frac{\partial \overset{\circ}{C}}{\partial x_j} dA_i - \int_{(\phi S \Delta A_i)} D_d \overset{\circ}{T}_{ij} \frac{\partial C}{\partial x_j} dA_i - \int_{(\phi S \Delta A_i)} D_d \overset{\circ}{T}_{ij} \frac{\partial \overset{\circ}{C}}{\partial x_j} dA_i \right] . \quad \text{(B-21)}$$

But by definition of the mean, Eq. B-21 is

$$J_i^* = CV_i + C\overline{\overset{\circ}{V}_i} + \overline{\overset{\circ}{C}}V_i + \overline{\overset{\circ}{C}\overset{\circ}{V}_i} - D_d T_{ij} \frac{\partial C}{\partial x_j} - D_d T_{ij} \overline{\frac{\partial \overset{\circ}{C}}{\partial x_j}} - D_d \overline{\overset{\circ}{T}}_{ij} \frac{\partial C}{\partial x_j} - D_d \overline{\overset{\circ}{T}_{ij} \frac{\partial \overset{\circ}{C}}{\partial x_j}} . \quad \text{(B-22)}$$

The following observations are made:

1. As previously noted, $\overline{\overset{\circ}{C}}$, $\overline{\overset{\circ}{V}_i}$, and $\overline{\overset{\circ}{T}_{ij}}$ are zero.

2. The average of a derivative is equal to the derivative of the average [Kells (1950), page 78]. Thus,

$$\overline{(\partial \overset{\circ}{C}/\partial x_j)} = (\partial \overline{\overset{\circ}{C}}/\partial x_j) = 0$$

3. Medium properties and fluid properties are assumed to be uncorrelated. Thus,

$$\overline{(\overset{\circ}{T}_{ij} \frac{\partial \overset{\circ}{C}}{\partial x_j})} = \overline{\overset{\circ}{T}}_{ij} \overline{(\partial \overset{\circ}{C}/\partial x_j)} = \overline{\overset{\circ}{T}}_{ij} (\partial \overline{\overset{\circ}{C}}/\partial x_j) = 0.$$

With the above observations, Eq. B-22 reduces to

$$J_i^* = CV_i + \overline{\overset{\circ}{C}\overset{\circ}{V}_i} - D_d T_{ij} \frac{\partial C}{\partial x_j} . \quad \text{(B-23)}$$

Thus, the averaged mass flux of the tracer over a cross-sectional area of the representative volume element is composed of three different flux terms. The first is a flux, CV_i , due to convection with the average velocity of the fluid. The second is a flux, $\overline{\overset{\circ}{C}\overset{\circ}{V}_i}$, which will be called the dispersive flux and is the result of microscopic spatial variations in velocity and concentration. The third is a flux, $D_d T_{ij} \frac{\partial C}{\partial x_j}$, due to molecular diffusion.

Dispersive Mass Flux. In order to use Eq. B-23, some relation between $\overline{\overset{\circ}{C}\overset{\circ}{V}_i}$ and C has to be postulated. By analogy with Fick's first law of mass transport, the following relationship is assumed:

$$\overline{\overset{\circ}{C}\overset{\circ}{V}_i} = - D_p \frac{\partial C}{\partial x_i} . \quad \text{(B-24)}$$

where D_p is called the dispersion coefficient of mass transport in porous media. The dispersion coefficient, D_p , is not a physical property characteristic of a given fluid; but depends on position, direction, velocity of flow, and the type of porous material.

Making such a postulation as Eq. B-24 is not without some foundation. For years, the theory of turbulent flow has used an analogy with Newton's law of viscosity to approximate the Reynold's stresses. Also, experimental evidence tends to match the approximation used in Eq. B-24.

Experimental evidence also indicates that D_p is not isotropic, but that transverse dispersion may occur and is less than dispersion in the longitudinal direction. Using a statistical approach, de Josselin de Jong (1958) determined analytically that longitudinal dispersion is larger than the transverse dispersion. His result is approximately a normal distribution of concentration in three dimensions.

Because longitudinal and transverse dispersion are different and must be invariant under a coordinate transformation, D_p must be treated as a tensor. By definition $\overline{\overset{\circ}{C}\overset{\circ}{V}_i}$ is a vector or tensor of rank 1. Also by definition $\partial C/\partial x_i$ is a vector or tensor of rank 1. Thus, Eq. B-24 is of the form

(Tensor of Rank 1)=-(Tensor of Rank ?)(Tensor of Rank 1). (B-25)

Since D_p is an anisotropic quantity, then the form of Eq. B-25 indicates that the multiplication must be that of finding the inner product of two tensors and that D_p must be a tensor of rank 2. Thus, Eq. B-24 may be written as

$$\overline{\overset{\circ}{C}\overset{\circ}{V}_i} = - D_{ij} \frac{\partial C}{\partial x_j} . \quad \text{(B-26)}$$

Introducing Eq. B-26 into Eq. B-23 gives

$$J_i^* = CV_i - D_{ij} \frac{\partial C}{\partial x_j} - D_d T_{ij} \frac{\partial C}{\partial x_j} \quad . \tag{B-27}$$

B.3 Dispersion Equation. The results of the flux determination given in Eq. B-27 are now introduced into Eq. B-4 to yield

$$\frac{\partial}{\partial t} (\phi S \Delta x_1 \Delta x_2 \Delta x_3 C) = \frac{\partial}{\partial x_i} \left[(D_{ij} + D_d T_{ij}) \frac{\partial C}{\partial x_j} \phi S \Delta A_i \right] \Delta x_i$$

$$- \frac{\partial}{\partial x_i} (CV_i \phi S \Delta A_i) \Delta x_i - C_p Q \quad . \tag{B-28}$$

Equation B-28 is the general form of the dispersion equation. However, since Eq. B-28 is to be solved numerically by the method of characteristics, a different form is required. Let the dispersive and molecular flux terms be denoted by DD , and rewrite Eq. B-28 as

$$\frac{\partial}{\partial t} (\phi S \Delta x_1 \Delta x_2 \Delta x_3 C) = DD - \frac{\partial}{\partial x_i} (CV_i \phi S \Delta A_i) \Delta x_i - C_p Q \quad . \tag{B-29}$$

The volume flux of a fluid flowing through a porous medium may be expressed as

$$q_i = V_i \phi S \quad , \tag{B-30}$$

where q_i is the volume flux in the ith direction. Using Eq. B-30 in Eq. B-29 and chaining out the derivatives of concentration results in

$$\frac{1}{\Delta x_1 \Delta x_2 \Delta x_3} \left[\frac{\partial}{\partial x_i} (q_i \Delta A_i) \Delta x_i + \frac{\partial}{\partial t} (\phi S \Delta x_1 \Delta x_2 \Delta x_3) \right] =$$

$$= \frac{DD}{C \Delta x_1 \Delta x_2 \Delta x_3} - \frac{\phi S}{C} \frac{\partial C}{\partial t} - \frac{q_i}{C} \frac{\partial C}{\partial x_i} - \frac{C_p}{C} \frac{Q}{\Delta x_1 \Delta x_2 \Delta x_3} \quad . \tag{B-31}$$

From Appendix A, Eq. A-6 for the flow equation is

$$\frac{\partial}{\partial x_i} (\rho q_i \Delta A_i) \Delta x_i = - \frac{\partial}{\partial t} (\rho \phi S \Delta x_1 \Delta x_2 \Delta x_3) - \rho_p Q \quad . \tag{B-32}$$

Chaining out the derivatives of density in Eq. B-32 gives

$$\frac{1}{\Delta x_1 \Delta x_2 \Delta x_3} \left[\frac{\partial}{\partial x_i} (q_i \Delta A_i) \Delta x_i + \frac{\partial}{\partial t} (\phi S \Delta x_1 \Delta x_2 \Delta x_3) \right]$$

$$= - \frac{\phi S}{\rho} \frac{\partial \rho}{\partial t} - \frac{q_i}{\rho} \frac{\partial \rho}{\partial x_i} - \frac{\rho_p}{\rho} \frac{Q}{\Delta x_1 \Delta x_2 \Delta x_3} \quad . \tag{B-33}$$

The left hand sides of Eqs. B-31 and B-33 are equal. Thus, the right hand sides must be equal also, i.e.,

$$- \frac{\phi S}{\rho} \frac{\partial \rho}{\partial t} - \frac{q_i}{\rho} \frac{\partial \rho}{\partial x_i} - \frac{\rho_p}{\rho} \frac{Q}{\Delta x_1 \Delta x_2 \Delta x_3} = \frac{DD}{C \Delta x_1 \Delta x_2 \Delta x_3}$$

$$- \frac{\phi S}{C} \frac{\partial C}{\partial t} - \frac{q_i}{C} \frac{\partial C}{\partial x_i} - \frac{C_p}{C} \frac{Q}{\Delta x_1 \Delta x_2 \Delta x_3} \quad . \tag{B-34}$$

Collecting like terms gives

$$\phi S \left(\frac{\partial C}{\partial t} - \frac{C}{\rho} \frac{\partial \rho}{\partial t} \right) = \frac{DD}{\Delta x_1 \Delta x_2 \Delta x_3} - q_i \left(\frac{\partial C}{\partial x_i} - \frac{C}{\rho} \frac{\partial \rho}{\partial x_i} \right)$$

$$- \left(C_p - \frac{\rho_p C}{\rho} \right) \frac{Q}{\Delta x_1 \Delta x_2 \Delta x_3} \quad . \tag{B-35}$$

Differentiating Eq. A-11 of Appendix A, the following relationships are obtained:

$$\frac{\partial \rho}{\partial x_i} = \beta \rho_o \frac{\partial P}{\partial x_i} + \alpha \frac{\partial C}{\partial x_i} \quad , \tag{B-36a}$$

and

$$\frac{\partial \rho}{\partial t} = \beta \rho_o \frac{\partial P}{\partial t} + \alpha \frac{\partial C}{\partial t} \quad . \tag{B-36b}$$

Substituting Eq. B-36 into Eq. B-35 and collecting like terms gives

$$\phi S (1 - \frac{\alpha C}{\rho}) \frac{\partial C}{\partial t} = \frac{DD}{\Delta x_1 \Delta x_2 \Delta x_3} - q_i (1 - \frac{\alpha C}{\rho}) \frac{\partial C}{\partial x_i}$$

$$- \left(C_p - \frac{\rho_p C}{\rho} \right) \frac{Q}{\Delta x_1 \Delta x_2 \Delta x_3} + C\beta \frac{\rho_o}{\rho} \left(\phi S \frac{\partial P}{\partial t} + q_i \frac{\partial P}{\partial x_i} \right) \quad , \tag{B-37}$$

where q_i is given by Eq. B-30. Upon division by $\phi S \left(\frac{\rho - \alpha C}{\rho} \right)$, Eq. B-37 becomes

$$\frac{\partial C}{\partial t} = \left(\frac{\rho}{\rho - \alpha C} \right) \left(\frac{DD}{\phi S \Delta x_1 \Delta x_2 \Delta x_3} \right) - V_i \frac{\partial C}{\partial x_i}$$

$$- (C_p - C) \frac{Q}{\phi S \Delta x_1 \Delta x_2 \Delta x_3} + \frac{\rho_o C \beta}{\rho - \alpha C} \left(\frac{\partial P}{\partial t} + V_i \frac{\partial P}{\partial x_i} \right) \quad . \tag{B-38}$$

If the volume element is completely saturated, i.e., $S \equiv 1$, then

$$\frac{\partial C}{\partial t} = \left(\frac{\rho}{\rho - \alpha C} \right) \left(\frac{1}{\phi \Delta A_i} \right) \frac{\partial}{\partial x_i} \left[(D_{ij} + D_d T_{ij}) \phi \Delta A_i \frac{\partial C}{\partial x_j} \right]$$

$$- V_i \frac{\partial C}{\partial x_i} - (C_p - C) \frac{Q}{\phi \Delta x_1 \Delta x_2 \Delta x_3} + \frac{\rho_o C \beta}{\rho - \alpha C} \left(\frac{\partial P}{\partial t} + V_i \frac{\partial P}{\partial x_i} \right) \quad . \tag{B-39}$$

Equation B-39 is a form of the dispersion equation containing two dependent variables, pressure and concentration, just as in the fundamental flow equation. Assuming that the terms of Eq. B-39 containing pressure and compressibility may be neglected, results in

$$\frac{\partial C}{\partial t} = \frac{\rho}{\phi \Delta A_i (\rho - \alpha C)} \frac{\partial}{\partial x_i} \left[(D_{ij} + D_d T_{ij}) \phi \Delta A_i \frac{\partial C}{\partial x_j} \right] - V_i \frac{\partial C}{\partial x_i} - (C_p - C) \left(\frac{Q}{\phi \Delta x_1 \Delta x_2 \Delta x_3} \right) . \quad \text{(B-40)}$$

Equation B-40 shall be called the dispersion equation.

APPENDIX C

DEVELOPMENT OF FINITE DIFFERENCE EQUATIONS FOR THE FLOW EQUATION

Since the same flow equation will be solved for all grids, a finite difference equation can be developed by considering a central grid (i,j,k) and the six immediately adjacent grids as shown in Fig. C-1. The general form of the flow equation given by Eq. A-17 may be rearranged into the following form for developing the finite difference equation:

$$\frac{1}{\phi_o \Delta x_1 \Delta x_2 \Delta x_3} \frac{\partial}{\partial x_i}\left[\frac{\rho k_{x_i} \Delta A_i}{\mu}\left(\frac{\partial p}{\partial x_i} + \rho g \frac{\partial h}{\partial x_i}\right)\right]\Delta x_i$$

$$= \rho_o (C_F + \beta) \frac{\partial P}{\partial t} + \alpha \frac{\partial C}{\partial t} + \frac{\rho_p Q}{\phi_o \Delta x_1 \Delta x_2 \Delta x_3} \quad , \qquad \text{(C-1)}$$

where x_i (i=1,2,3) indicates a cartesian coordinate system.

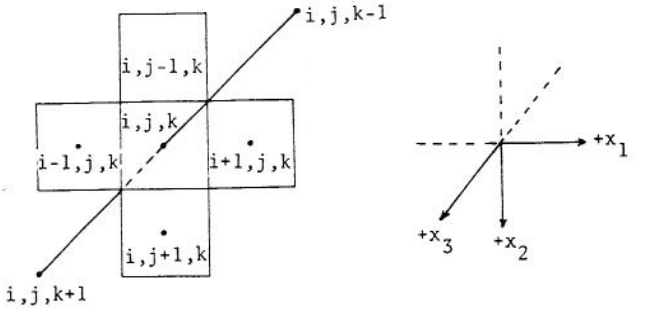

Fig. C-1 Central grid and six adjacent grids with the subscripting used in the finite difference equations.

Because of the symmetry of the spatial derivatives in Eq. C-1, only a detailed description of the finite difference equation in the x_1-direction will be given. Analogous equations for the x_2- and x_3-directions may be easily developed. Looking at a point on the boundary between grids i,j,k and i+1,j,k , the terms $(\partial p/\partial x_1)_{i+\frac{1}{2},j,k}$ and $(\partial h/\partial x_1)_{i+\frac{1}{2},j,k}$ are approximated by:

$$\left(\frac{\partial p}{\partial x_1}\right)_{i+\frac{1}{2},j,k} = \frac{P_{i+1,j,k} - P_{i,j,k}}{\Delta x_1} \quad , \qquad \text{(C-2a)}$$

and

$$\left(\frac{\partial h}{\partial x_1}\right)_{i+\frac{1}{2},j,k} = \frac{h_{i+1,j,k} - h_{i,j,k}}{\Delta x_1} \quad . \qquad \text{(C-2b)}$$

Likewise, for a point on the boundary between grids i,j,k and i-1,j,k ;

$$\left(\frac{\partial p}{\partial x_1}\right)_{i-\frac{1}{2},j,k} = \frac{P_{i,j,k} - P_{i-1,j,k}}{\Delta x_1} \quad , \qquad \text{(C-3a)}$$

and

$$\left(\frac{\partial h}{\partial x_1}\right)_{i-\frac{1}{2},j,k} = \frac{h_{i,j,k} - h_{i-1,j,k}}{\Delta x_1} \quad . \qquad \text{(C-3b)}$$

The x_1-component of the left hand side of Eq. C-1 may be approximated by:

$$(\text{lhs})_{x_1} = \left(\frac{\Delta x_1}{\phi_o \Delta x_1 \Delta x_2 \Delta x_3}\right)_{i,j,k}\left(\frac{1}{\Delta x_1}\right)\left\{\left[\frac{\rho k_{x_1} \Delta x_2 \Delta x_3}{\mu}\left(\frac{\partial p}{\partial x_1} + \rho g \frac{\partial h}{\partial x_1}\right)\right]_{i+\frac{1}{2},j,k} - \left[\frac{\rho k_{x_1} \Delta x_2 \Delta x_3}{\mu}\left(\frac{\partial p}{\partial x_1} + \rho g \frac{\partial h}{\partial x_1}\right)\right]_{i-\frac{1}{2},j,k}\right\} \quad . \qquad \text{(C-4)}$$

Introducing Eqs. C-2 and C-3 into Eq. C-4 gives

$$(\text{lhs})_{x_1} = \left(\frac{1}{\phi_o \Delta x_1 \Delta x_2 \Delta x_3}\right)_{i,j,k}\left\{\left(\frac{\rho k_{x_1} \Delta x_2 \Delta x_3}{\mu}\right)_{i+\frac{1}{2},j,k}\left[\frac{P_{i+1,j,k} - P_{i,j,k}}{\Delta x_1} + (\rho g)_{i+\frac{1}{2},j,k}\frac{h_{i+1,j,k} - h_{i,j,k}}{\Delta x_1}\right]\right.$$

$$\left. - \left(\frac{\rho k_{x_1} \Delta x_2 \Delta x_3}{\mu}\right)_{i-\frac{1}{2},j,k}\left[\frac{P_{i,j,k} - P_{i-1,j,k}}{\Delta x_1} + (\rho g)_{i-\frac{1}{2},j,k}\frac{h_{i,j,k} - h_{i-1,j,k}}{\Delta x_1}\right]\right\} \quad . \qquad \text{(C-5)}$$

In developing Eqs. C-2 thru C-5, the grid dimensions, x_1, x_2, and x_3 , are assumed to be constant. This is just a matter of convenience. Allowing the grid dimensions to vary spatially can be accomplished without great difficulty.

The coefficients of the form $[(k_{x_1}\Delta x_2\Delta x_3)/\mu]_{i+\frac{1}{2},j,k}$ are calculated using the harmonic mean concept:

$$\left(\frac{k_{x_1}\Delta x_2\Delta x_3}{\mu}\right)_{i+\frac{1}{2},j,k} =$$

$$\frac{2\Delta x_2\Delta x_3 (k_{x_1})_{i,j,k} (k_{x_1})_{i+1,j,k}}{\mu_{i,j,k}(k_{x_1})_{i+1,j,k} + \mu_{i+1,j,k}(k_{x_1})_{i,j,k}} . \quad \text{(C-6)}$$

Using Eq. C-6, the following definitions are made:

$$N^+_{x_1} = \left(\frac{1}{\phi_o \Delta x_1 \Delta x_2 \Delta x_3}\right)_{i,j,k} \left(\frac{k_{x_1}\Delta x_2\Delta x_3}{\mu}\right)_{i+\frac{1}{2},j,k} \left(\frac{1}{\Delta x_1}\right)$$

$$= \frac{2(k_{x_1})_{i,j,k} (k_{x_1})_{i+1,j,k}}{(\phi_o)_{i,j,k} (\Delta x_1)^2 [\mu_{i,j,k}(k_{x_1})_{i+1,j,k} + \mu_{i+1,j,k}(k_{x_1})_{i,j,k}]} \quad \text{(C-7a)}$$

$$N^-_{x_1} = \frac{2(k_{x_1})_{i,j,k} (k_{x_1})_{i-1,j,k}}{(\phi_o)_{i,j,k} (\Delta x_1)^2 [\mu_{i,j,k}(k_{x_1})_{i-1,j,k} + \mu_{i-1,j,k}(k_{x_1})_{i,j,k}]} \quad \text{(C-7b)}$$

$$N^+_{x_2} = \frac{2(k_{x_2})_{i,j,k} (k_{x_2})_{i,j+1,k}}{(\phi_o)_{i,j,k} (\Delta x_2)^2 [\mu_{i,j,k}(k_{x_2})_{i,j+1,k} + \mu_{i,j+1,k}(k_{x_2})_{i,j,k}]} \quad \text{(C-7c)}$$

$$N^-_{x_2} = \frac{2(k_{x_2})_{i,j,k} (k_{x_2})_{i,j-1,k}}{(\phi_o)_{i,j,k} (\Delta x_2)^2 [\mu_{i,j,k}(k_{x_2})_{i,j-1,k} + \mu_{i,j-1,k}(k_{x_2})_{i,j,k}]} \quad \text{(C-7d)}$$

$$N^+_{x_3} = \frac{2(k_{x_3})_{i,j,k} (k_{x_3})_{i,j,k+1}}{(\phi_o)_{i,j,k} (\Delta x_3)^2 [\mu_{i,j,k}(k_{x_3})_{i,j,k+1} + \mu_{i,j,k+1}(k_{x_3})_{i,j,k}]} \quad \text{(C-7e)}$$

$$N^-_{x_3} = \frac{2(k_{x_3})_{i,j,k} (k_{x_3})_{i,j,k-1}}{(\phi_o)_{i,j,k} (\Delta x_3)^2 [\mu_{i,j,k}(k_{x_3})_{i,j,k-1} + \mu_{i,j,k-1}(k_{x_3})_{i,j,k}]} \quad \text{(C-7f)}$$

$$\rho^+_{x_1} = 0.5(\rho_{i+1,j,k} + \rho_{i,j,k}) \quad \text{(C-7g)}$$

$$\rho^-_{x_1} = 0.5(\rho_{i-1,j,k} + \rho_{i,j,k}) \quad \text{(C-7h)}$$

$$\rho^+_{x_2} = 0.5(\rho_{i,j+1,k} + \rho_{i,j,k}) \quad \text{(C-7i)}$$

$$\rho^-_{x_2} = 0.5(\rho_{i,j-1,k} + \rho_{i,j,k}) \quad \text{(C-7j)}$$

$$\rho^+_{x_3} = 0.5(\rho_{i,j,k+1} + \rho_{i,j,k}) \quad \text{(C-7k)}$$

$$\rho^-_{x_3} = 0.5(\rho_{i,j,k-1} + \rho_{i,j,k}) \quad \text{(C-7l)}$$

$$\Delta h^+_{x_1} = (h_{i+1,j,k} - h_{i,j,k}) \quad \text{(C-7m)}$$

$$\Delta h^-_{x_1} = (h_{i-1,j,k} - h_{i,j,k}) \quad \text{(C-7n)}$$

$$\Delta h^+_{x_2} = (h_{i,j+1,k} - h_{i,j,k}) \quad \text{(C-7p)}$$

$$\Delta h^-_{x_2} = (h_{i,j-1,k} - h_{i,j,k}) \quad \text{(C-7q)}$$

$$\Delta h^+_{x_3} = (h_{i,j,k+1} - h_{i,j,k}) \quad \text{(C-7r)}$$

$$\Delta h^-_{x_3} = (h_{i,j,k-1} - h_{i,j,k}) \quad \text{(C-7s)}$$

Using the notation of Eqs. C-7 and substituting difference approximations for all pressure and elevation derivatives, the left hand side of Eq. C-1 may be written as:

$$\text{lhs} = \rho^+_{x_1} N^+_{x_1} P_{i+1,j,k} + \rho^-_{x_1} N^-_{x_1} P_{i-1,j,k}$$

$$+ \rho^+_{x_2} N^+_{x_2} P_{i,j+1,k} + \rho^-_{x_2} N^-_{x_2} P_{i,j-1,k}$$

$$+ \rho^+_{x_3} N^+_{x_3} P_{i,j,k+1} + \rho^-_{x_3} N^-_{x_3} P_{i,j,k-1}$$

$$- (\rho^+_{x_1} N^+_{x_1} + \rho^-_{x_1} N^-_{x_1} + \rho^+_{x_2} N^+_{x_2} + \rho^-_{x_2} N^-_{x_2} + \rho^+_{x_3} N^+_{x_3} + \rho^-_{x_3} N^-_{x_3}) P_{i,j,k}$$

$$+ (\rho^+_{x_1})^2 N^+_{x_1} g\Delta h^+_{x_1} + (\rho^-_{x_1})^2 N^-_{x_1} g\Delta h^-_{x_1}$$

$$+ (\rho^+_{x_2})^2 N^+_{x_2} g\Delta h^+_{x_2} + (\rho^-_{x_2})^2 N^-_{x_2} g\Delta h^-_{x_2}$$

$$+ (\rho^+_{x_3})^2 N^+_{x} g\Delta h^+_{x_3} + (\rho^-_{x_3})^2 N^-_{x_3} g\Delta h^-_{x_3} \quad . \qquad \text{(C-8)}$$

The right hand side of Eq. C-1 contains derivatives with respect to time. The derivatives of pressure with respect to time will be represented by an implicit finite difference form:

$$\frac{\partial P}{\partial t} = \frac{P^{t+1}_{i,j,k} - P^{t}_{i,j,k}}{\Delta t} \quad . \qquad \text{(C-9)}$$

The derivatives of concentration with respect to time will be approximated from the previous, not the present, time interval:

$$\frac{\partial C}{\partial t} = \frac{C^{t}_{i,j,k} - C^{t-1}_{i,j,k}}{\Delta t_o} \quad , \qquad \text{(C-10)}$$

where Δt_o is the time increment used in the preceding time step. Combining Eqs. C-9 and C-10, the right hand side of Eq. C-1 becomes:

$$\text{rhs} = \frac{(\rho_o)_{i,j,k}(C_F{}^{+\beta})_{i,j,k}}{\Delta t} P^{t+1}_{i,j,k}$$

$$- \frac{(\rho_o)_{i,j,k}(C_F{}^{+\beta})_{i,j,k}}{\Delta t} P^{t}_{i,j,k}$$

$$+ \frac{\alpha_{i,j,k}(C^{t}_{i,j,k} - C^{t-1}_{i,j,k})}{\Delta t_o} + \frac{(\rho_p Q)_{i,j,k}}{(\phi_o \Delta x_1 \Delta x_2 \Delta x_3)_{i,j,k}} \quad . \qquad \text{(C-11)}$$

An implicit finite difference representation of Eq. C-1 may be obtained by combining Eqs. C-8 and C-11 to give:

$$\rho^+_{x_1} N^+_{x_1} P^{t+1}_{i+1,j,k} + \rho^-_{x_1} N^-_{x_1} P^{t+1}_{i-1,j,k} + \rho^+_{x_2} N^+_{x_2} P^{t+1}_{i,j+1,k}$$

$$+ \rho^-_{x_2} N^-_{x_2} P^{t+1}_{i,j-1,k} + \rho^+_{x_3} N^+_{x_3} P^{t+1}_{i,j,k+1} + \rho^-_{x_3} N^-_{x_3} P^{t+1}_{i,j,k-1}$$

$$- \left[\rho^+_{x_1} N^+_{x_1} + \rho^-_{x_1} N^-_{x_1} + \rho^+_{x_2} N^+_{x_2} + \rho^-_{x_2} N^-_{x_2} + \rho^+_{x_3} N^+_{x_3} + \rho^-_{x_3} N^-_{x_3} \right.$$

$$\left. + \frac{(\rho_o)_{i,j,k}(C_F{}^{+\beta})_{i,j,k}}{\Delta t} \right] P^{t+1}_{i,j,k}$$

$$= - \frac{(\rho_o)_{i,j,k}(C_F{}^{+\beta})_{i,j,k}}{\Delta t} P^{t}_{i,j,k}$$

$$+ \frac{\alpha_{i,j,k}(C^{t}_{i,j,k} - C^{t-1}_{i,j,k})}{\Delta t_o} + \left(\frac{\rho_p Q}{\phi_o \Delta x_1 \Delta x_2 \Delta x_3} \right)_{i,j,k}$$

$$- [(\rho^+_{x_1})^2 N^+_{x_1} g\Delta h^+_{x_1} + (\rho^-_{x_1})^2 N^-_{x_1} g\Delta h^-_{x_1} + (\rho^+_{x_2})^2 N^+_{x_2} g\Delta h^+_{x_2}$$

$$+ (\rho^-_{x_2})^2 N^-_{x_2} g\Delta h^-_{x_2} + (\rho^+_{x_3})^2 N^+_{x_3} g\Delta h^+_{x_3} + (\rho^-_{x_3})^2 N^-_{x_3} g\Delta h^-_{x_3}] \quad . \qquad \text{(C-12)}$$

The analogous implicit finite difference scheme for the two-dimensional vertical flow problem may be formulated by allowing no flow to take place across grids in the x_2-direction, i.e., $\partial P/\partial x_2 = 0$ and $\partial h/\partial x_2 = 0$. The flow in the x_1- and x_3-directions will be in terms of flow per unit width, i.e., $\Delta x_2 = 1$. Under these conditions, Eq. C-12 reduces to:

$$\rho^+_{x_1} N^+_{x_1} P^{t+1}_{i+1,k} + \rho^-_{x_1} N^-_{x_1} P^{t+1}_{i-1,k} + \rho^+_{x_3} N^+_{x_3} P^{t+1}_{i,k+1} +$$

$$\rho^-_{x_3} N^-_{x_3} P^{t+1}_{i,k-1} - \left[\rho^+_{x_1} N^+_{x_1} + \rho^-_{x_1} N^-_{x_1} + \rho^+_{x_3} N^+_{x_3} + \rho^-_{x_3} N^-_{x_3} \right.$$

$$\left. + \frac{(\rho_o)_{i,k}(C_F{}^{+\beta})_{i,k}}{\Delta t} \right] P^{t+1}_{i,k} = - \frac{(\rho_o)_{i,k}(C_F{}^{+\beta})_{i,k}}{\Delta t} P^{t}_{i,k}$$

$$+ \frac{\alpha_{i,k}(C^{t}_{i,k} - C^{t-1}_{i,k})}{\Delta t_o} + \left(\frac{\rho_p Q}{\phi_o \Delta x_1 \Delta x_3} \right)_{i,k} - [(\rho^+_{x_1})^2 N^+_{x_1} g\Delta h^+_{x_1}$$

$$+ (\rho^-_{x_1})^2 N^-_{x_1} g\Delta h^-_{x_1} + (\rho^+_{x_3})^2 N^+_{x_3} g\Delta h^+_{x_3} + (\rho^-_{x_3})^2 N^-_{x_3} g\Delta h^-_{x_3}] \quad . \qquad \text{(C-13)}$$

All coefficients in Eq. C-13 are calculated from Eq. C-7 with $\Delta x_2 = 1$ for all grids.

APPENDIX D

DEVELOPMENT OF FINITE DIFFERENCE EQUATION FOR THE DISPERSION EQUATION

A numerical solution to the dispersion equation will be obtained by using the method of characteristics. The dispersion equation was given by Eq. B-40, and is reproduced here in the form:

$$\frac{\partial C}{\partial t} = \frac{\omega}{\phi \Delta A_i} \frac{\partial}{\partial x_i} \left[D^*_{ij} \phi \Delta A_i \frac{\partial C}{\partial x_j} \right] - V_i \frac{\partial C}{\partial x_i} - (C_p - C) \frac{Q}{\phi \Delta x_1 \Delta x_2 \Delta x_3} \quad , \tag{D-1}$$

where $\omega = \frac{\rho}{\rho - \alpha C}$, and

$$D^*_{ij} = D_{ij} + D_d T_{ij} \quad .$$

Following the development of Garder et al. (1964), the second order terms of Eq. D-1 are regarded as given functions of x_1 , x_2 , x_3 , and t , and Eq. D-1 treated as a first-order equation. Such an equation will then have four characteristic curves which are the solutions to the following ordinary differential equation:

$$\frac{dx_1}{dt} = V_1 \quad , \tag{D-2}$$

$$\frac{dx_2}{dt} = V_2 \quad , \tag{D-3}$$

$$\frac{dx_3}{dt} = V_3 \quad , \tag{D-4}$$

and

$$\frac{\partial C}{\partial t} = \frac{\omega}{\phi \Delta A_i} \frac{\partial}{\partial x_i} \left[D^*_{ij} \phi \Delta A_i \frac{\partial C}{\partial x_j} \right] \quad . \tag{D-5}$$

A fifth characteristic curve could be written for the production term, $(C_p - C)(Q/\phi \Delta x_1 \Delta x_2 \Delta x_3)$. However, the production term will be treated as a boundary condition of the moving points described below.

In addition to the usual division of the flow region into a grid system, a set of moving points is introduced into this numerical solution. Each one of the moving points has associated with it a concentration, which varies with time. Within each time interval, the moving points are relocated using the finite difference equations,

$$X_{1_\ell}^{t+1} = X_{1_\ell}^{t} + \Delta t \, V_{1_\ell}^{t+1} \quad , \tag{D-6}$$

$$X_{2_\ell}^{t+1} = X_{2_\ell}^{t} + \Delta t \, V_{2_\ell}^{t+1} \quad , \tag{D-7}$$

and

$$X_{3_\ell}^{t+1} = X_{3_\ell}^{t} + \Delta t \, V_{3_\ell}^{t+1} \quad , \tag{D-8}$$

where $t+1$ is the new time level and t is the old time level. Each cell in the grid system is assigned a concentration equal to the average of the concentrations of the moving points located inside the cell at time $t+1$. The concentration of the cell is then modified for dispersion by solving the explicit form of Eq. D-5.

Because of symmetry only a detailed description of the finite difference form of Eq. D-5 in the x_1-direction will be given. Expanding the x_1-derivative on the right hand side of Eq. D-5 gives

$$(\text{rhs})_{x_1} = \frac{\omega}{\phi \Delta x_2 \Delta x_3} \frac{\partial}{\partial x_i} \left[D^*_{11} \phi \Delta x_2 \Delta x_3 \frac{\partial C}{\partial x_2} + D^*_{12} \phi \Delta x_2 \Delta x_3 \frac{\partial C}{\partial x_2} + D^*_{13} \phi \Delta x_2 \Delta x_3 \frac{\partial C}{\partial x_3} \right] \quad . \tag{D-9}$$

As can be seen, Eq. D-9 involves the cross derivatives of the concentration. Also, there are six more second order terms in Eq. D-5 in addition to the three given in Eq. D-9,

To develop a finite difference form of Eq. D-9, consider the cell (i,j,k) as shown in Fig. D-1, and the 18 indicated adjacent cells. The spatial derivatives at a point on the boundary between cells (i,j,k) and (i+1,j,k) may be approximated by

$$\left(\frac{\partial C}{\partial x_1} \right)_{i+\frac{1}{2},j,k} = \frac{C_{i+1,j,k} - C_{i,j,k}}{\Delta x_1} \quad , \tag{D-10a}$$

$$\left(\frac{\partial C}{\partial x_2} \right)_{i+\frac{1}{2},j,k} = \frac{C_{i+\frac{1}{2},j+1,k} - C_{i+\frac{1}{2},j-1,k}}{2\Delta x_2} \quad , \tag{D-10b}$$

$$\left(\frac{\partial C}{\partial x_3} \right)_{i+\frac{1}{2},j,k} = \frac{C_{i+\frac{1}{2},j,k+1} - C_{i+\frac{1}{2},j,k-1}}{2\Delta x_3} \quad . \tag{D-10c}$$

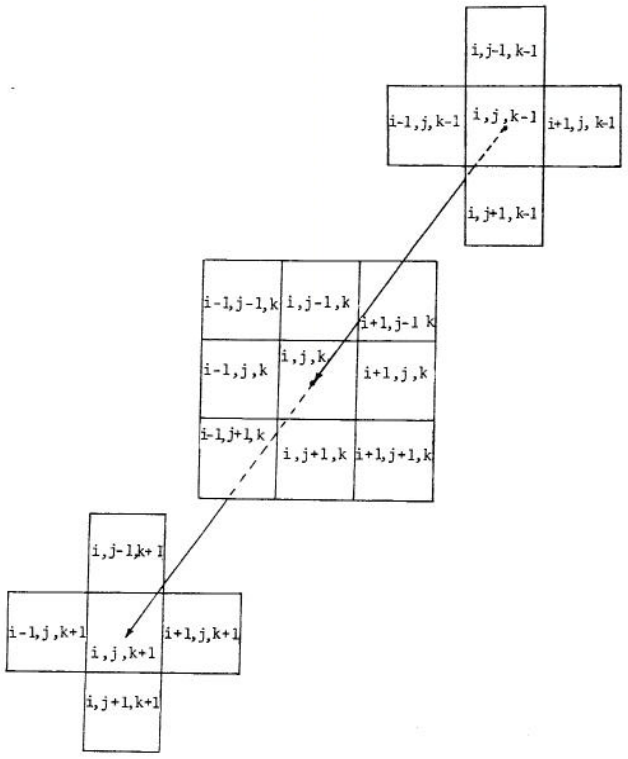

Fig. D-1 Three-dimensional grid system with subscripting used to develop the finite difference form of the dispersion equation.

Using a linear interpolation scheme,

$$C_{i+\frac{1}{2},j+1,k} = \frac{C_{i,j+1,k} + C_{i+1,j+1,k}}{2} , \qquad \text{(D-11a)}$$

$$C_{i+\frac{1}{2},j-1,k} = \frac{C_{i,j-1,k} + C_{i+1,j-1,k}}{2} , \qquad \text{(D-11b)}$$

$$C_{i+\frac{1}{2},j,k+1} = \frac{C_{i,j,k+1} + C_{i+1,j,k+1}}{2} , \qquad \text{(D-11c)}$$

$$C_{i+\frac{1}{2},j,k-1} = \frac{C_{i,j,k-1} + C_{i+1,j,k-1}}{2} . \qquad \text{(D-11d)}$$

In writing Eqs. D-10 and D-11, all spatial increments, Δx_1, Δx_2, and Δx_3, are assumed to be equal. This is in keeping with the finite difference grid system proposed in Chapter IV, and the problems that are solved in Chapter V.

Substituting Eqs. D-11 into Eqs. D-10 gives

$$\left(\frac{\partial C}{\partial x_1}\right)_{i+\frac{1}{2},j,k} = \frac{C_{i+1,j,k} - C_{i,j,k}}{\Delta x_1} , \qquad \text{(D-12a)}$$

$$\left(\frac{\partial C}{\partial x_2}\right)_{i+\frac{1}{2},j,k} = \frac{C_{i,j+1,k}+C_{i+1,j+1,k}-C_{i,j-1,k}-C_{i+1,j-1,k}}{4\Delta x_2} \qquad \text{(D-12b)}$$

$$\left(\frac{\partial C}{\partial x_3}\right)_{i+\frac{1}{2},j,k} = \frac{C_{i,j,k+1}+C_{i+1,j,k+1}-C_{i,j,k-1}-C_{i+1,j,k-1}}{4\Delta x_3} . \qquad \text{(D-12c)}$$

Similarly, for a point on the boundary between cells (i,j,k) and (i-1,j,k), the spatial derivatives are

$$\left(\frac{\partial C}{\partial x_1}\right)_{i-\frac{1}{2},j,k} = \frac{C_{i,j,k} - C_{i-1,j,k}}{\Delta x_1} , \qquad \text{(D-13a)}$$

$$\left(\frac{\partial C}{\partial x_2}\right)_{i-\frac{1}{2},j,k} = \frac{C_{i,j+1,k}+C_{i-1,j+1,k}-C_{i,j-1,k}-C_{i-1,j-1,k}}{4\Delta x_2} , \qquad \text{(D-13b)}$$

$$\left(\frac{\partial C}{\partial x_3}\right)_{i-\frac{1}{2},j,k} = \frac{C_{i,j,k+1}+C_{i-1,j,k+1}-C_{i,j,k-1}-C_{i-1,j,k-1}}{4\Delta x_3} . \qquad \text{(D-13c)}$$

Now using a central finite difference scheme, Eq. D-9 may be written as

$$(rhs)_{x_1} = \left(\frac{\omega}{\phi\Delta x_2\Delta x_3}\right)_{i,j,k} \left\{ \frac{\left(D^*_{11}\phi\Delta x_2\Delta x_3 \frac{\partial C}{\partial x_1}\right)_{i+\frac{1}{2},j,k}}{\Delta x_1} - \frac{\left(D^*_{11}\phi\Delta x_2\Delta x_3 \frac{\partial C}{\partial x_1}\right)_{i-\frac{1}{2},j,k}}{\Delta x_1} + \frac{\left(D^*_{12}\phi\Delta x_2\Delta x_3 \frac{\partial C}{\partial x_2}\right)_{i+\frac{1}{2},j,k}}{\Delta x_1} - \frac{\left(D^*_{12}\phi\Delta x_2\Delta x_3 \frac{\partial C}{\partial x_2}\right)_{i-\frac{1}{2},j,k}}{\Delta x_1} + \frac{\left(D^*_{13}\phi\Delta x_2\Delta x_3 \frac{\partial C}{\partial x_3}\right)_{i+\frac{1}{2},j,k}}{\Delta x_1} - \frac{\left(D^*_{13}\phi\Delta x_2\Delta x_3 \frac{\partial C}{\partial x_3}\right)_{i-\frac{1}{2},j,k}}{\Delta x_1} \right\} . \qquad \text{(D-14)}$$

Introducing Eqs. D-12 and D-13 into Eq. D-14 gives

$$(rhs)_{x_1} =$$

$$\left(\frac{\omega}{\phi\Delta x_2\Delta x_3}\right)_{i,j,k} \left\{ \frac{(D^*_{11}\phi\Delta x_2\Delta x_3)_{i+\frac{1}{2},j,k}(C_{i+1,j,k}-C_{i,j,k})}{(\Delta x_1)^2} \right.$$

$$- \frac{(D^*_{11}\phi\Delta x_2\Delta x_3)_{i-\frac{1}{2},j,k}(C_{i,j,k}-C_{i-1,j,k})}{(\Delta x_1)^2}$$

$$+ \frac{(D^*_{12}\phi\Delta x_2\Delta x_3)_{i+\frac{1}{2},j,k}(C_{i,j+1,k}+C_{i+1,j+1,k}-C_{i,j-1,k}-C_{i+1,j-1,k})}{4\Delta x_1\Delta x_2}$$

$$- \frac{(D^*_{12}\phi\Delta x_2\Delta x_3)_{i-\frac{1}{2},j,k}(C_{i,j+1,k}+C_{i-1,j+1,k}-C_{i,j-1,k}-C_{i-1,j-1,k})}{4\Delta x_1\Delta x_2}$$

$$+ \frac{(D^*_{13}\phi\Delta x_2\Delta x_3)_{i+\frac{1}{2},j,k}(C_{i,j,k+1}+C_{i+1,j.k+1}-C_{i,j,k-1}-C_{i+1,j,k-1})}{4\Delta x_1\Delta x_3}$$

$$\left. - \frac{(D^*_{13}\phi\Delta x_2\Delta x_3)_{i-\frac{1}{2},j,k}(C_{i,j,k+1}+C_{i-1,j,k+1}-C_{i,j,k-1}-C_{i-1,j,k-1})}{4\Delta x_1\Delta x_3} \right\}$$

(D-15)

Coefficients of the form $(D^*_{11}\phi\Delta x_2\Delta x_3)_{i+\frac{1}{2},j,k}$ will be calculated using the harmonic mean, i.e.:

$$(D^*_{11}\phi\Delta x_2\Delta x_3)_{i+\frac{1}{2},j,k} = \frac{2(\phi D^*_{11})_{i,j,k}(\phi D^*_{11})_{i+1,j,k}\Delta x_2\Delta x_3}{(\phi D^*_{11})_{i,j,k}+(\phi D^*_{11})_{i+1,j,k}} .$$

(D-16)

Thus, the coefficients of concentration in Eq. D-15 are of the form

$$\frac{\omega_{i,j,k}(D^*_{11}\phi\Delta x_2\Delta x_3)_{i+\frac{1}{2},j,k}}{\phi_{i,j,k}\Delta x_2\Delta x_3(\Delta x_1)^2} = \frac{2(\omega D^*_{11})_{i,j,k}(\phi D^*_{11})_{i+1,j,k}}{(\Delta x_1)^2[(\phi D^*_{11})_{i,j,k}+(\phi D^*_{11})_{i+1,j,k}]}$$

(D-17)

In a completely analogous development to that used in Eqs. D-10 thru D-16, the x_2-derivative and x_3-derivative on the right hand side of Eq. D-5 may be obtained. In obtaining the x_2-derivative, a central difference scheme using the points $(i,j+\frac{1}{2},k)$ and $(i,j-\frac{1}{2},k)$ is used, while the x_3-derivative uses the points $(i,j,k+\frac{1}{2})$ and $(i,j,k-\frac{1}{2})$. An explicit form of the left hand side of Eq. D-5 is

$$\frac{dC}{dt} = \frac{C^{t+1}_{i,j,k} - C^t_{i,j,k}}{\Delta t} . \qquad \text{(D-18)}$$

To simplify notation the following definitions are made:

$$E^+_{x_1x_1} = \frac{2(\omega D^*_{11})_{i,j,k}(\phi D^*_{11})_{i+1,j,k}\Delta t}{(\Delta x_1)^2[(\phi D^*_{11})_{i,j,k}+(\phi D^*_{11})_{i+1,j,k}]} , \qquad \text{(D-19a)}$$

$$E^-_{x_1x_1} = \frac{2(\omega D^*_{11})_{i,j,k}(\phi D^*_{11})_{i-1,j,k}\Delta t}{(\Delta x_1)^2[(\phi D^*_{11})_{i,j,k}+(\phi D^*_{11})_{i-1,j,k}]} , \qquad \text{(D-19b)}$$

$$E^+_{x_2x_2} = \frac{2(\omega D^*_{22})_{i,j,k}(\phi D^*_{22})_{i,j+1,k}\Delta t}{(\Delta x_2)^2[(\phi D^*_{22})_{i,j,k}+(\phi D^*_{22})_{i,j+1,k}]} , \qquad \text{(D-19c)}$$

$$E^-_{x_2x_2} = \frac{2(\omega D^*_{22})_{i,j,k}(\phi D^*_{22})_{i,j-1,k}\Delta t}{(\Delta x_2)^2[(\phi D^*_{22})_{i,j,k}+(\phi D^*_{22})_{i,j-1,k}]} , \qquad \text{(D-19d)}$$

$$E^+_{x_3x_3} = \frac{2(\omega D^*_{33})_{i,j,k}(\phi D^*_{33})_{i,j,k+1}\Delta t}{(\Delta x_3)^2[(\phi D^*_{33})_{i,j,k}+(\phi D^*_{33})_{i,j,k+1}]} , \qquad \text{(D-19e)}$$

$$E^-_{x_3x_3} = \frac{2(\omega D^*_{33})_{i,j,k}(\phi D^*_{33})_{i,j,k-1}\Delta t}{(\Delta x_3)^2[(\phi D^*_{33})_{i,j,k}+(\phi D^*_{33})_{i,j,k-1}]} , \qquad \text{(D-19f)}$$

$$F^+_{x_1x_2} = \frac{(\omega D^*_{12})_{i,j,k}(\phi D^*_{12})_{i+1,j,k}\Delta t}{2\Delta x_1\Delta x_2[(\phi D^*_{12})_{i,j,k}+(\phi D^*_{12})_{i+1,j,k}]} , \qquad \text{(D-19g)}$$

$$F^-_{x_1x_2} = \frac{(\omega D^*_{12})_{i,j,k}(\phi D^*_{12})_{i-1,j,k}\Delta t}{2\Delta x_1\Delta x_2[(\phi D^*_{12})_{i,j,k}+(\phi D^*_{12})_{i-1,j,k}]} , \qquad \text{(D-19h)}$$

$$F^+_{x_2x_1} = \frac{(\omega D^*_{21})_{i,j,k}(\phi D^*_{21})_{i,j+1,k}\Delta t}{2\Delta x_1\Delta x_2[(\phi D^*_{21})_{i,j,k}+(\phi D^*_{21})_{i,j+1,k}]} , \qquad \text{(D-19i)}$$

$$F^-_{x_2x_1} = \frac{(\omega D^*_{21})_{i,j,k}(\phi D^*_{21})_{i,j-1,k}\Delta t}{2\Delta x_1\Delta x_2[(\phi D^*_{21})_{i,j,k}+(\phi D^*_{21})_{i,j-1,k}]} , \qquad \text{(D-19j)}$$

$$G^{+}_{x_1x_3} = \frac{(\omega D^{*}_{13})_{i,j,k}(\phi D^{*}_{13})_{i+1,j,k}\Delta t}{2\Delta x_1\Delta x_3[(\phi D^{*}_{13})_{i,j,k}+(\phi D^{*}_{13})_{i+1,j,k}]} \quad , \quad \text{(D-19k)}$$

$$G^{-}_{x_1x_3} = \frac{(\omega D^{*}_{13})_{i,j,k}(\phi D^{*}_{13})_{i-1,j,k}\Delta t}{2\Delta x_1\Delta x_3[(\phi D^{*}_{13})_{i,j,k}+(\phi D^{*}_{13})_{i-1,j,k}]} \quad , \quad \text{(D-19ℓ)}$$

$$G^{+}_{x_3x_1} = \frac{(\omega D^{*}_{31})_{i,j,k}(\phi D^{*}_{31})_{i,j,k+1}\Delta t}{2\Delta x_1\Delta x_3[(\phi D^{*}_{31})_{i,j,k}+(\phi D^{*}_{31})_{i,j,k+1}]} \quad , \quad \text{(D-19m)}$$

$$G^{-}_{x_3x_1} = \frac{(\omega D^{*}_{31})_{i,j,k}(\phi D^{*}_{31})_{i,j,k-1}\Delta t}{2\Delta x_1\Delta x_3[(\phi D^{*}_{31})_{i,j,k}+(\phi D^{*}_{31})_{i,j,k-1}]} \quad , \quad \text{(D-19n)}$$

$$H^{+}_{x_2x_3} = \frac{(\omega D^{*}_{23})_{i,j,k}(\phi D^{*}_{23})_{i,j+1,k}\Delta t}{2\Delta x_2\Delta x_3[(\phi D^{*}_{23})_{i,j,k}+(\phi D^{*}_{23})_{i,j+1,k}]} \quad , \quad \text{(D-19p)}$$

$$H^{-}_{x_2x_3} = \frac{(\omega D^{*}_{23})_{i,j,k}(\phi D^{*}_{23})_{i,j-1,k}\Delta t}{2\Delta x_2\Delta x_3[(\phi D^{*}_{23})_{i,j,k}+(\phi D^{*}_{23})_{i,j-1,k}]} \quad , \quad \text{(D-19q)}$$

$$H^{+}_{x_3x_2} = \frac{(\omega D^{*}_{32})_{i,j,k}(\phi D^{*}_{32})_{i,j,k+1}\Delta t}{2\Delta x_2\Delta x_3[(\phi D^{*}_{32})_{i,j,k}+(\phi D^{*}_{32})_{i,j,k+1}]} \quad , \quad \text{(D-19r)}$$

$$H^{-}_{x_3x_2} = \frac{(\delta D^{*}_{32})_{i,j,k}(\phi D^{*}_{32})_{i,j,k-1}\Delta t}{2\Delta x_2\Delta x_3[(\phi D^{*}_{32})_{i,j,k}+(\phi D^{*}_{32})_{i,j,k-1}]} \quad . \quad \text{(D-19s)}$$

Using Eq. D-18, the notation of Eqs. D-19, and substituting difference approximations for all concentration derivatives, the explicit form of Eq. D-5 becomes:

$$\begin{aligned}
C^{t+1}_{i,j,k} = {} & C^{t}_{i,j,k} + E^{+}_{x_1x_1}(C^{t}_{i+1,j,k} - C^{t}_{i,j,k}) \\
& - E^{-}_{x_1x_1}(C^{t}_{i,j,k} - C^{t}_{i-1,j,k}) + E^{+}_{x_2x_2}(C^{t}_{i,j+1,k} - C^{t}_{i,j,k}) \\
& - E^{-}_{x_2x_2}(C^{t}_{i,j,k} - C^{t}_{i,j-1,k}) + E^{+}_{x_3x_3}(C^{t}_{i,j,k+1} - C^{t}_{i,j,k}) \\
& - E^{-}_{x_3x_3}(C^{t}_{i,j,k} - C^{t}_{i,j,k-1}) \\
& + F^{+}_{x_1x_2}(C^{t}_{i,j+1,k} + C^{t}_{i+1,j+1,k} - C^{t}_{i,j-1,k} - C^{t}_{i+1,j-1,k}) \\
& - F^{-}_{x_1x_2}(C^{t}_{i,j+1,k} + C^{t}_{i-1,j+1,k} - C^{t}_{i,j-1,k} - C^{t}_{i-1,j-1,k}) \\
& + F^{+}_{x_2x_1}(C^{t}_{i+1,j,k} + C^{t}_{i+1,j+1,k} - C^{t}_{i-1,j,k} - C^{t}_{i-1,j+1,k}) \\
& - F^{-}_{x_2x_1}(C^{t}_{i+1,j,k} + C^{t}_{i+1,j-1,k} - C^{t}_{i-1,j,k} - C^{t}_{i-1,j-1,k}) \\
& + G^{+}_{x_1x_3}(C^{t}_{i,j,k+1} + C^{t}_{i+1,j,k+1} - C^{t}_{i,j,k-1} - C^{t}_{i+1,j,k-1}) \\
& - G^{-}_{x_1x_3}(C^{t}_{i-1,j,k+1} + C^{t}_{i,j,k+1} - C^{t}_{i,j,k-1} - C^{t}_{i-1,j,k-1}) \\
& + G^{+}_{x_3x_1}(C^{t}_{i+1,j,k+1} + C^{t}_{i+1,j,k} - C^{t}_{i-1,j,k+1} - C^{t}_{i-1,j,k}) \\
& - G^{-}_{x_3x_1}(C^{t}_{i+1,j,k} + C^{t}_{i+1,j,k-1} - C^{t}_{i-1,j,k} - C^{t}_{i-1,j,k-1}) \\
& + H^{+}_{x_2x_3}(C^{t}_{i,j,k+1} + C^{t}_{i,j+1,k+1} - C^{t}_{i,j,k-1} - C^{t}_{i,j+1,k-1}) \\
& - H^{-}_{x_2x_3}(C^{t}_{i,j-1,k+1} + C^{t}_{i,j,k+1} - C^{t}_{i,j-1,k-1} - C^{t}_{i,j,k-1}) \\
& + H^{+}_{x_3x_2}(C^{t}_{i,j+1,k+1} + C^{t}_{i,j+1,k} - C^{t}_{i,j-1,k+1} - C^{t}_{i,j-1,k}) \\
& - H^{-}_{x_3x_2}(C^{t}_{i,j+1,k} + C^{t}_{i,j+1,k-1} - C^{t}_{i,j-1,k} - C^{t}_{i,j-1,k-1}) \quad .
\end{aligned} \quad \text{(D-20)}$$

The analogous explicit finite difference equation for the two-dimensional dispersion equation may be obtained by allowing no flow to take place across grids in the x_2-direction, i.e., $(\partial C/\partial x_2)=0$. The flow in the x_1- and x_3-directions will be for a unit width of the model $(\Delta x_2=1)$. Under these conditions, the two-dimensional form of Eq. D-20 is:

$$C^{t+1}_{i,k}=C^{t}_{i,k}+E^{+}_{x_1x_1}(C^{t}_{i+1,k}-C^{t}_{i,k})-E^{-}_{x_1x_1}(C^{t}_{i,k}-C^{t}_{i-1,k})$$

$$+ E^{+}_{x_3x_3}(C^{t}_{i,k+1}-C^{t}_{i,k})-E^{-}_{x_3x_3}(C^{t}_{i,k}-C^{t}_{i,k-1})$$

$$+ G^{+}_{x_1x_3}(C^{t}_{i,k+1}+C^{t}_{i+1,k+1}-C^{t}_{i,k-1}-C^{t}_{i+1,k-1})$$

$$- G^{-}_{x_1x_3}(C^{t}_{i-1,k+1}+C^{t}_{i,k+1}-C^{t}_{i,k-1}-C^{t}_{i-1,k-1})$$

$$+ G^{+}_{x_3x_1}(C^{t}_{i+1,k+1}+C^{t}_{i+1,k}-C^{t}_{i-1,k+1}-C^{t}_{i-1,k})$$

$$- G^{-}_{x_3x_1}(C^{t}_{i+1,k}+C^{t}_{i+1,k-1}-C^{t}_{i-1,k}-C^{t}_{i-1,k-1}) \quad . \qquad \text{(D-21)}$$

The coefficients in Eq. D-21 are calculated using the definitions given in Eq. D-19 with $\Delta x_2=1$.

APPENDIX E

STABILITY ANALYSIS FOR DISPERSION EQUATION

E.1 Method of Determining Stability. The explicit finite difference form of the dispersion equation (Eq. D-20) has a stability criterion attached to its use. To examine the stability of this equation, the linear form of Eq. D-20 with constant coefficients will be used, i.e.:

$$C^{t+1}_{i,j,k} = C^{t}_{i,j,k} +$$

$$+ \frac{\omega D^*_{11}\Delta t}{(\Delta x_1)^2}\,(C^{t}_{i+1,j,k} + C^{t}_{i-1,j,k} - 2C^{t}_{i,j,k})$$

$$+ \frac{\omega D^*_{22}\Delta t}{(\Delta x_2)^2}\,(C^{t}_{i,j+1,k} + C^{t}_{i,j-1,k} - 2C^{t}_{i,j,k})$$

$$+ \frac{\omega D^*_{33}\Delta t}{(\Delta x_3)^2}\,(C^{t}_{i,j,k+1} + C^{t}_{i,j,k-1} - 2C^{t}_{i,j,k})$$

$$+ \frac{\omega(D^*_{12}+D^*_{21})\Delta t}{4\Delta x_1\Delta x_2}\,(C^{t}_{i+1,j+1,k}+C^{t}_{i-1,j-1,k}-C^{t}_{i+1,j-1,k}$$

$$-C^{t}_{i-1,j+1,k}) + \frac{\omega(D^*_{13}+D^*_{31})\Delta t}{4\Delta x_1\Delta x_3}\,(C^{t}_{i+1,j,k+1}+C^{t}_{i-1,j,k-1}$$

$$- C^{t}_{i+1,j,k-1}-C^{t}_{i-1,j,k+1}) + \frac{\omega(D^*_{23}+D^*_{32})\Delta t}{4\Delta x_2\Delta x_3}\,(C^{t}_{i,j+1,k+1}$$

$$+ C^{t}_{i,j-1,k-1}-C^{t}_{i,j+1,k-1}-C^{t}_{i,j-1,k+1}) \quad . \qquad \text{(E-1)}$$

The method used for the stability analysis is that of a Fourier series developed by von Neumann and discussed by O'Brien et al. (1951) and Smith (1960, p. 102). This technique expresses an initial line of errors in terms of a finite Fourier series, and considers the growth of a function that reduces to this series for $t=0$ by a 'variables separable' method. The errors at the nodes of the grid system for $t=0$, $0\le x_1\le N\Delta x_1$, $0\le x_2\le M\Delta x_2$, and $0\le x_3\le L\Delta x_3$ are denoted by $E_{\bar{P},\bar{Q},\bar{R}}$ where $\bar{P}=1,2,\ldots N$; $\bar{Q}=1,2,\ldots M$; $\bar{R}=1,2,\ldots L$; N = the number of grids in the x_1-direction; M = the number of grids in the x_2-direction; and L = the number of grids in the x_3-direction.

The MNL equations,

$$E_{\bar{P},\bar{Q},\bar{R}} = \sum_{n=1}^{MNL} A_n \exp[i(\psi_n\bar{P}\Delta x_1+\zeta_n\bar{Q}\Delta x_2+\gamma_n\bar{R}\Delta x_3)] \qquad \text{(E-2)}$$

are sufficient to determine the MNL unknowns A_1, $A_2,\ldots,A_{MNL}$ uniquely, thus demonstrating that an arbitrary distribution of initial errors can be expressed in the complex exponential form. In Eq. E-2, $\psi_n = \frac{n\pi}{N\Delta x_1}$, $\zeta_n = \frac{n\pi}{M\Delta x_2}$, $\gamma_n = \frac{n\pi}{L\Delta x_3}$ and $i = \sqrt{-1}$. Equation E-1 is a linear finite difference equation and separate solutions are additive. Thus, only an analysis of the error propagation in a single term of the series is necessary. This makes A_n a constant and can be neglected. As t increases, a solution of the finite difference equation is wanted such that it reduces to $\exp[i(\psi\bar{P}\Delta x_1+\zeta\bar{Q}\Delta x_2+\gamma\bar{R}\Delta x_3)]$ when $t=\bar{S}\Delta t=0$. Thus, it is assumed that

$$E^{\bar{S}}_{\bar{P},\bar{Q},\bar{R}} = \exp[i(\psi x_1 + \zeta x_2 + \gamma x_3) + \lambda t]$$

$$= \exp[i(\psi\bar{P}\Delta x_1 + \zeta\bar{Q}\Delta x_2 + \gamma\bar{R}\Delta x_3)]\xi^{\bar{S}} \quad , \qquad \text{(E-3)}$$

where $\xi = \exp(\lambda\Delta t)$, and λ is a complex constant. Note that Eq. E-3 reduces to $\exp[i(\psi\bar{P}\Delta x_1+\zeta\bar{Q}\Delta x_2+\gamma\bar{R}\Delta x_3)]$ when $\bar{S}=0$, which is the desired result. Also, the error, $E^{\bar{S}}_{\bar{P},\bar{Q},\bar{R}}$, will not increase as t increases provided

$$|\xi| \le 1 \quad . \qquad \text{(E-4)}$$

E.2 Stability Function for Three-Dimensional Dispersion Equation. Since the error $E^{\bar{S}}_{\bar{P},\bar{Q},\bar{R}}$ satisfies the same finite difference equation as $C^{t}_{i,j,k}$, then Eq. E-1 may be written in terms of $E^{\bar{S}}_{\bar{P},\bar{Q},\bar{R}}$.

For example, the first few terms of Eq. E-1 would look like

$$E^{\bar{S}+1}_{\bar{P},\bar{Q},\bar{R}} = E^{\bar{S}}_{\bar{P},\bar{Q},\bar{R}} +$$

$$\frac{\omega D^*_{11}\Delta t}{(\Delta x_1)^2}\,(E^{\bar{S}}_{\bar{P}+1,\bar{Q},\bar{R}} + E^{\bar{S}}_{\bar{P}-1,\bar{Q},\bar{R}} - 2E^{\bar{S}}_{\bar{P},\bar{Q},\bar{R}})+\ldots \quad . \qquad \text{(E-5)}$$

Substituting Eq. E-3 for the values of $E^{\overline{S}}_{\overline{P},\overline{Q},\overline{R}}$, Eq. E-5 may be written as

$$\exp[i(\psi\overline{P}\Delta x_1 + \zeta\overline{Q}\Delta x_2 + \gamma\overline{R}\Delta x_3)]\xi^{\overline{S}+1}$$

$$= \exp[i(\psi\overline{P}\Delta x_1 + \zeta\overline{Q}\Delta x_2 + \gamma\overline{R}\Delta x_3)]\xi^{\overline{S}}$$

$$+ \frac{\omega D^*_{11}\Delta t}{(\Delta x_1)^2} \exp[i(\psi(\overline{P}+1)\Delta x_1+\zeta\overline{Q}\Delta x_2+\gamma\overline{R}\Delta x_3)]\xi^{\overline{S}}$$

$$+ \exp[i(\psi(\overline{P}-1)\Delta x_1+\zeta\overline{Q}\Delta x_2+\gamma\overline{R}\Delta x_3)]\xi^{\overline{S}}$$

$$- 2\exp[i(\psi\overline{P}\Delta x_1+\zeta\overline{Q}\Delta x_2+\gamma\overline{R}\Delta x_3)]\xi^{\overline{S}} + \ldots \quad . \qquad \text{(E-6)}$$

Equation E-6 contains only the first three terms and similar terms are implied for the other five terms of the equation. Note that Eq. E-6 shows a pattern of each term containing the factor $\exp[i(\psi\overline{P}\Delta x_1 + \zeta\overline{Q}\Delta x_2 + \gamma\overline{R}\Delta x_3)]\xi^{\overline{S}}$. Thus, if Eq. E-6 were expanded in its complete form and divided thru by $\exp[i(\psi\overline{P}\Delta x_1 +\zeta\overline{Q}\Delta x_2+\gamma\overline{R}\Delta x_3)]\xi^{\overline{S}}$, the following result would be obtained:

$$\xi = 1 + \frac{\omega D^*_{11}\Delta t}{(\Delta x_1)^2}\{\exp(i\psi\Delta x_1)+\exp(-i\psi\Delta x_1)-2\}$$

$$+ \frac{\omega D^*_{22}\Delta t}{(\Delta x_2)^2}\{\exp(i\zeta\Delta x_2)+\exp(-i\zeta\Delta x_2)-2\}$$

$$+ \frac{\omega D^*_{33}\Delta t}{(\Delta x_3)^2}\{\exp(i\gamma\Delta x_3)+\exp(-i\gamma\Delta x_3)-2\}$$

$$+ \frac{\omega(D^*_{12}+D^*_{21})\Delta t}{4\Delta x_1\Delta x_2}\{\exp[i(\psi\Delta x_1+\zeta\Delta x_2)]+\exp[i(-\psi\Delta x_1-\zeta\Delta x_2)]$$

$$- \exp[i(\psi\Delta x_1-\zeta\Delta x_2)]-\exp[i(-\psi\Delta x_1+\zeta\Delta x_2)]\}$$

$$+ \frac{\omega(D^*_{13}+D^*_{31})\Delta t}{4\Delta x_1\Delta x_3}\{\exp[i(\psi\Delta x_1+\gamma\Delta x_3)]+\exp[i(-\psi\Delta x_1-\gamma\Delta x_3)]$$

$$- \exp[i(\psi\Delta x_1-\gamma\Delta x_3)] - \exp[i(-\psi\Delta x_1+\gamma\Delta x_3)]\}$$

$$+ \frac{\omega(D^*_{23}+D^*_{32})\Delta t}{4\Delta x_2\Delta x_3}\{\exp[i(\zeta\Delta x_2+\gamma\Delta x_3)]+\exp[i(-\zeta\Delta x_2-\gamma\Delta x_3)]$$

$$- \exp[i(\zeta\Delta x_2-\gamma\Delta x_3)] - \exp[i(-\zeta\Delta x_2+\gamma\Delta x_3)]\} \quad . \qquad \text{(E-7)}$$

Noting that $\exp(i\theta)=\cos\theta+i\sin\theta$, $\exp(-i\theta)=\cos\theta - i\sin\theta$, and $i^2 = -1$, Eq. E-7 becomes

$$\xi=1+\frac{2\omega D^*_{11}\Delta t}{(\Delta x_1)^2}[\cos(\psi\Delta x_1)-1]+\frac{2\omega D^*_{22}\Delta t}{(\Delta x_2)^2}[\cos(\zeta\Delta x_2)-1]$$

$$+ \frac{2\omega D^*_{33}\Delta t}{(\Delta x_3)^2}[\cos(\gamma\Delta x_3)-1] - \frac{\omega(D^*_{12}+D^*_{21})\Delta t}{\Delta x_1\Delta x_2}[$$

$$\sin(\psi\Delta x_1)\sin(\zeta\Delta x_2)]- \frac{\omega(D^*_{13}+D^*_{31})\Delta t}{\Delta x_1\Delta x_3}[\sin(\psi\Delta x_1)\sin(\gamma\Delta x_3)]$$

$$- \frac{\omega(D^*_{23}+D^*_{32})\Delta t}{\Delta x_2\Delta x_3}[\sin(\zeta\Delta x_2)\sin(\gamma\Delta x_3)] \quad . \qquad \text{(E-8)}$$

From trigonometric identities, $\cos 2\theta-1 = -2\sin^2\theta$ and $\sin 2\theta = 2\sin\theta\cos\theta$. Thus, by letting $a = \frac{\psi\Delta x_1}{2}$, $b = \frac{\zeta\Delta x_2}{2}$, and $d = \frac{\gamma\Delta x_3}{2}$, Eq. E-8 may be written as

$$\xi = 1 - \frac{4\omega D^*_{11}\Delta t}{(\Delta x_1)^2}\sin^2 a - \frac{4\omega D^*_{22}\Delta t}{(\Delta x_2)^2}\sin^2 b$$

$$- \frac{4\omega D^*_{33}\Delta t}{(\Delta x_3)^2}\sin^2 d - \frac{4\omega(D^*_{12}+D^*_{21})\Delta t}{\Delta x_1\Delta x_2}(\sin a\cos a\sin b\cos b)$$

$$- \frac{4\omega(D^*_{13}+D^*_{31})\Delta t}{\Delta x_1\Delta x_3}(\sin a\cos a\sin d\cos d)$$

$$- \frac{4\omega(D^*_{23}+D^*_{32})\Delta t}{\Delta x_2\Delta x_3}(\sin b\cos b\sin d\cos d) \quad . \qquad \text{(E-9)}$$

Thus, upon substituting Eq. E-9 into Eq. E-4, the stability of Eq. E-1 is assured if

$$0 \leq F(a,b,d) \leq \tfrac{1}{2} \quad , \qquad \text{(E-10)}$$

where

$$F_{(a,b,d)} = \frac{\omega D^*_{11}\Delta t}{(\Delta x_1)^2}\sin^2 a + \frac{\omega D^*_{22}\Delta t}{(\Delta x_2)^2}\sin^2 b$$

$$+ \frac{\omega D^*_{33}\Delta t}{(\Delta x_3)^2}\sin^2 d + \frac{\omega(D^*_{12}+D^*_{21})\Delta t}{\Delta x_1 \Delta x_2}(\sin a \cos a \sin b \cos b) +$$

$$+ \frac{\omega(D^*_{13}+D^*_{31})\Delta t}{\Delta x_1 \Delta x_3}(\sin a \cos a \sin d \cos d) +$$

$$+ \frac{\omega(D^*_{23}+D^*_{32})\Delta t}{\Delta x_2 \Delta x_3}(\sin b \cos b \sin d \cos d) \quad . \qquad \text{(E-11)}$$

$F_{(a,b,d)}$ shall be referred to as the stability function, and must satisfy Eq. E-10 for all values of a, b, and d. To investigate the range of $F_{(a,b,d)}$, an absolute maximum and minimum value of $F_{(a,b,d)}$ must be obtained. A necessary condition for a relative maximum or minimum to exist at a point is for the first partial derivatives of F to be zero when evaluated at the point (Taylor, 1955, p. 154). Taking the derivatives of Eq. E-11 and setting them equal to zero gives

$$\frac{\partial F}{\partial a} = \frac{2\omega D^*_{11}\Delta t}{(\Delta x_1)^2}\sin a \cos a + \frac{\omega(D^*_{12}+D^*_{21})\Delta t}{\Delta x_1 \Delta x_2}\Big[$$

$$\sin b \cos b(\cos^2 a - \sin^2 a)\Big] + \frac{\omega(D^*_{13}+D^*_{31})\Delta t}{\Delta x_1 \Delta x_3}\Big[$$

$$\sin d \cos d(\cos^2 a - \sin^2 a)\Big] = 0 \quad , \qquad \text{(E-12)}$$

$$\frac{\partial F}{\partial b} = \frac{2\omega D^*_{22}\Delta t}{(\Delta x_2)^2}\sin b \cos b + \frac{\omega(D^*_{12}+D^*_{21})\Delta t}{\Delta x_1 \Delta x_2}\Big[$$

$$\sin a \cos a(\cos^2 b - \sin^2 b)\Big] + \frac{\omega(D^*_{23}+D^*_{32})\Delta t}{\Delta x_2 \Delta x_3}\Big[$$

$$\sin d \cos d(\cos^2 b - \sin^2 b)\Big] = 0 \quad , \qquad \text{(E-13)}$$

and

$$\frac{\partial F}{\partial d} = \frac{2\omega D^*_{33}\Delta t}{(\Delta x_3)^2}\sin d \cos d + \frac{\omega(D^*_{13}+D^*_{31})\Delta t}{\Delta x_1 \Delta x_3}\Big[$$

$$\sin a \cos a(\cos^2 d - \sin^2 d)\Big] + \frac{\omega(D^*_{23}+D^*_{32})\Delta t}{\Delta x_2 \Delta x_3}\Big[$$

$$\sin b \cos b(\cos^2 d - \sin^2 d)\Big] = 0 \quad . \qquad \text{(E-14)}$$

By inspection, Eqs. E-12, E-13, and E-14 are satisfied when

$$\sin a = \sin b = \sin d = 0 \quad ,$$

$$\sin a = \cos b = \sin d = 0 \quad ,$$

$$\sin a = \sin b = \cos d = 0 \quad ,$$

$$\sin a = \cos b = \cos d = 0 \quad ,$$

$$\cos a = \sin b = \sin d = 0 \quad ,$$

$$\cos a = \sin b = \cos d = 0 \quad ,$$

$$\cos a = \cos b = \sin d = 0 \quad ,$$

$$\cos a = \cos b = \cos d = 0 \quad . \qquad \text{(E-15)}$$

There are other solutions to Eqs. E-12, E-13, and E-14 which shall be discussed later. At the present time, an investigation of the points given by Eq. E-15 for an absolute maximum and minimum shall be undertaken. Substituting Eqs. E-15 into Eq. E-11 gives

$$F(\sin a = \sin b = \sin d = 0) = 0 \quad ,$$

$$F(\sin a = \cos b = \sin d = 0) = \frac{\omega D^*_{22}\Delta t}{(\Delta x_2)^2} \quad ,$$

$$F(\sin a = \sin b = \cos d = 0) = \frac{\omega D^*_{33}\Delta t}{(\Delta x_3)^2} \quad .$$

$$F(\sin a = \cos b = \cos d = 0) = \frac{\omega D^*_{22}\Delta t}{(\Delta x_2)^2} + \frac{\omega D^*_{33}\Delta t}{(\Delta x_3)^2} \quad .$$

$$F(\cos a = \sin b = \sin d = 0) = \frac{\omega D^*_{11}\Delta t}{(\Delta x_1)^2} \quad ,$$

$$F(\cos a = \cos b = \sin d = 0) = \frac{\omega D^*_{11}\Delta t}{(\Delta x_1)^2} + \frac{\omega D^*_{22}\Delta t}{(\Delta x_2)^2} \quad ,$$

$$F(\cos a = \cos b = \cos d = 0) = \frac{\omega D^*_{11}\Delta t}{(\Delta x_1)^2} + \frac{\omega D^*_{22}\Delta t}{(\Delta x_2)^2} + \frac{\omega D^*_{33}\Delta t}{(\Delta x_3)^2} \quad .$$

$$F(\cos a = \cos b = \cos d = 0) \quad \frac{\omega D^*_{11}\Delta t}{(\Delta x_1)^2} + \frac{\omega D^*_{33}\Delta t}{(\Delta x_3)^2} \qquad \text{(E-16)}$$

If the coefficients ω, D^*_{11}, D^*_{22}, D^*_{33} and Δt are positive, then from Eq. E-16 F(a,b,d) has a minimum value of zero at $\sin a = \sin b = \sin d = 0$ and a maximum value of $\frac{\omega D^*_{11}\Delta t}{(\Delta x_1)^2} + \frac{\omega D^*_{22}\Delta t}{(\Delta x_2)^2} + \frac{\omega D^*_{33}\Delta t}{(\Delta x_3)^2}$ at the points where $\cos a = \cos b = \cos d = 0$.

To investigate the sufficiency conditions for a local maximum and minimum, Eq. E-11 is expanded in a Taylor's series about the point of interest, i.e.,

$$F(a,b,d)=F(\bar{a},\bar{b},\bar{d}) + \left[(a-\bar{a})\frac{\partial}{\partial a} + (b-\bar{b})\frac{\partial}{\partial b} + (d-\bar{d})\frac{\partial}{\partial d}\right]F(a,b,d)\Big|_{\bar{a},\bar{b},\bar{d}} + \frac{1}{2!}\left[(a-\bar{a})\frac{\partial}{\partial a} + (b-\bar{b})\frac{\partial}{\partial b} + (d-\bar{d})\frac{\partial}{\partial d}\right]^2 F(a,b,d)\Big|_{\bar{a},\bar{b},\bar{d}} + \text{higher order terms,} \qquad \text{(E-17)}$$

where $\bar{a}$, $\bar{b}$ and $\bar{d}$ are the values of the variables a, b and d at the point of interest. By hypothesis, the points at a maximum or minimum value of $F(a,b,d)$ have

$$\frac{\partial F}{\partial a}\Big|_{\bar{a},\bar{b},\bar{d}} = \frac{\partial F}{\partial b}\Big|_{\bar{a},\bar{b},\bar{d}} = \frac{\partial F}{\partial d}\Big|_{\bar{a},\bar{b},\bar{d}} = 0 \quad . \qquad \text{(E-18)}$$

Hence, Eq. E-17 may be written as

$$F(a,b,d) - F(\bar{a},\bar{b},\bar{d}) = \frac{1}{2}(a-\bar{a})^2\frac{\partial^2 F}{\partial a^2}\Big|_{\bar{a},\bar{b},\bar{d}} + \frac{1}{2}(b-\bar{b})^2\frac{\partial^2 F}{\partial b^2}\Big|_{\bar{a},\bar{b},\bar{d}} + \frac{1}{2}(d-\bar{d})^2\frac{\partial^2 F}{\partial d^2}\Big|_{\bar{a},\bar{b},\bar{d}} + (a-\bar{a})(b-\bar{b})\frac{\partial^2 F}{\partial a\partial b}\Big|_{\bar{a},\bar{b},\bar{d}} + (a-\bar{a})(d-\bar{d})\frac{\partial^2 F}{\partial a\partial d}\Big|_{\bar{a},\bar{b},\bar{d}} + (b-\bar{b})(d-\bar{d})\frac{\partial^2 F}{\partial b\partial d}\Big|_{\bar{a},\bar{b},\bar{d}} + \text{higher order terms.} \qquad \text{(E-19)}$$

In the neighborhood of the point (a,b,d), the principal part of the right hand side of Eq. E-19 is composed of second order terms, which may be written in a quadratic matrix form (Wylie, 1966, Chapter 11) as

$$F(a,b,d) - F(\bar{a},\bar{b},\bar{d}) = \tfrac{1}{2} \cdot \left\| (a-\bar{a})\ (b-\bar{b})\ (d-\bar{d}) \right\| \cdot \left\| \begin{matrix} \frac{\partial^2 F}{\partial a^2}\Big|_{\bar{a},\bar{b},\bar{d}} & \frac{\partial^2 F}{\partial a\partial b}\Big|_{\bar{a},\bar{b},\bar{d}} & \frac{\partial^2 F}{\partial a\partial d}\Big|_{\bar{a},\bar{b},\bar{d}} \\ \frac{\partial^2 F}{\partial a\partial b}\Big|_{\bar{a},\bar{b},\bar{d}} & \frac{\partial^2 F}{\partial b^2}\Big|_{\bar{a},\bar{b},\bar{d}} & \frac{\partial^2 F}{\partial b\partial d}\Big|_{\bar{a},\bar{b},\bar{d}} \\ \frac{\partial^2 F}{\partial a\partial d}\Big|_{\bar{a},\bar{b},\bar{d}} & \frac{\partial^2 F}{\partial b\partial d}\Big|_{\bar{a},\bar{b},\bar{d}} & \frac{\partial^2 F}{\partial d^2}\Big|_{\bar{a},\bar{b},\bar{d}} \end{matrix} \right\| \cdot \left\| \begin{matrix} (a-\bar{a}) \\ (b-\bar{b}) \\ (d-\bar{d}) \end{matrix} \right\| \qquad \text{(E-20)}$$

Eq. E-20 is of the general matrix form $[Y]=[X^T][A][X]$, where $[A]$ is a symmetric matrix and $[X]$ is a column vector. In this notation, $[A]$ is the matrix of the quadratic form and is positive-or negative-definite, semidefinite, or indefinite according to the nature of $[Y]$.

By the definition of positive-or negative-definite and maximum or minimum values, the following results may be deduced [Wylie (1966, Chapter 11)]. If $F(a,b,d)-F(\bar{a},\bar{b},\bar{d})$ is negative for all sufficiently small values of $(a-\bar{a})$, $(b-\bar{b})$, and $(d-\bar{d})$ which are not all zero, then $F(a,b,d)-F(\bar{a},\bar{b},\bar{d})$ is negative-definite and the point $(\bar{a},\bar{b},\bar{d})$ is a local maximum. If $F(a,b,d)-F(\bar{a},\bar{b},\bar{d})$ is positive for all sufficiently small values of $(a-\bar{a})$, $(b-\bar{b})$, and $(d-\bar{d})$ which are not all zero, then $F(a,b,d)-F(\bar{a},\bar{b},\bar{d})$ is positive definite and the point $(\bar{a},\bar{b},\bar{d})$ is a local minimum. The point $(\bar{a},\bar{b},\bar{d})$ is neither a maximum nor a minimum if $F(a,b,d)-F(\bar{a},\bar{b},\bar{d})$ is sometimes positive and sometimes negative in the neighborhood of the point $(\bar{a},\bar{b},\bar{d})$, and this is the case if the quadratic form is indefinite. If the quadratic form is semidefinite, then no decision about the nature of the point $(\bar{a},\bar{b},\bar{d})$ may be deduced and a consideration of the higher order terms of the Taylor's series would be necessary.

From Wylie (1966, p. 468), a necessary and sufficient condition that the real quadratic form, $[X^T]\ [A]\ [X]$, be positive-definite (or negative-definite) is that the quantities

$$\det|a_{11}|\ ,\quad \det\begin{vmatrix} a_{11} & a_{12} \\ a_{21} & a_{22} \end{vmatrix}\ ,\ldots\ \det\begin{vmatrix} a_{11} & \cdots & a_{1n} \\ \cdots & \cdots & \cdots \\ a_{n1} & \cdots & a_{nn} \end{vmatrix} \qquad \text{(E-21)}$$

all be positive (or for negative-definite to alternate in sign, with $\det|a_{11}|$ negative), where a_{11}, a_{12}, ..., a_{nn} are the elements of matrix [A] . Applying the above discussion and Eq. E-21 to Eq. E-20, the following conclusions may be obtained:
If

$$\frac{\partial^2 F}{\partial a^2}\bigg|_{\bar{a},\bar{b},\bar{d}} > 0 \quad , \tag{E-22}$$

$$\left\{\frac{\partial^2 F}{\partial a^2}\frac{\partial^2 F}{\partial b^2} - \left(\frac{\partial^2 F}{\partial a \partial b}\right)^2\right\}\bigg|_{\bar{a},\bar{b},\bar{d}} > 0 \quad , \tag{E-23}$$

and

$$\left\{\frac{\partial^2 F}{\partial a^2}\frac{\partial^2 F}{\partial b^2}\frac{\partial^2 F}{\partial d^2} + 2\frac{\partial^2 F}{\partial a \partial b}\frac{\partial^2 F}{\partial b \partial d}\frac{\partial^2 F}{\partial a \partial d} - \left(\frac{\partial^2 F}{\partial a \partial d}\right)^2\frac{\partial^2 F}{\partial b^2} - \left(\frac{\partial^2 F}{\partial b \partial d}\right)^2\frac{\partial^2 F}{\partial a^2} - \left(\frac{\partial^2 F}{\partial a \partial b}\right)^2\frac{\partial^2 F}{\partial d^2}\right\}\bigg|_{\bar{a},\bar{b},\bar{d}} > 0 \quad , \tag{E-24}$$

then Eq. E-20 is positive-definite and the point $(\bar{a},\bar{b},\bar{d})$ is a relative minimum. If Eq. E-22 is negative, Eq. E-23 is positive, and Eq. E-24 is negative, then Eq. E-20 is negative-definite and the point $(\bar{a},\bar{b},\bar{d})$ is a relative maximum.

Taking the second partial derivatives of Eq. E-11 gives

$$\frac{\partial^2 F}{\partial a^2} = \frac{2\omega D^*_{11}\Delta t}{(\Delta x_1)^2}(\cos^2 a - \sin^2 a) - \frac{4\omega(D^*_{12}+D^*_{21})\Delta t}{\Delta x_1 \Delta x_2}\sin b \cos b \sin a \cos a - \frac{4\omega(D^*_{13}+D^*_{31})\Delta t}{\Delta x_1 \Delta x_3}\sin d \cos d \sin a \cos a \quad , \tag{E-25a}$$

$$\frac{\partial^2 F}{\partial b^2} = \frac{2\omega D^*_{22}\Delta t}{(\Delta x_2)^2}(\cos^2 b - \sin^2 b) - \frac{4\omega(D^*_{12}+D^*_{21})\Delta t}{\Delta x_1 \Delta x_2}\sin a \cos a \sin b \cos b - \frac{4\omega(D^*_{23}+D^*_{32})\Delta t}{\Delta x_2 \Delta x_3}\sin d \cos d \sin b \cos b \quad , \tag{E-25b}$$

$$\frac{\partial^2 F}{\partial d^2} = \frac{2\omega D^*_{33}\Delta t}{(\Delta x_3)^2}(\cos^2 d - \sin^2 d) - \frac{4\omega(D^*_{13}+D^*_{31})\Delta t}{\Delta x_1 \Delta x_3}\sin a \cos a \sin d \cos d - \frac{4\omega(D^*_{23}+D^*_{32})\Delta t}{\Delta x_2 \Delta x_3}\sin b \cos b \sin d \cos d \quad , \tag{E-25c}$$

$$\frac{\partial^2 F}{\partial a \partial b} = \frac{\omega(D^*_{12}+D^*_{21})\Delta t}{\Delta x_1 \Delta x_2}(\cos^2 b - \sin^2 b)(\cos^2 a - \sin^2 a) \quad , \tag{E-25d}$$

$$\frac{\partial^2 F}{\partial a \partial d} = \frac{\omega(D^*_{13}+D^*_{31})\Delta t}{\Delta x_1 \Delta x_3}(\cos^2 d - \sin^2 d)(\cos^2 a - \sin^2 a) \quad , \tag{E-25e}$$

$$\frac{\partial^2 F}{\partial b \partial d} = \frac{\omega(D^*_{23}+D^*_{32})\Delta t}{\Delta x_2 \Delta x_3}(\cos^2 d - \sin^2 d)(\cos^2 b - \sin^2 b) \quad . \tag{E-25f}$$

From Eq. E-16, a candidate for a minimum value of F is the point where $\sin a = \sin b = \sin d = 0$. Using this point to evaluate Eqs. E-25 gives:

$$\frac{\partial^2 F}{\partial a^2}\bigg|_{\sin a=\sin b=\sin d=0} = \frac{2\omega D^*_{11}\Delta t}{(\Delta x_1)^2} \quad , \tag{E-26a}$$

$$\frac{\partial^2 F}{\partial b^2}\bigg|_{\sin a=\sin b=\sin d=0} = \frac{2\omega D^*_{22}\Delta t}{(\Delta x_2)^2} \quad , \tag{E-26b}$$

$$\frac{\partial^2 F}{\partial d^2}\bigg|_{\sin a=\sin b=\sin d=0} = \frac{2\omega D^*_{33}\Delta t}{(\Delta x_3)^2} \quad , \tag{E-26c}$$

$$\frac{\partial^2 F}{\partial a \partial b}\bigg|_{\sin a=\sin b=\sin d=0} = \frac{\omega(D^*_{12}+D^*_{21})\Delta t}{\Delta x_1 \Delta x_2} \quad . \tag{E-26d}$$

$$\frac{\partial^2 F}{\partial a \partial d}\bigg|_{\sin a=\sin b=\sin d=0} = \frac{\omega(D^*_{13}+D^*_{31})\Delta t}{\Delta x_1 \Delta x_3} \quad , \tag{E-26e}$$

$$\frac{\partial^2 F}{\partial b \partial d}\bigg|_{\sin a=\sin b=\sin d=0} = \frac{\omega(D^*_{23}+D^*_{32})\Delta t}{\Delta x_2 \Delta x_3} \quad . \tag{E-26f}$$

Using Eqs. E-22, E-23, E-24, and E-26, the points where $\sin a = \sin b = \sin d = 0$ will be a minimum if the following conditions hold:

$$\frac{2\omega D_{11}^{*}\Delta t}{(\Delta x_1)^2} > 0 \quad , \tag{E-27a}$$

$$\frac{4\omega^2 D_{11}^{*} D_{22}^{*}\Delta t^2}{(\Delta x_1)^2(\Delta x_2)^2} > \frac{\omega^2(D_{12}+D_{21})^2\Delta t^2}{(\Delta x_1)^2(\Delta x_2)^2} \quad , \tag{E-27b}$$

and

$$\frac{8\omega^3 D_{11}^{*} D_{22}^{*} D_{33}^{*}\Delta t^3}{(\Delta x_1)^2(\Delta x_2)^2(\Delta x_3)^2} + \frac{2\omega^3(D_{12}^{*}+D_{21}^{*})(D_{13}^{*}+D_{31}^{*})(D_{23}^{*}+D_{32}^{*})\Delta t^3}{(\Delta x_1)^2(\Delta x_2)^2(\Delta x_3)^2}$$

$$- \frac{2\omega^3 D_{22}^{*}(D_{13}^{*}+D_{31}^{*})^2\Delta t^3}{(\Delta x_1)^2(\Delta x_2)^2(\Delta x_3)^2} - \frac{2\omega^3 D_{11}^{*}(D_{23}^{*}+D_{32}^{*})^2\Delta t^3}{(\Delta x_1)^2(\Delta x_2)^2(\Delta x_3)^2}$$

$$- \frac{2\omega^3 D_{33}^{*}(D_{12}^{*}+D_{21}^{*})\Delta t^3}{(\Delta x_1)^2(\Delta x_2)^2(\Delta x_3)^2} > 0 \quad . \tag{E-27c}$$

Noting that Δt , Δx_1 , Δx_2 , Δx_3 , and ω are all positive, then Eq. E-27 reduces to

$$D_{11}^{*} > 0 \quad , \tag{E-28a}$$

$$4D_{11}^{*}D_{22}^{*} > (D_{12}^{*}+D_{21}^{*})^2 \quad , \tag{E-28b}$$

$$4D_{11}^{*}D_{22}^{*}D_{33}^{*} + (D_{12}^{*}+D_{21}^{*})(D_{13}^{*}+D_{31}^{*})(D_{23}^{*}+D_{32}^{*})$$

$$- D_{22}^{*}(D_{13}^{*}+D_{31}^{*})^2 - D_{11}^{*}(D_{23}^{*}+D_{32}^{*})^2 - D_{33}^{*}(D_{12}^{*}+D_{21}^{*})^2 > 0 \quad . \tag{E-28c}$$

The third inequality of Eq. E-28 may be written as

$$D_{11}^{*}[D_{22}^{*}D_{23}^{*} - (D_{23}^{*}+D_{32}^{*})^2] + D_{22}^{*}[D_{11}^{*}D_{33}^{*} - (D_{13}^{*}+D_{31}^{*})^2]$$

$$+ D_{33}^{*}[D_{11}^{*}D_{22}^{*} - (D_{12}^{*}+D_{21}^{*})^2]$$

$$+ [D_{11}^{*}D_{22}^{*}D_{33}^{*} + (D_{12}^{*}+D_{21}^{*})(D_{13}^{*}+D_{31}^{*})(D_{23}^{*}+D_{32}^{*})] > 0 \quad . \tag{E-29}$$

The first two inequalities of Eq. E-28 are a subset of those required by the third inequality, i.e.,

$$D_{11}^{*} \; ; \; D_{22}^{*} \; ; \; D_{33}^{*} > 0 \quad , \tag{E-30a}$$

$$D_{22}^{*} D_{33}^{*} > (D_{23}^{*} + D_{32}^{*})^2 \quad , \tag{E-30b}$$

$$D_{11}^{*} D_{33}^{*} > (D_{13}^{*} + D_{31}^{*})^2 \quad , \tag{E-30c}$$

$$D_{11}^{*} D_{22}^{*} > (D_{12}^{*} + D_{21}^{*})^2 \quad , \tag{E-30d}$$

$$D_{11}^{*}D_{22}^{*}D_{33}^{*} > (D_{12}^{*}+D_{21}^{*})(D_{13}^{*}+D_{31}^{*})(D_{23}^{*}+D_{32}^{*}) \quad . \tag{E-30e}$$

From Eq. E-16, the candidate for the maximum value of F was the points where $\cos a = \cos b = \cos d = 0$. Evaluating Eqs. E-25 at these points gives:

$$\left.\frac{\partial^2 F}{\partial a^2}\right|_{\cos a=\cos b=\cos d=0} = \frac{-2\omega D_{11}^{*}\Delta t}{(\Delta x_1)^2} \quad , \tag{E-31a}$$

$$\left.\frac{\partial^2 F}{\partial b^2}\right|_{\cos a=\cos b=\cos d=0} = \frac{-2\omega D_{22}^{*}\Delta t}{(\Delta x_2)^2} \quad , \tag{E-31b}$$

$$\left.\frac{\partial^2 F}{\partial d^2}\right|_{\cos a=\cos b=\cos d=0} = \frac{-2\omega D_{33}^{*}\Delta t}{(\Delta x_3)^2} \quad , \tag{E-31c}$$

$$\left.\frac{\partial^2 F}{\partial a \partial b}\right|_{\cos a=\cos b=\cos d=0} = \frac{-\omega(D_{12}^{*}+D_{21}^{*})\Delta t}{\Delta x_1 \Delta x_2} \quad , \tag{E-31d}$$

$$\left.\frac{\partial^2 F}{\partial a \partial d}\right|_{\cos a=\cos b=\cos d=0} = \frac{-\omega(D_{13}^{*}+D_{31}^{*})\Delta t}{x_1 \; x_3} \quad , \tag{E-31e}$$

$$\left.\frac{\partial^2 F}{\partial b \partial d}\right|_{\cos a=\cos b=\cos d=0} = \frac{-\omega(D_{23}^{*}+D_{32}^{*})\Delta t}{\Delta x_2 \Delta x_3} \quad . \tag{E-31f}$$

Comparing Eqs. E-26 and E-31, it is seen that all elements of Eq. E-31 are just the negative value of the elements in Eq. E-26. Since the inequalities of Eq. E-30 will assure that the elements of Eq. E-26 form a positive-definite matrix, then Eq. E-30 will also assure that the elements of Eq. E-31 form a negative-definite matrix. Thus, when the inequalities of Eq. E-30 are satisfied, the points $\sin a = \sin b = \sin d = 0$ and $\cos a = \cos b = \cos d = 0$ are assured to be minimum and maximum values respectively of $F(a,b,d)$.

Although not shown here, each of the remaining six points of Eq. E-15 results in an indefinite

quadratic matrix when the inequalities of Eq. E-30 are used. Thus, each of these points are saddle points of $F(a,b,d)$, and are not relative extremes of the function.

There still remains the possibility of solutions to Eqs. E-12, E-13, and E-14 besides those given by Eq. E-15. Using the trigonometric identity $\sin 2\theta = 2 \sin\theta \cos\theta$, and solving Eq. E-12 for $\sin 2a$ gives

$$\sin 2a = -\frac{(D^*_{12}+D^*_{21})}{2D^*_{11}} \frac{\Delta x_1}{\Delta x_2} \sin 2b \cos 2a - \frac{(D^*_{13}+D^*_{31})}{2D^*_{11}} \frac{\Delta x_1}{\Delta x_3} \sin 2d \cos 2a \quad . \qquad \text{(E-32)}$$

In a similar manner, Eq. E-14 is solved for $\sin 2d$, i.e.,

$$\sin 2d = -\frac{(D^*_{13}+D^*_{31})}{2D^*_{33}} \frac{\Delta x_3}{\Delta x_1} \sin 2a \cos 2d - \frac{(D^*_{23}+D^*_{32})}{2D^*_{33}} \frac{\Delta x_3}{\Delta x_2} \sin 2b \cos 2d \quad . \qquad \text{(E-33)}$$

Substituting Eq. E-33 into Eq. E-32 gives

$$\sin 2a = \frac{\Delta x_1 \sin 2b \cos 2a}{\Delta x_2 [4D^*_{11}D^*_{33} - (D^*_{13}+D^*_{31})\cos 2a \cos 2d} [(D^*_{13}+D^*_{31}) (D^*_{23}+D^*_{32}) \cos 2d - 2D^*_{33}(D^*_{12}+D^*_{21})] \quad . \qquad \text{(E-34)}$$

Substituting Eq. E-32 into Eq. E-33 gives

$$\sin 2d = \frac{\Delta x_3 \sin 2b \cos 2d}{\Delta x_2 [4D^*_{11}D^*_{33} - (D^*_{13}+D^*_{31})^2 \cos 2a \cos 2d} [(D^*_{13}+D^*_{31}) (D^*_{12}+D^*_{21}) \cos 2a - 2D^*_{11}(D^*_{23}+D^*_{32})] \quad . \qquad \text{(E-35)}$$

Now then, a substitution of Eqs. E-34 and E-35 into Eq. E-13 gives

$$4D^*_{11}D^*_{22}D^*_{33} - D^*_{22}(D^*_{13}+D^*_{31})^2 \cos 2a \cos 2d - D^*_{33}(D^*_{12}+D^*_{21})^2 \cos 2a \cos 2b - D^*_{11}(D^*_{23}+D^*_{32})^2 \cos 2d \cos 2b + (D^*_{12}+D^*_{21})(D^*_{13}+D^*_{31}) (D^*_{23}+D^*_{32}) \cos 2d \cos 2a \cos 2b = 0 \quad . \qquad \text{(E-36)}$$

Although Eq. E-36 is not in an explicit form yet, it is easily observed that Eq. E-36 is almost of the same form as the third inequality of Eq. E-28. In fact since $|\cos\theta| \leq 1$, there is no way in which Eq. E-36 may be satisfied if Eqs. E-28 (or Eqs. E-30) hold.

From this analysis it may be concluded that if Eqs E-30 are valid, then $F(a,b,d)$ has only one minimum value located at the points $\sin a = \sin b = \sin d = 0$, and from Eq. E-16,

$$\text{Absolute Min. } F(a,b,d) = 0 \qquad \text{(E-37)}$$

Also, $F(a,b,d)$ has only one maximum value located at the points $\cos a = \cos b = \cos d = 0$, and from Eq. E-16:

$$\text{Absolute Max. } F(a,b,d) = \frac{\omega D^*_{11}\Delta t}{(\Delta x_1)^2} + \frac{\omega D^*_{22}\Delta t}{(\Delta x_2)^2} + \frac{\omega D^*_{33}\Delta t}{(\Delta x_3)^2} \quad . \qquad \text{(E-38)}$$

Combining Eqs. E-37, E-38, and E-10 results in:

$$0 \leq F(a,b,d) \leq \frac{\omega D^*_{11}\Delta t}{(\Delta x_1)^2} + \frac{\omega D^*_{22}\Delta t}{(\Delta x_2)^2} + \frac{\omega D^*_{33}\Delta t}{(\Delta x_3)^2} \leq \frac{1}{2} \quad . \qquad \text{(E-39)}$$

In summary, stability of Eq. E-1 is assured for any a, b, and d if:

$$D^*_{11} \; ; \; D^*_{22} \; ; \; D^*_{33} > 0 \quad , \qquad \text{(E-40a)}$$

$$D^*_{11} D^*_{33} > (D^*_{13}+D^*_{31})^2 \quad , \qquad \text{(E-40b)}$$

$$D^*_{11} D^*_{22} > (D^*_{12}+D^*_{21})^2 \quad , \qquad \text{(E-40c)}$$

$$D^*_{22} D^*_{33} > (D^*_{23} + D^*_{32})^2 \quad , \qquad \text{(E-40d)}$$

$$D^*_{11} D^*_{22} D^*_{33} > (D^*_{13}+D^*_{31})(D^*_{12}+D^*_{21})(D^*_{23}+D^*_{32}) \quad , \qquad \text{(E-40e)}$$

$$\frac{\omega D^*_{11}\Delta t}{(\Delta x_1)^2} + \frac{\omega D^*_{22}\Delta t}{(\Delta x_2)^2} + \frac{\omega D^*_{33}\Delta t}{(\Delta x_3)^2} \leq \frac{1}{2} \quad . \qquad \text{(E-40f)}$$

E.3 Stability Function for Two-Dimensional Dispersion Equation. The linear, constant coefficient, explicit difference form of the two-dimensional dispersion equation has the following form:

$$C^{t+1}_{i,k} = C^{t}_{i,k} + \frac{\omega D^*_{11}\Delta t}{(\Delta x_1)^2}\left(C^{t}_{i+1,k}+C^{t}_{i-1,k}-2C^{t}_{i,k}\right)$$

$$+ \frac{\omega D^*_{33}\Delta t}{(\Delta x_3)^2}\left(C^{t}_{i,k+1}+C^{t}_{i,k-1}-2C^{t}_{i,k}\right)$$

$$+ \frac{(D^*_{13}+D^*_{31})\ t}{x_1\ x_3}\left(C^{t}_{i+1,k+1}+C^{t}_{i-1,k-1}-C^{t}_{i+1,k-1}-C^{t}_{i-1,k+1}\right) . \qquad \text{(E-41)}$$

Designating the error in the two-dimensional space region as, $E^{\overline{S}}_{\overline{P},\overline{R}}$, and approximating it in a manner similar to that of Eq. E-3 gives

$$E^{\overline{S}}_{\overline{P},\overline{R}} = \exp[i(\psi\overline{P}\Delta x_1 + \gamma\overline{R}\Delta x_3)]\xi^{\overline{S}} . \qquad \text{(E-42)}$$

In a manner analogous to that used in developing Eqs. E-5, E-6, E-7, E-8, and E-9, the amplification factor is given by

$$\xi = 1 - \frac{4\omega D^*_{11}\Delta t}{(\Delta x_1)^2}\sin^2 a - \frac{4\omega D^*_{33}\Delta t}{(\Delta x_3)^2}\sin^2 d$$

$$- \frac{4\omega(D^*_{13}+D^*_{31})\Delta t}{\Delta x_1 \Delta x_3}(\sin a \cos a \sin d \cos d) . \qquad \text{(E-43)}$$

Substituting Eq. E-43 into Eq. E-4, the stability of Eq. E-41 is assured if

$$0 \le F(a,d) \le \frac{1}{2} , \qquad \text{(E-44)}$$

where

$$F(a,d) = \frac{\omega D^*_{11}\Delta t}{(\Delta x_1)^2}\sin^2 a + \frac{\omega D^*_{33}\Delta t}{(\Delta x_3)^2}\sin^2 d$$

$$+ \frac{\omega(D^*_{13}+D^*_{31})\Delta t}{\Delta x_1 \Delta x_3}(\sin a \cos a \sin d \cos d) . \qquad \text{(E-45)}$$

The necessary condition for a maximum or minimum value of $F(a,d)$ is for the first partial derivatives of F to vanish at the point of local extreme, i.e.,

$$\frac{\partial F}{\partial a} = \frac{2\omega D^*_{11}\Delta t}{(\Delta x_1)^2}\sin a \cos a$$

$$+ \frac{\omega(D^*_{13}+D^*_{31})\Delta t}{\Delta x_1 \Delta x_3}\sin d \cos d(\cos^2 a - \sin^2 a) = 0 , \qquad \text{(E-46)}$$

$$\frac{\partial F}{\partial d} = \frac{2\omega D^*_{33}\Delta t}{(\Delta x_3)^2}\sin d \cos d$$

$$+ \frac{\omega(D^*_{13}+D^*_{31})\Delta t}{\Delta x_1 \Delta x_3}\sin a \cos a(\cos^2 d - \sin^2 d) = 0 . \qquad \text{(E-47)}$$

By inspection, Eqs. E-46 and E-47 are satisfied when

$$\sin a = \sin d = 0 , \qquad \text{(E-48a)}$$

$$\sin a = \cos d = 0 , \qquad \text{(E-48b)}$$

$$\cos a = \sin d = 0 , \qquad \text{(E-48c)}$$

$$\cos a = \cos d = 0 . \qquad \text{(E-48d)}$$

Disregarding other possible solutions of Eqs. E-46 and E-47 at the present time, the values of $F(a,d)$ at the points suggested by Eq. E-48 become

$$F(\sin a = \sin d = 0) = 0 , \qquad \text{(E-49a)}$$

$$F(\sin a = \cos d = 0) = \frac{\omega D^*_{33}\Delta t}{(\Delta x_3)^2} , \qquad \text{(E-49b)}$$

$$F(\cos a = \sin d = 0) = \frac{\omega D^*_{11}\Delta t}{(\Delta x_1)^2} , \qquad \text{(E-49c)}$$

$$F(\cos a = \cos d = 0) = \frac{\omega D^*_{11}\Delta t}{(\Delta x_1)^2} + \frac{\omega D^*_{33}\Delta t}{(\Delta x_3)^2} . \qquad \text{(E-49d)}$$

If the coefficients ω , D^*_{11} , D^*_{33} , and Δt are positive, then $F(a,d)$ has a minimum value of zero at $(\sin a = \sin d = 0)$ and a maximum value of $\frac{\omega D^*_{11}\Delta t}{(\Delta x_1)^2} + \frac{\omega D^*_{33}\Delta t}{(\Delta x_3)^2}$ at the points where $\cos a = \cos d = 0$.

A two variable analysis of the sufficiency conditions, analogous to Eqs. E-17, E-18, E-19, and E-20, leads to the following quadratic form:

$$F(a,d) - F(\overline{a},\overline{d}) = \frac{1}{2} \cdot \| (a-\overline{a})\ (d-\overline{d}) \| \cdot \left\| \begin{matrix} \left.\frac{\partial^2 F}{\partial a^2}\right|_{\overline{a},\overline{d}} & \left.\frac{\partial^2 F}{\partial a \partial d}\right|_{\overline{a},\overline{d}} \\ \left.\frac{\partial^2 F}{\partial a \partial d}\right|_{\overline{a},\overline{d}} & \left.\frac{\partial^2 F}{\partial d^2}\right|_{\overline{a},\overline{d}} \end{matrix} \right\| \cdot \left\| \begin{matrix} (a-\overline{a}) \\ (b-\overline{b}) \end{matrix} \right\| . \qquad \text{(E-50)}$$

From Eq. E-21, it is concluded that if

$$\left.\frac{\partial^2 F}{\partial a^2}\right|_{\bar{a},\bar{d}} > 0 \quad , \tag{E-51}$$

and

$$\left\{\frac{\partial^2 F}{\partial a^2}\ \frac{\partial^2 F}{\partial d^2} - \left(\frac{\partial^2 F}{\partial a \partial d}\right)^2\right\}\Bigg|_{\bar{a},\bar{d}} \quad 0 \quad , \tag{E-52}$$

then Eq. E-50 is positive-definite and the point $(\bar{a},\bar{d})$ is a relative minimum. If Eq. E-51 is negative and Eq. E-52 is positive, then Eq. E-50 is negative-definite and the point $(\bar{a},\bar{d})$ is a relative maximum.

Taking the second partial derivative of $F(a,d)$ gives

$$\frac{\partial^2 F}{\partial a^2} = \frac{2\omega D^*_{11}\Delta t}{(\Delta x_1)^2}(\cos^2 a - \sin^2 a) - \frac{4\omega(D^*_{13}+D^*_{31})\Delta t}{\Delta x_1 \Delta x_3}\sin d \cos d \sin a \cos a \quad , \tag{E-53a}$$

$$\frac{\partial^2 F}{\partial b^2} = \frac{2\omega D^*_{33}\Delta t}{(\Delta x_3)^2}(\cos^2 d - \sin^2 d) - \frac{4\omega(D^*_{13}+D^*_{31})\Delta t}{\Delta x_1 \Delta x_3}\sin a \cos a \sin d \cos d \quad , \tag{E-53b}$$

and

$$\frac{\partial^2 F}{\partial a \partial d} = \frac{\omega(D^*_{13}+D^*_{31})\Delta t}{\Delta x_1 \Delta x_3}(\cos^2 d - \sin^2 d)(\cos^2 a - \sin^2 a) \quad . \tag{E-53c}$$

When $(\sin a = \sin d = 0)$, then

$$\left.\frac{\partial^2 F}{\partial a^2}\right|_{\sin a=\sin d=0} = \frac{2\omega D^*_{11}\Delta t}{(\Delta x_1)^2} \quad ,$$

$$\left.\frac{\partial^2 F}{\partial d^2}\right|_{\sin a=\sin d=0} = \frac{2\omega D^*_{33}\Delta t}{(\Delta x_3)^2} \quad ,$$

$$\left.\frac{\partial^2 F}{\partial a \partial d}\right|_{\sin a=\sin d=0} = \frac{\omega(D^*_{13}+D^*_{31})\Delta t}{\Delta x_1 \Delta x_3} \quad .$$

From Eqs. E-51 and E-52, the points $(\sin a = \sin d = 0)$ are a relative minimum if

$$D^*_{11} \ ; \ D^*_{33} > 0 \tag{E-54a}$$

and

$$4D^*_{11}D^*_{33} > (D^*_{13}+D^*_{31})^2 \quad . \tag{E-54b}$$

when $(\cos a = \cos d = 0)$, then

$$\left.\frac{\partial^2 F}{\partial a^2}\right|_{\sin a = \sin d = 0} = \frac{-2\omega D^*_{11}\Delta t}{(\Delta x_1)^2} \quad ,$$

$$\left.\frac{\partial^2 F}{\partial d^2}\right|_{\sin a = \sin d = 0} = \frac{-2\omega D^*_{33}\Delta t}{(\Delta x_3)^2} \quad , \text{ and}$$

$$\left.\frac{\partial^2 F}{\partial a \partial d}\right|_{\sin a = \sin d = 0} = \frac{-\omega(D^*_{13}+D^*_{31})\Delta t}{\Delta x_1 \Delta x_3} \quad .$$

From Eqs. E-51 and E-52, the points $(\cos a = \cos d = 0)$ are a relative maximum if the inequalities of Eq. E-54 hold. Thus, when the inequalities of Eq. E-54 are satisfied, the points $(\sin a = \sin d = 0)$ and $(\cos a = \cos d = 0)$ are assured to be a minimum values respectively of $F(a,d)$.

The remaining two points of Eq. E-48, $(\sin a = \cos d = 0)$ and $(\cos a = \sin d = 0)$, result in an indefinite quadratic matrix when the inequalities of Eq. E-54 are used. Therefore, each of these two points are saddle points of $F(a,d)$.

The possibility of other solutions to Eqs. E-46 and E-47 still exists. Solving the two equations simultaneously gives

$$\frac{2D^*_{11}}{(\Delta x_1)^2}\sin a \cos a = \frac{(D^*_{13}+D^*_{31})}{\Delta x_1 \Delta x_3}\sin d \cos d(\cos^2 a - \sin^2 a), \tag{E-55a}$$

and

$$\frac{2D^*_{33}}{(\Delta x_3)^2}\sin d \cos d = \frac{(D^*_{13}+D^*_{31})}{\Delta x_1 \Delta x_3}\sin a \cos a\,(\cos^2 d - \sin^2 d). \tag{E-55b}$$

Multiplying Eq. E-55a by E-55b gives

$$4D^*_{11}D^*_{33} = (D^*_{13}+D^*_{31})^2 \cos 2a \cos 2b \quad , \tag{E-56}$$

where the trigonometric identity $\cos^2\theta - \sin^2\theta = \cos 2\theta$ has been used. If Eq. E-54 holds, then there is no way for Eq. E-56 to be valid because $|\cos 2a \cos 2b| \leq 1$. Therefore, all the points of relative extreme are included in Eq. E-48.

From this analysis, $F(a,d)$ has only one minimum value located at the point $(\sin a = \sin d = 0)$, and the

$$\text{Absolute Min. } F(a,d) = 0 \quad . \tag{E-57}$$

Also, $F(a,d)$ has only one maximum value located at the point $(\cos a = \cos d = 0)$, and the

$$\text{Absolute Max. } F(a,d) = \frac{\omega D^*_{11} \Delta t}{(\Delta x_1)^2} + \frac{\omega D^*_{33} \Delta t}{(\Delta x_3)^2} \quad . \tag{E-58}$$

Combining Eqs. E-57, E-58, and E-44 results in:

$$0 \leq F(a,d) \leq \frac{\omega D^*_{11} \Delta t}{(\Delta x_1)^2} + \frac{\omega D^*_{33} \Delta t}{(\Delta x_3)^2} \leq \frac{1}{2} \quad . \tag{E-59}$$

In summary, the stability of Eq. E-41 is assured for any (a,d) if

$$D^*_{11} \; ; \; D^*_{33} > 0 \quad , \tag{E-60a}$$

$$4 D^*_{11} D^*_{33} > \left(D^*_{13} + D^*_{31}\right)^2 \quad , \tag{E-60b}$$

$$\frac{\omega D^*_{11} \Delta t}{(\Delta x_1)^2} + \frac{\omega D^*_{33} \Delta t}{(\Delta x_3)^2} \leq \frac{1}{2} \quad . \tag{E-60c}$$

APPENDIX F

FLOW CHART OF PROGRAM

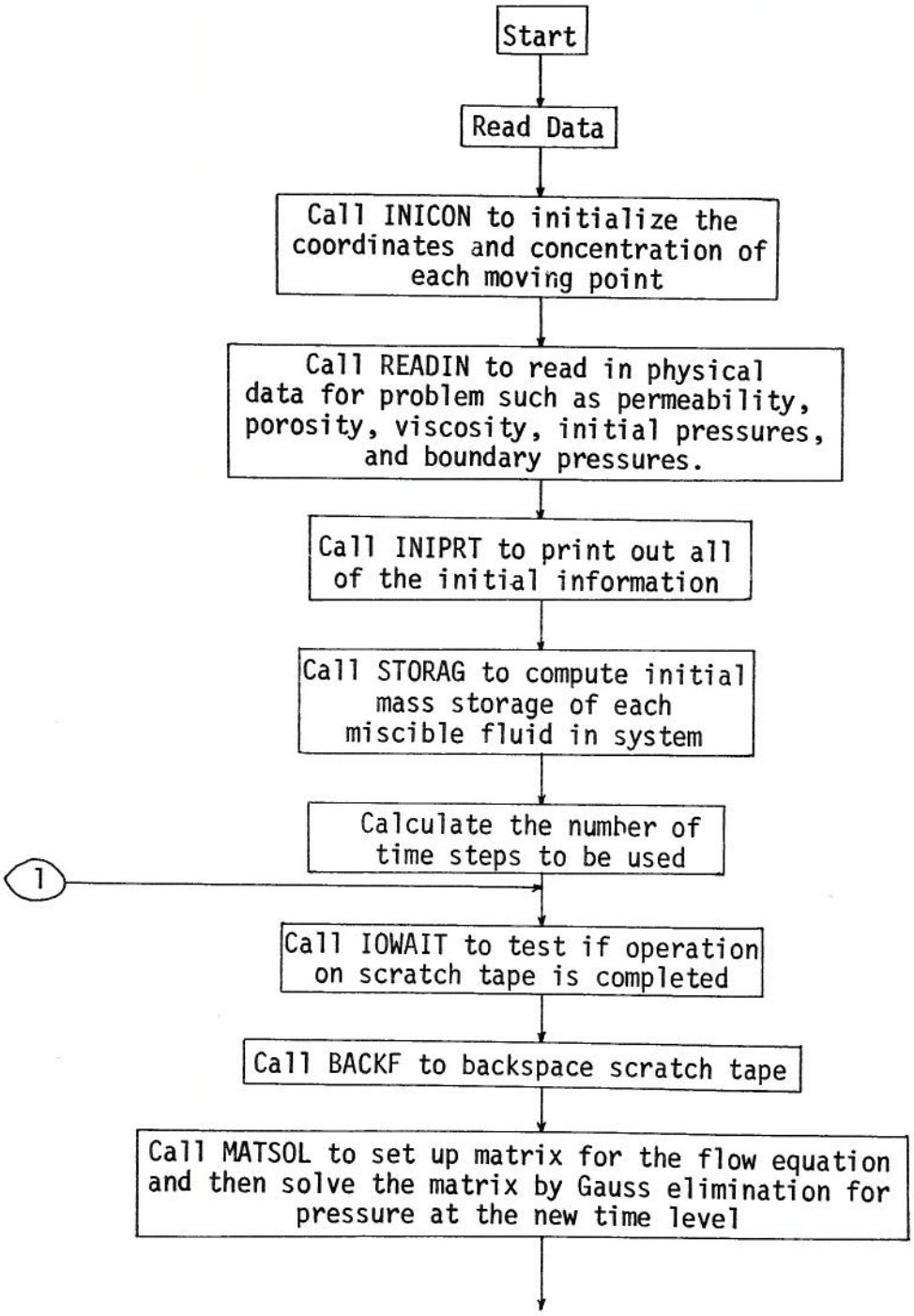

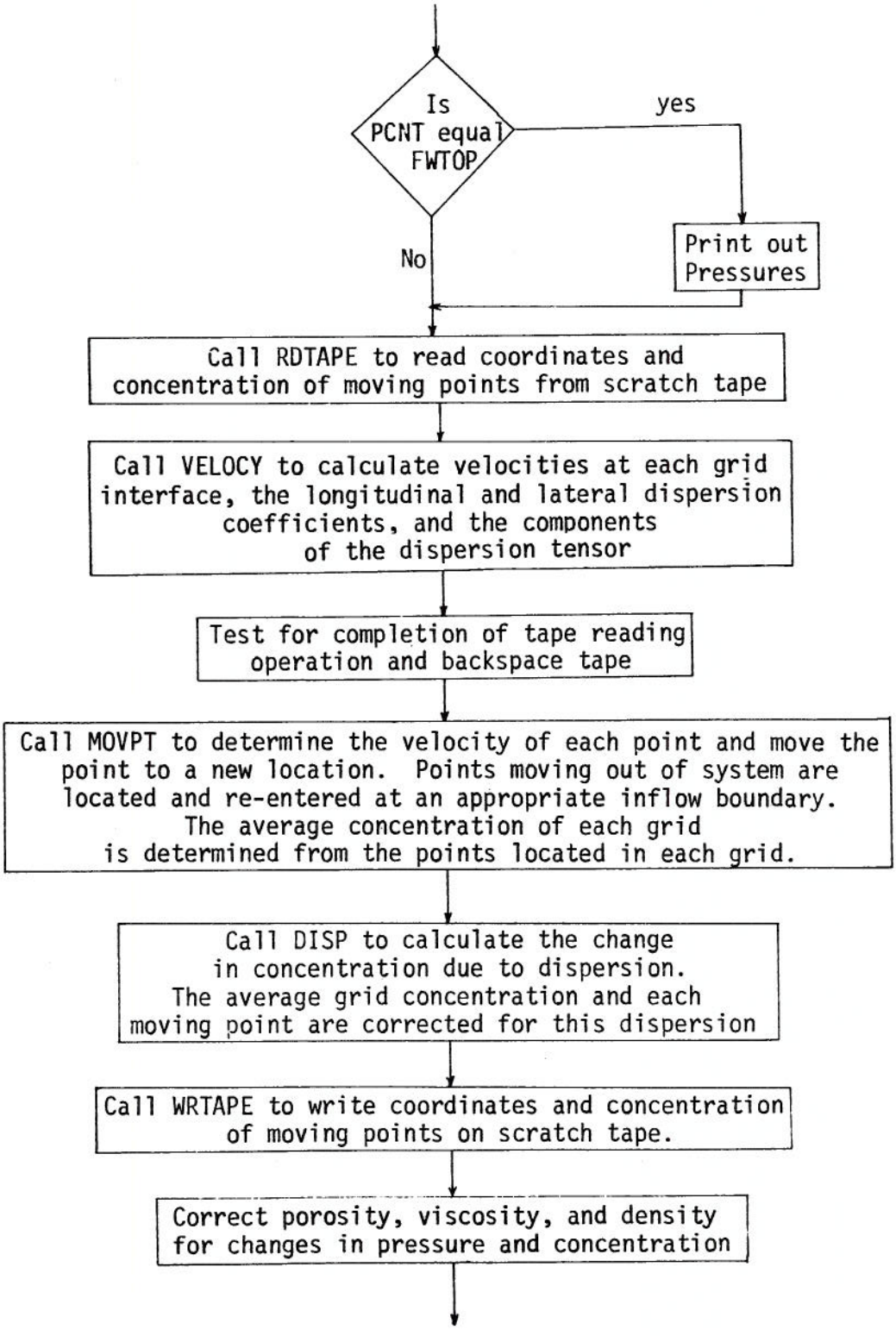
Is PCNT equal FWTOP
yes
No
Print out Pressures
Call RDTAPE to read coordinates and concentration of moving points from scratch tape
Call VELOCY to calculate velocities at each grid interface, the longitudinal and lateral dispersion coefficients, and the components of the dispersion tensor
Test for completion of tape reading operation and backspace tape
Call MOVPT to determine the velocity of each point and move the point to a new location. Points moving out of system are located and re-entered at an appropriate inflow boundary. The average concentration of each grid is determined from the points located in each grid.
Call DISP to calculate the change in concentration due to dispersion. The average grid concentration and each moving point are corrected for this dispersion
Call WRTAPE to write coordinates and concentration of moving points on scratch tape.
Correct porosity, viscosity, and density for changes in pressure and concentration

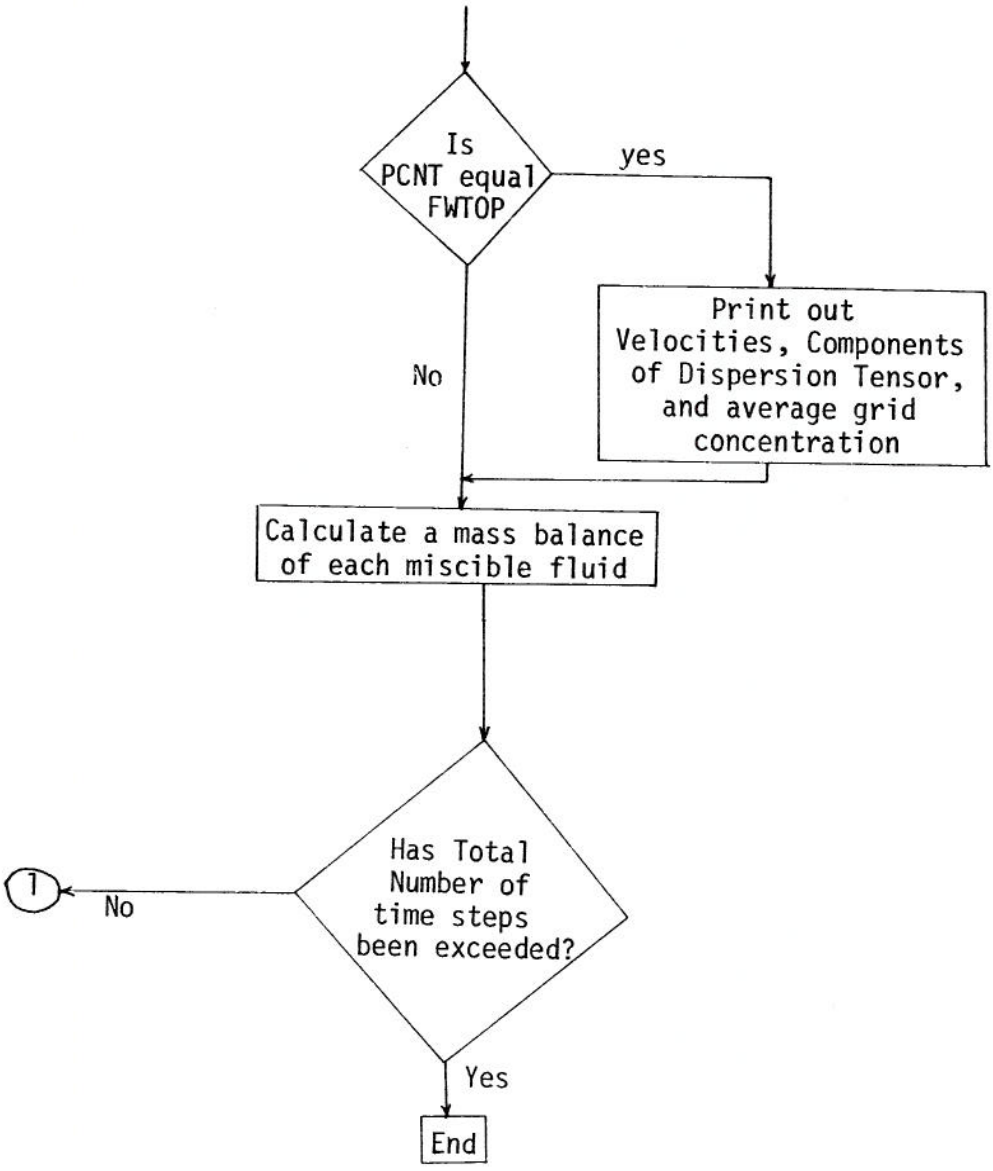
Is PCNT equal FWTOP
yes
No
Print out Velocities, Components of Dispersion Tensor, and average grid concentration
Calculate a mass balance of each miscible fluid
Has Total Number of time steps been exceeded?
No
1
Yes
End

MAIN PROGRAM

```
      PROGRAM MAIN
      DIMENSION FK(12,27),POR(12,27),H(12,27),P(12,27),PT(12,27),
     1PP(12,27),POT(12,27),RHO(12,27),VIS(12,27),Q(12,27),CAVG(12,27),
     2CAVGP(12,27),DELC(12,27),SUMC(12,27),COUNT(12,27),D11(12,27),
     3D22(12,27),D12(12,27),VX(12,28),VZ(13,27),CCMAT(5500),X(1496),
     4Z(1496),C(1496),CMATRX(250,21),CR(250),XB1(24),ZB1(24),CB1(24),
     5XB2(24),ZB2(24),CB2(24)
      COMMON DELT,ST,FWTOP,DELX,DELZ,FK,POR,H,P,PT,PP,RHO,VIS,Q,RHOP,
     1CAVG,CAVGP,DELC,G,BETA,ALPHA,GAMMA,RCOMP,SUMC,COUNT,D11,D22,D12,
     2VX,VZ,NWDCNT,XB1,ZB1,CB1,XB2,ZB2,CB2,CCMAT
      EQUIVALENCE (CCMAT(1),POT(1),X(1),CMATRX(1)), (CCMAT(1497),Z(1)),
     1(CCMAT(2993),C(1)), (CCMAT(5251),CR(1))
C
C'*****************************************************************''
C*****THE MAIN PROGRAM IS THE CONTROL PROGRAM AND DIRECTS THE SEQUENCE**
C*****     OF OPERATIONS FOR SOLVING THE FLOW EQUATION AND DISPERSION***
C*****     EQUATION.  APPROPRIATE SUBROUTINES ARE CALLED AS NEEDED TO **
C*****     MAKE THE NECESSARY CALCULATIONS.  THEPROGRAM DESCRIBED HERE**
C*****     IS FOR A TWO DIMENSIONAL VERTICAL FLOW PROBLEM.          *****
C*****NR = NUMBER OF ROWS                                           *****
C*****NC = NUMBER OF COLUMNS                                        *****
C*****     NOTE THAT THE NUMBER OF ROWS,NR, SHOULD ALWAYS BE EQUAL *****
C*****     TO OR LESS THAN THE NUMBER OF COLUMNS,NC.                *****
C*****NA = ROW DIMENSION OF THE REDUCED COEFFICIENT MATRIX USED IN *****
C*****     GAUSS ELIMINATION.                                       *****
C*****NB = COLUMN DIMENSION OF THE REDUCED COEFFICIENT MATRIX USED IN **
C*****     GAUSS ELIMINATION.                                       *****
C*****DELT = TIME INCREMENT (SEC.)                                  *****
C*****ST = TOTAL TIME OF ANALYSIS (SEC.)                            *****
C*****FWTOP = PRINT OUT CONTROL. FWTOP SHOULD ALWAYS BE A MULTIPLE  *****
C******    OF DELT.                                                 *****
C*****DELX = SPATIAL INCREMENT IN THE X'DIRECTION (FT.)             *****
C*****DELZ = SPATIAL INCREMENT IN THE Z'DIRECTION (FT.)             *****
C*****FK = PERMEABILITY (SQ.FT.)                                    *****
C*****POR = POROSITY                                                *****
C*****H = ELEVATION AT CENTER OF GRID (FT.)                         *****
C*****P = PRESSURE AT CENTER OF GRID FOR INITIAL TIME LEVEL (LBS. PER **
C*****     SQ. FT.)                                                 *****
C*****PT = PRESSURE AT CENTER OF GRID AT PRESENT TIME LEVEL (LBS. PER **
C*****     SQ. FT.)                                                 *****
C*****PP=PRESSURE AT CENTER OF GRID AT PREVIOUS TIME LEVEL (LBS. PER ***
C*****     SQ. FT.)                                                 *****
C*****POT = POTENTIAL AT CENTER OF GRID (FT.)                       *****
C*****RHO = DENSITY OF FLUID (SLUGS PER CUBIC FOOT)                 *****
C*****RHOP = DENSITY OF PRODUCED FLUID (SLUGS PER CUBIC FOOT)       *****
C*****VIS= VISCOSITY OF FLUID (LBF.-SEC. PER SQ. FT.)               *****
C*****Q = PRODUCTION TERM (CUBIC FEET PER SEC.)                     *****
C*****CAVG = AVERAGE CONCENTRATION OF TRACER (SLUGS PER CUB. FT.)   *****
C*****CAVGP=AVERAGE CONCENTRATION FROM PREVIOUS TIME STEP.          *****
C*****DELC= CHANGE IN CONCENTRATION DUE TO DISPERSION.              *****
C*****G = ACCELERATION OF GRAVITY (FT. PER SQ. SEC.)                *****
C*****BETA = FLUID COMPRESSIBILITY (SQ. FT. PER LB.)                *****
C*****RCOMP = ROCK COMPRESSIBILITY (SQ. FT. PER LB.)                *****
C*****ALPHA = CONSTANT RELATING DENSITY TO CONCENTRATION            *****
C*****GAMMA = CONSTANT RELATING VISCOSITY TO CONCENTRATION.         *****
C*****STOR = TOTAL MASS STORAGE OF AREA (SLUGS)                     *****
C*****WRTAPE = SUBROUTINE TO WRITE INFORMATION ON A TAPE.  THIS IS A ***
C*****     SYSTEMS PROGRAM OF THE CSU COMPUTER CENTER.              *****
C*****RDTAPE = SUBROUTINE TO READ INFORMATION FROM A TAPE. THIS IS A ***
C*****     SYSTEMS PROGRAM OF THE CSU COMPUTER CENTER.              *****
C*****CCMAT = DUMMY ARRAY TO BE USED BY DIFFERENT VARIABLES AT DIFFER-**
C*****     ENT LOCATIONS THROUGHOUT PROGRAM AND SUBPROGRAMS.        *****
C'*****************************************************************''
C
      READ (5,12) NR,NC,NPX,NPZ
      READ (5,2) DELX,DELZ,ALPHA
      NA=(NR-2)*(NC-2)
      NB=(2*NR)-3
      MAA=NR-1
      M=MAA-1
      NAA=NC-1
      N=NAA-1
      AM=M
      AN=N
      NP1=NPZ*NR
      NP2=NPX*NC
      NWDCNT=(3*NR*NC*NPX*NPZ)+600
      TIME=0.0
      CALL INICON (NR,NC,NP1,NP2,NPX,NPZ)
      CALL READIN (NR,NC,NA,NB)
      DO 20 I=1,NR
      DO 20 J=1,NC
      POT(I,J)=( PT(I,J)/(RHO(I,J)*G))+H(I,J)
   20 CONTINUE
      CALL INIPRT (NR,NC,NA,NB)
      CALL STORAG (NR,NC,NA,NB,STOR,ADD)
      WRITE (6,9) STOR,ADD
      STORI=STOR
      STORP=STOR
      ADDI=ADD
      ADDP=ADD
      SQSO=0.0
      SQTO=0.0
      LOOPUL=ST/DELT
      PCNT=1.0
      DO 8 ILAST=1,LOOPUL
      TIME=TIME+DELT
      DO 50 I=1,NR
      DO 50 J=1,NC
      PP(I,J)=PT(I,J)
   50 CONTINUE
      CALL IOWAIT (1,NSTAT,NWDS)
      CALL BACKF(1)
      CALL MATSOL (NR,NC,NA,NB)
      IF(PCNT.EQ.FWTOP) GO TO 3
      GO TO 22
    3 WRITE (6,10) TIME
      CALL MATROP (NR,NC,PT)
      DO 21 I=1,NR
      DO 21 J=1,NC
      POT(I,J)=(PT(I,J)/(RHO(I,J)*G))+H(I,J)
   21 CONTINUE
      WRITE (6,11) TIME
      CALL MATROP (NR,NC,POT)
   22 CALL RDTAPE (1,1,1,CCMAT(1),NWDCNT)
      IC=NC+1
      IR=NR+1
      CALL VELOCY (NR,NC,IR,IC)
      CALL IOWAIT (1,NSTAT,NWDS)
```

```
      CALL BACKF (1)
      CALL MOVPT(NR,NC,NP1,NP2,NPX,NPZ)
      CALL WRTAPE (1,1,1,CCMAT(1),NWDCNT)
      CALL DISP (NR,NC,NP1,NP2,NPX,NPZ)
      DO 60 I=1,NR
      DO 60 J=1,NC
      POR(I,J)=POR(I,J)*(1.0+(RCOMP*(PT(I,J)-PP(I,J))))
      RHO(I,J)=RHO(I,J)+(BETA*RHO(I,J)*(PT(I,J)-PP(I,J)))+(ALPHA*(CAVG(
     1I,J)-CAVGP(I,J)))
      VIS(I,J)=VIS(I,J)+(GAMMA*(CAVG(I,J)-CAVGP(I,J)))
   60 CONTINUE
      IF(PCNT.EQ.FWTOP) GO TO 65
      GO TO 23
   65 WRITE (6,14) TIME
      CALL MATROP (12,28,VX)
      WRITE (6,15) TIME
      CALL MATROP (13,27,VZ)
      WRITE (6,16) TIME
      CALL MATROP (NR,NC,D11)
      WRITE (6,17) TIME
      CALL MATROP (NR,NC,D22)
      WRITE (6,18) TIME
      CALL MATROP (NR,NC,D12)
      WRITE (6,19) TIME
      CALL MATROP (NR,NC,CAVGP)
      WRITE (6,25) TIME
      CALL MATROP (NR,NC,CAVG)
      WRITE (6,100) (XB1(I),I=1,NP1)
      WRITE (6,100) (ZB1(I),I=1,NP1)
      WRITE (6,100) (CB1(I),I=1,NP1)
      WRITE (6,100) (XB2(I),I=1,NP1)
      WRITE (6,100) (ZB2(I),I=1,NP1)
      WRITE (6,100) (CB2(I),I=1,NP1)
  100 FORMAT (1X,12F10.3)
      PCNT=0.0
   23 CALL MBAL (NR,NC,NA,NB,STORI,ADDI,STORP,ADDP,SQSO,SQTO,TIME)
      PCNT=PCNT+1.0
    8 CONTINUE
    2 FORMAT (3F10.3)
    9 FORMAT (1HO,10X,9HSTORAGE =,F10.3,10X,16HTRACER STORAGE =,F10.3  )
   10 FORMAT (1HO,47X,46HNEW PRESSURE MAP (LBS. PER SQ. FT.) AT TIME = ,
     1F10.2,1H   /)
   11 FORMAT (1HO,52X,34HNEW POTENTIAL MAP (FT.) AT TIME = ,F10.2,1H  /)
   12 FORMAT (4I10)
   13 FORMAT (1H ,15F8.3)
   14 FORMAT(1HO,52X,20HX-VELOCITY AT TIME =,F10.2,1H  /)
   15 FORMAT(1HO,52X,20HZ-VELOCITY AT TIME =,F10.2,1H  /)
   16 FORMAT(1HO,52X,13HD11 AT TIME =,F10.2,1H  /)
   17 FORMAT(1HO,52X,13HD22 AT TIME =,F10.2,1H  /)
   18 FORMAT(1HO,52X,13HD12 AT TIME =,F10.2,1H  /)
   19 FORMAT(1HO,52X,15HCAVGP AT TIME =,F10.2,1H  /)
   25 FORMAT(1HO,52X,14HCAVG AT TIME =,F10.2,1H  /)
      END
```

SUBROUTINE READIN

```
      SUBROUTINE READIN (NR, NC, NA, NB)
      DIMENSION FK(12,27),POR(12,27),H(12,27),P(12,27),PT(12,27),
     1PP(12,27),POT(12,27),RHO(12,27),VIS(12,27),Q(12,27),CAVG(12,27),
     2CAVGP(12,27),DELC(12,27),SUMC(12,27),COUNT(12,27),D11(12,27),
     3D22(12,27),D12(12,27),VX(12,28),VZ(13,27),CCMAT(5500),X(1496),
     4Z(1496),C(1496),CMATRX(250,21),CR(250),XB1(24),ZB1(24),CB1(24),
     5XB2(24),ZB2(24),CB2(24)
      COMMON DELT,ST,FWTOP,DELX,DELZ,FK,POR,H,P,PT,PP,RHO,VIS,Q,RHOP,
     1CAVG,CAVGP,DELC,G,BETA,ALPHA,GAMMA,RCOMP,SUMC,COUNT,D11,D22,D12,
     2VX,VZ,NWDCNT,XB1,ZB1,CB1,XB2,ZB2,CB2,CCMAT
      EQUIVALENCE (CCMAT(1),POT(1),X(1),CMATRX(1)), (CCMAT(1497),Z(1)),
     1(CCMAT(2993),C(1)), (CCMAT(5251),CR(1))
C'''''''''''''''''''''''''''''''''''''''''''''''''''''''''''''''''''''''''''''''''
C*****THIS SUBROUTINE READS IN THE PHYSICAL DATA NEEDED TO SOLVE THE ***
C*****     PROBLEM.                                                    *****
C*****P(I,J) GREATER THAN 100,000 INDICATES CONSTANT PRESSURE BOUNDARY.*
C'''''''''''''''''''''''''''''''''''''''''''''''''''''''''''''''''''''''''''''''''
C
      READ (5,1) DELT, ST, FWTOP
      READ (5,3) G,BETA,RCOMP,ALPHA,RHOP,GAMMA
      IR=NR-1
      IC=NC-1
      DO 10 J=1,NC
      FK(1,J)=0.0
   10 FK(NR,J)=0.0
      DO 11 I=2,IR
      DO 11 J=1,NC
   11 FK(I,J)=0.000009885
      DO 12 I=1,NR
      DO 12 J=1,NC
      POR(I,J)=0.39
      VIS(I,J)=0.0116
   12 Q(I,J)=0.0
      H(1,1)=69.0
      P(1,1)=129993.88
      H(1,NC)=69.0
      P(1,NC)=129576.40
      DO 13 I=2,NR
      H(I,1)=H(I-1,1)-DELZ
      H(I,NC)=H(I-1,NC)-DELZ
      P(I,NC)=P(I-1,NC)+(RHO(I,NC)*G*DELZ)
   13 P(I,1)=P(I-1,1)+(RHO(I,1)*G*DELZ)
      DO 14 J=2,IC
      P(1,J)=29576.4
      H(1,J)=69.0
      DO 14 I=2,NR
      H(I,J)=H(I-1,J)-DELZ
   14 P(I,J)=P(I-1,J)+(RHO(I,J)*G*DELZ)
      DO 4 I=1,NR
      DO 4 J=1,NC
      IF(P(I,J).LT.100000.0) PT(I,J)=P(I,J)
      IF(P(I,J).GT.100000.0) PT(I,J)=P(I,J)-100000.0
    4 CONTINUE
      RETURN
    1 FORMAT (3F10.3)
    3 FORMAT (6F10.3)
    5 FORMAT (E11.4,E11.4,F8.3,4F10.3)
      END
```

SUBROUTINE INICON

```
      SUBROUTINE INICON (NR,NC,NP1,NP2,NPX,NPZ)
      DIMENSION FK(12,27),POR(12,27),H(12,27),P(12,27),PT(12,27),
     1PP(12,27),POT(12,27),RHO(12,27),VIS(12,27),Q(12,27),CAVG(12,27),
     2CAVGP(12,27),DELC(12,27),SUMC(12,27),COUNT(12,27),D11(12,27),
     3D22(12,27),D12(12,27),VX(12,28),VZ(13,27),CCMAT(5500),X(1496),
     4Z(1496),C(1496),CMATRX(250,21),CR(250),XB1(24),ZB1(24),CB1(24),
     5XB2(24),ZB2(24),CB2(24)
      COMMON DELT,ST,FWTOP,DELX,DELZ,FK,POR,H,P,PT,PP,RHO,VIS,Q,RHOP,
     1CAVG,CAVGP,DELC,G,BETA,ALPHA,GAMMA,RCOMP,SUMC,COUNT,D11,D22,D12,
     2VX,VZ,NWDCNT,XB1,ZB1,CB1,XB2,ZB2,CB2,CCMAT
      EQUIVALENCE (CCMAT(1),POT(1),X(1),CMATRX(1)), (CCMAT(1497),Z(1)),
     1(CCMAT(2993),C(1)), (CCMAT(5251),CR(1))
C
C--*********************************************************************--
C*****THIS SUBROUTINE DETERMINES THE INITIAL X-Z COORDINATES OF THE ****
C*****      MOVING POINTS AND ASSIGNS AN INITIAL CONCENTRATION TO EACH **
C*****      OF THE POINTS.  THE MOVING POINTS ARE UNIFORMLY DISTRIBUTED**
C*****      THROUGHOUT THE GRID SYSTEM, INCLUDING THE BOUNDARY GRIDS.****
C*****X =X-COORDINATE OF MOVING POINT.                                 *****
C*****Z = Z-COORDINATE OF MOVING POINT.                                *****
C*****C = CONCENTRATION OF MOVING POINT.                               *****
C*****NPX = NUMBER OF MOVING POINTS PER GRID IN X-DIRECTION.           *****
C*****NPZ = NUMBER OF MOVING POINTS PER GRID IN Z-DIRECTION.           *****
C*****      NOTE THAT NPX*NPZ IS THE TOTAL NUMBER OF MOVING POINTS PER***
C*****      GRID INITIALLY.                                           *****
C*****PX = FLOATING POINT DESIGNATION OF NPX.                          *****
C*****PZ = FLOATING POINT DESIGNATION OF NPZ.                          *****
C*****NP1 = NUMBER OF MOVING POINTS IN VERTICAL DIMENSION OF MODEL.*****
C*****NP2 = NUMBER OF MOVING POINTS IN HORIZONTAL DIMENSION OF MODEL.***
C*****      NOTE THAT NP1*NP2 IS THE TOTAL NUMBER OF MOVING POINTS IN ***
C*****      THE MODEL INITIALLY.                                      *****
C*****SUMC = SUMMATION OF CONCENTRATION OF MOVING POINTS IN A GRID. ****
C*****COUNT = A COUNT OF THE NUMBER OF MOVING POINTS IN A GRID.        *****
C*****CAVG = AVERAGE CONCENTRATION OF TRACER (SLUGS PER CUB. FT.)) *****
C*****      AND IS DETERMINED BY SUMC/COUNT.                          *****
C*****DELC =CHANGE IN CONCENTRATION DUE TO DISPERSION.                 *****
C*****LOG,NOG,DOG,XD = INCREMENTING FACTORS USED IN DO LOOP.           *****
C*****NI1,NI2 = ROW NUMBER AND COLUMN NUMBER OF GRID IN WHICH POINT IS**
C*****      LOCATED.                                                  *****
C--*********************************************************************--
C*****XB1,ZB1,CB1 = COORDINATES AND CONCENTRATIONS OF BOUNDARY MOVING **
C*****      POINTS ALONG X=0.                                         *****
C*****XB2,ZB2,CB2 = COORDINATES AND CONCENTRATIONS OF BOUNDARY MOVING **
C*****      POINTS ALONG X=MODEL LENGTH.                              *****
C
      REWIND 1
      LOG=1-NP1
      NOG=0
      PX=NPX
      PZ=NPZ
      DO 67 I=1,NR
      DO 67 J=1,NC
      SUMC(I,J)=0.0
      COUNT(I,J)=0.0
   67 DELC(I,J)=0.0
      DO 10 J=1,NP2
      DOG=J-1
      XD=(DELX/PX)*(0.5+DOG)
      IF(XD.LT.156.0) YD=SQRT(39.99*(156.0-XD)+220.0)
      IF(XD  .GT.156.0) YD=0.0
   14 LOG=LOG+NP1
      NOG=NOG+NP1
      DO 10 I=LOG,NOG
      DOG=I-LOG
      Z(I)=(DELZ/PZ)*(0.5+DOG)
      X(I)=XD
      IF(Z(I).LT.YD) C(I)=0.0
      IF(Z(I).GE.YD) C(I)=0.10
      NI1=Z(I)/DELZ+1.0
      NI2=X(I)/DELX+1.0
      SUMC(NI1,NI2)=SUMC(NI1,NI2)+C(I)
      COUNT(NI1,NI2)=COUNT(NI1,NI2)+1.0
   10 CONTINUE
C*****FROM HERE THRU STATEMENT 2, A BUFFER ZONE OF 200 MOVING POINTS ***
C*****      IS CREATED FOR USE IN INJECTING AT INFLOW BOUNDARY COND- ****
C*****      ITIONS.                                                   *****
      ALENX=(NC*DELX)+150.0
      ALENZ=(NR*DELZ)/2.0
      LOG=(NP1*NP2)+1
      NOG=(NP1*NP2)+200
      DO 2 I=LOG,NOG
      X(I)=ALENX
      Z(I)=ALENZ
      C(I)=0.10
    2 CONTINUE
      CALL WRTAPE (1,1,1,CCMAT(1),NWDCNT)
      XD=(DELX/PX)*0.5
      DO 12 I=1,NP1
      DOG=I-1
      ZB1(I)=(DELZ/PZ)*(0.5+DOG)
      XB1(I)=XD
      CB1(I)=0.0
   12 CONTINUE
      LOG=(NP1*(NP2-1))+1
      NOG=NP1*NP2
      DOG=NP2-1
      XD=(DELX/PX)*(0.5+DOG)
      DO 13 I=LOG,NOG
      DOG=I-LOG
      J=I-LOG+1
      ZB2(J)=(DELZ/PZ)*(0.5+DOG)
      XB2(J)=XD
      CB2(J)=0.10
   13 CONTINUE
      DO 1 I=1,NR
      DO 1 J=1,NC
      IF(COUNT(I,J).EQ.0.0) COUNT(I,J)=1.0
      CAVG(I,J)=SUMC(I,J)/COUNT(I,J)
      CAVGP(I,J)=CAVG(I,J)
    1 RHO(I,J)=1.0+ALPHA*CAVG(I,J)
      CALL IOWAIT (1,NSTAT,NWDS)
      CALL BACKF (1)
      RETURN
      END
```

SUBROUTINE BSOLVE

```
      SUBROUTINE BSOLVE (C,N,M,V)
      DIMENSION C(N,M),V(N)
C
C--*********************************************************************--
C*****THIS SUBROUTINE SOLVES THE MATRIX SET UP IN MATSOL BY GAUSS  *****
C*****      ELIMINATION.                                           *****
C--*********************************************************************--
C
      LR=(M-1)/2
      DO 2 L=1,LR
      IM=LR-L+1
      DO 2 I=1,IM
      DO 1 J=2,M
    1 C(L,J-1)=C(L,J)
      KN=N-L
      KM=M-I
      C(L,M)=0.0
    2 C(KN+1,KM+1)=0.0
      LR=LR+1
      IM=N-1
      DO 10 I=1,IM
      NPIV=I
      LS=I+1
      DO 3 L=LS,LR
      IF (ABS(C(L,1)).GT.ABS(C(NPIV,1))) NPIV=L
    3 CONTINUE
      IF (NPIV.EQ.I) 6,4
    4 DO 5 J=1,M
      TEMP=C(I,J)
      C(I,J)=C(NPIV,J)
    5 C(NPIV,J)=TEMP
      TEMP=V(I)
      V(I)=V(NPIV)
      V(NPIV)=TEMP
    6 V(I)=V(I)/C(I,1)
      DO 7 J=2,M
    7 C(I,J)=C(I,J)/C(I,1)
      DO 9 L=LS,LR
      TEMP=C(L,1)
      V(L)=V(L)-TEMP*V(I)
      DO 8 J=2,M
    8 C(L,J-1)=C(L,J)-TEMP*C(I,J)
    9 C(L,M)=0.0
      IF (LR.LT.N) LR=LR+1
   10 CONTINUE
      V(N)=V(N)/C(N,1)
      JM=2
      DO 12 I=1,IM
      L=N-I
      DO 11 J=2,JM
      KM=L+J
   11 V(L)=V(L)-C(L,J)*V(KM-1)
      IF (JM.LT.M) JM=JM+1
   12 CONTINUE
      RETURN
      END
```

SUBROUTINE MATROP

```
      SUBROUTINE MATROP (NR, NC, B)
      DIMENSION B(NR,NC), A(12)
C
C!!*********************************************************************!!
C*****THIS SUBROUTINE ORGANIZES THE INITIAL DATA OR THE RESULTS INTO*****
C*****      A SUITABLE FORM FOR PRINTOUT.                          *****
C!!*********************************************************************!!
C
      DO 11 I=1,NC,12
      IN=I/12
      DO 9 J=1,NR
      IF((IN+1)*12.LE.NC) 1,3
    1 DO 2 JJ=1,12
      JJJ=IN*12+JJ
    2 A(JJ)=B(J,JJJ)
      GO TO 6
    3 LL=NC-12*IN
      DO 4 JJ=1,LL
      JJJ=IN*12+JJ
    4 A(JJ)=B(J,JJJ)
      LL=LL+1
      DO 5 JJ=LL,12
    5 A(JJ)=0.0
    6 IF (A(1).LT.0.001) GO TO 14
      IF (IN) 7,7,8
    7 WRITE (6,12) (A(II),II=1,12),J
      GO TO 9
    8 WRITE (6,12) (A(II),II=1,12), IN
      GO TO 9
   14 IF(IN) 15,15,16
   15 WRITE (6,17) (A(II),II=1,12), J
      GO TO 9
   16 WRITE (6,17) (A(II),II=1,12), IN
    9 CONTINUE
      IF(NC.LE.(IN+1)*12) 11,10
   10 WRITE (6,13)
   11 CONTINUE
      RETURN
   12 FORMAT (1H ,12E10.3,I4)
   13 FORMAT (1H0,//)
   17 FORMAT (1H ,12E10.3,I4)
      END
```

SUBROUTINE INIPRT

```
      SUBROUTINE INIPRT (NR, NC, NA, NB)
      DIMENSION FK(12,27),POR(12,27),H(12,27),P(12,27),PT(12,27),
     1PP(12,27),POT(12,27),RHO(12,27),VIS(12,27),Q(12,27),CAVG(12,27),
     2CAVGP(12,27),DELC(12,27),SUMC(12,27),COUNT(12,27),D11(12,27),
     3D22(12,27),D12(12,27),VX(12,28),VZ(13,27),CCMAT(5500),X(1496),
     4Z(1496),C(1496),CMATRX(250,21),CR(250),XB1(24),ZB1(24),CB1(24),
     5XB2(24),ZB2(24),CB2(24)
      COMMON DELT,ST,FWTOP,DELX,DELZ,FK,POR,H,P,PT,PP,RHO,VIS,Q,RHOP,
     1CAVG,CAVGP,DELC,G,BETA,ALPHA,GAMMA,RCOMP,SUMC,COUNT,D11,D22,D12,
     2VX,VZ,NWDCNT,XB1,ZB1,CB1,XB2,ZB2,CB2,CCMAT
      EQUIVALENCE (CCMAT(1),POT(1),X(1),CMATRX(1)), (CCMAT(1497),Z(1)),
     1(CCMAT(2993),C(1)), (CCMAT(5251),CR(1))
C
C''*********************************************************************''
C*****THIS SUBROUTINE WRITES OUT ALL OF THE INITIAL DATA BY USE OF *****
C*****     SUBROUTINE MATROP.                                      *****
C''*********************************************************************''
C
      WRITE (6,1)
      WRITE (6,2) NR, NC, NA, NB
      WRITE (6,3) DELT, ST, FWTOP
      WRITE (6,4) DELX, DELZ
      WRITE (6,5) G, ALPHA,RHOP
      WRITE (6,6) BETA, RCOMP,GAMMA
      WRITE (6,7)
      CALL MATROP (NR, NC, FK)
      WRITE (6,8)
      CALL MATROP (NR, NC, POR)
      WRITE (6,9)
      CALL MATROP (NR, NC, H)
      WRITE (6,10)
      CALL MATROP (NR, NC, PT)
      WRITE (6,11)
      CALL MATROP (NR, NC, POT)
      WRITE (6,12)
      CALL MATROP (NR, NC, RHO)
      WRITE (6,13)
      CALL MATROP (NR, NC, VIS)
      WRITE (6,14)
      CALL MATROP (NR, NC, Q)
      WRITE (6,15)
      CALL MATROP (NR, NC, CAVG)
      WRITE (6,16)
      CALL MATROP (NR, NC, DELC)
      RETURN
    1 FORMAT (1H1,36X,57H**********TWO-DIMENSIONAL VERTICAL FLOW PROBLEM
     1********** //)
    2 FORMAT (1HO,15HROW DIMENSION =,I4,10X,18HCOLUMN DIMENSION =,I4,
     110X,19HCMATRX DIMENSIONS =,I4,1X,2HBY,1X,I4)
    3 FORMAT (1HO,12HDELTA-TIME =,F10.3,1X,5HSECS.,10X,16HTOTAL RUN TIME
     1 =,F10.3,1X,5HSECS.,10X,19HPRINT OUT CONTROL =,F10.3)
    4 FORMAT (1HO,9HDELTA-X =,F10.3,1X,3HFT.,10X,9HDELTA-Z =,F10.3,1X,
     13HFT. )
    5 FORMAT (1HO,17HACC. OF GRAVITY =,F10.3,1X,16HFT. PER SQ. SEC.,10X,
     17HALPHA =,F10.3,10X,21HPROD. FLUID DENSITY =,F10.3,1X,17HSLUG PER
     2CUB. FT.  )
    6 FORMAT (1HO,13HFLUID COMP. =,F10.3,1X,15HSQ. FT. PER LB.,10X,12HRO
     1CK COMP. =,F10.3,1X,15HSQ. FT. PER LB.,10X,7HGAMMA =,F10.3 )
    7 FORMAT (1HO,52X,27HPERMEABILITY MAP (SQ. FT.).  /)
    8 FORMAT (1HO,58X,13HPOROSITY MAP.  /)
    9 FORMAT (1HO,52X,25HGRID ELEVATION MAP (FT.).  /)
   10 FORMAT (1HO,45X,40HINITIAL PRESSURE MAP (LBS. PER SQ. FT.).  /)
   11 FORMAT (1HO,51X,28HINITIAL POTENTIAL MAP (FT.).  /)
   12 FORMAT (1HO,45X,41HINITIAL DENSITY MAP (SLUG PER CUBIC FT.).  /)
   13 FORMAT (1HO,43X,45HINITIAL VISCOSITY MAP (LB.-SEC. PER SQ. FT.)./)
   14 FORMAT (1HO,46X,37HPRODUCTION MAP (CUBIC FEET PER SEC.).  /)
   15 FORMAT (1HO,41X,48HINITIAL CONCENTRATION MAP (SLUG PER CUBIC FOOT)
     1.  /)
   16 FORMAT (1HO,41X,49HCHANGE IN CONCENTRATION MAP (SLUG PER CUBIC FT.
     1).  /)
      END
```

SUBROUTINE STORAG

```
      SUBROUTINE STORAG (NR,NC,NA,NB,STOR,ADD)
      DIMENSION FK(12,27),POR(12,27),H(12,27),P(12,27),PT(12,27),
     1PP(12,27),POT(12,27),RHO(12,27),VIS(12,27),Q(12,27),CAVG(12,27),
     2CAVGP(12,27),DELC(12,27),SUMC(12,27),COUNT(12,27),D11(12,27),
     3D22(12,27),D12(12,27),VX(12,28),VZ(13,27),CCMAT(5500),X(1496),
     4Z(1496),C(1496),CMATRX(250,21),CR(250),XB1(24),ZB1(24),CB1(24),
     5XB2(24),ZB2(24),CB2(24)
      COMMON DELT,ST,FWTOP,DELX,DELZ,FK,POR,H,P,PT,PP,RHO,VIS,Q,RHOP,
     1CAVG,CAVGP,DELC,G,BETA,ALPHA,GAMMA,RCOMP,SUMC,COUNT,D11,D22,D12,
     2VX,VZ,NWDCNT,XB1,ZB1,CB1,XB2,ZB2,CB2,CCMAT
      EQUIVALENCE (CCMAT(1),POT(1),X(1),CMATRX(1)), (CCMAT(1497),Z(1)),
     1(CCMAT(2993),C(1)), (CCMAT(5251),CR(1))
C
C''*********************************************************************''
C*****THIS SUBROUTINE COMPUTES THE MASS STORAGE FOR THE TOTAL AREA. ****
C*****STOR=TOTAL MASS STORAGE OF AREA (SLUGS)                       *****
C*****ADD = TRACER MASS STORAGE OF AREA (SLUGS).                    *****
C''*********************************************************************''
C
      NC1=NC-1
      NR1=NR-1
      ADD=0.0
      STOR=0.0
      DO 1 L=2,NC1
      DO 1 K=2,NR1
      STOR=(1.0*DELX*DELZ*POR(K,L)*RHO(K,L))+STOR
      ADD=(1.0*DELX*DELZ*POR(K,L)*CAVG(K,L))+ADD
    1 CONTINUE
      RETURN
      END
```

SUBROUTINE MATSOL

```
      SUBROUTINE MATSOL (NR,NC,NA,NB)
      DIMENSION FK(12,27),POR(12,27),H(12,27),P(12,27),PT(12,27),
     1PP(12,27),POT(12,27),RHO(12,27),VIS(12,27),Q(12,27),CAVG(12,27),
     2CAVGP(12,27),DELC(12,27),SUMC(12,27),COUNT(12,27),D11(12,27),
     3D22(12,27),D12(12,27),VX(12,28),VZ(13,27),CCMAT(5500),X(1496),
     4Z(1496),C(1496),CMATRX(250,21),CR(250),XB1(24),ZB1(24),CB1(24),
     5XB2(24),ZB2(24),CB2(24)
      COMMON DELT,ST,FWTOP,DELX,DELZ,FK,POR,H,P,PT,PP,RHO,VIS,Q,RHOP,
     1CAVG,CAVGP,DELC,G,BETA,ALPHA,GAMMA,RCOMP,SUMC,COUNT,D11,D22,D12,
     2VX,VZ,NWDCNT,XB1,ZB1,CB1,XB2,ZB2,CB2,CCMAT
      EQUIVALENCE (CCMAT(1),POT(1),X(1),CMATRX(1)), (CCMAT(1497),Z(1)),
     1(CCMAT(2993),C(1)), (CCMAT(5251),CR(1))
C
C--*****************************************************************--
C*****THIS SUBROUTINE SETS UP THE COEFFICIENT MATRIX AND THE RIGHT *****
C*****     HAND SIDE COLUMN VECTOR.                                *****
C*****THE COEFFICIENTS ARE COMPUTED BY THE FUNCTIONS PARAM, RHOAM, *****
C*****     AND ELVAM.                                              *****
C*****THE MATRIX OBTAINED HAS ALL OF THE LOWER LEFT HAND AND UPPER *****
C*****     RIGHT HAND ZERO ELEMENTS ELIMINATED.                    *****
C*****CMATRX = ELEMENTS OF COEFFICIENT MATRIX                      *****
C*****CR = ELEMENTS OF RIGHT HAND SIDE COLUMN VECTOR               *****
C--*****************************************************************--
C
      PARAM(AFK1,AFK2,APOR,ADELS,AMU1,AMU2)=(2.0*AFK1*AFK2)/(APOR*ADELS*
     1ADELS*(AMU1*AFK2+AMU2*AFK1))
      RHOAM(ARHO1,ARHO2)=0.5*(ARHO1+ARHO2)
      ELVAM(AH1,AH2)=AH1-AH2
      DO 1 J=1,NB
      DO 1 I=1,NA
    1 CMATRX(I,J)=0.0
      NT=0
      NC1=NC-1
      NR1=NR-1
      IB=NR-2
      IM=IB+1
      IC=IM+1
      ID=2*IB+1
      DO 12 J=2,NC1
      DO 12 I=2,NR1
      NT=NT+1
      CR(NT)=0.0
      IF(FK(I,J).EQ.0.0) 11,22
   22 IF(P(I,J).GE.100000.0) 11,2
    2 JA=I
      JD=I
      CMATRX(NT, 1)=RHOAM(RHO( JA,J-1),RHO(I,J))*PARAM(FK( JA,J-1),
     1FK(I,J),POR(I,J),DELX,VIS( JA,J-1),VIS(I,J))
      CMATRX(NT,IB)=RHOAM(RHO(I-1,  J),RHO(I,J))*PARAM(FK(I-1,  J),
     1FK(I,J),POR(I,J),DELZ,VIS(I-1,  J),VIS(I,J))
      CMATRX(NT,IC)=RHOAM(RHO(I+1,  J),RHO(I,J))*PARAM(FK(I+1,  J),
     1FK(I,J),POR(I,J),DELZ,VIS(I+1,  J),VIS(I,J))
      CMATRX(NT,ID)=RHOAM(RHO( JD,J+1),RHO(I,J))*PARAM(FK( JD,J+1),
     1FK(I,J),POR(I,J),DELX,VIS( JD,J+1),VIS(I,J))
C*****THE FOLLOWING STATEMENTS (THRU 10) TRANSFER COEFFICIENTS,    *****
C*****     MULTIPLIED BY RESPECTIVE PRESSURE TERM, TO RIGHT HAND  *****
C*****     SIDE COLUMN VECTOR FOR KNOWN  BOUNDARY CONDITIONS.     *****
      IF(P(JA,J-1).GE.100000.0) 3,4
    3 CR(NT)=CR(NT)-(CMATRX(NT, 1)*PT( JA,J-1))-(G*CMATRX(NT, 1)*RHOAM
     1(RHO( JA,J-1),RHO(I,J))*ELVAM(H( JA,J-1),H(I,J)))
      CMATRX(NT,IM)=CMATRX(NT,IM)-CMATRX(NT, 1)
      CMATRX(NT, 1)=0.0
    4 IF(P(I-1,J).GE.100000.0) 5,6
    5 CR(NT)=CR(NT)-(CMATRX(NT,IB)*PT(I-1,  J))-(G*CMATRX(NT,IB)*RHOAM
     1(RHO(I-1,  J),RHO(I,J))*ELVAM(H(I-1,  J),H(I,J)))
      CMATRX(NT,IM)=CMATRX(NT,IM)-CMATRX(NT,IB)
      CMATRX(NT,IB)=0.0
    6 IF(P(I+1,J).GE.100000.0) 7,8
    7 CR(NT)=CR(NT)-(CMATRX(NT,IC)*PT(I+1,  J))-(G*CMATRX(NT,IC)*RHOAM
     1(RHO(I+1,  J),RHO(I,J))*ELVAM(H(I+1,  J),H(I,J)))
      CMATRX(NT,IM)=CMATRX(NT,IM)-CMATRX(NT,IC)
      CMATRX(NT,IC)=0.0
    8 IF(P(JD,J+1).GE.100000.0) 9,10
    9 CR(NT)=CR(NT)-(CMATRX(NT,ID)*PT( JD,J+1))-(G*CMATRX(NT,ID)*RHOAM
     1(RHO( JD,J+1),RHO(I,J))*ELVAM(H( JD,J+1),H(I,J)))
      CMATRX(NT,IM)=CMATRX(NT,IM)-CMATRX(NT,ID)
      CMATRX(NT,ID)=0.0
   10 CMATRX(NT,IM)=CMATRX(NT,IM)-(CMATRX(NT,1)+CMATRX(NT,IB)+CMATRX(NT,
     1IC)+CMATRX(NT,ID)+((RHO(I,J)*(RCOMP+BETA))/DELT))
      DELCCP=CAVG(I,J)-CAVGP(I,J)
      CR(NT)=CR(NT)-((RHO(I,J)*(RCOMP+BETA)*PT(I,J))/DELT)+((ALPHA*DELC
     1CP  ) /DELT)+((RHOP*Q(I,J))/(POR(I,J)*DELX*DELZ))-(G*CMATRX(NT,1)*
     2RHOAM(RHO(JA,J-1),RHO(I,J))*ELVAM(H(JA,J-1),H(I,J)))-(G*CMATRX(NT,
     3IB)*RHOAM(RHO(I-1,J),RHO(I,J))*ELVAM(H(I-1,J),H(I,J)))-(G*CMATRX(
     4NT,IC)*RHOAM(RHO(I+1,J),RHO(I,J))*ELVAM(H(I+1,J),H(I,J)))-(G*CMATR
     5X(NT,ID)*RHOAM(RHO(JD,J+1),RHO(I,J))*ELVAM(H(JD,J+1),H(I,J)))
      GO TO 12
   11 CMATRX(NT,IM)=1.0
      CR(NT)=PT(I,J)
   12 CONTINUE
      CALL BSOLVE (CMATRX,NA,NB,CR)
      NT=0
      DO 13 J=2,NC1
      DO 13 I=2,NR1
      NT=NT+1
   13 PT(I,J)=CR(NT)
      RETURN
      END
```

SUBROUTINE VELOCY

```
      SUBROUTINE VELOCY (NR,NC,IR,IC)
      DIMENSION FK(12,27),POR(12,27),H(12,27),P(12,27),PT(12,27),
     1PP(12,27),POT(12,27),RHO(12,27),VIS(12,27),Q(12,27),CAVG(12,27),
     2CAVGP(12,27),DELC(12,27),SUMC(12,27),COUNT(12,27),D11(12,27),
     3D22(12,27),D12(12,27),VX(12,28),VZ(13,27),CCMAT(5500),X(1496),
     47(1496),C(1496),CMATRX(250,21),CR(250),XB1(24),ZB1(24),CB1(24),
     5XB2(24),ZB2(24),CB2(24)
      COMMON DELT,ST,FWTOP,DELX,DELZ,FK,POR,H,P,PT,PP,RHO,VIS,Q,RHOP,
     1CAVG,CAVGP,DELC,G,BETA,ALPHA,GAMMA,RCOMP,SUMC,COUNT,D11,D22,D12,
     2VX,VZ,NWDCNT,XB1,ZB1,CB1,XB2,ZB2,CB2,CCMAT
      EQUIVALENCE (CCMAT(1),POT(1),X(1),CMATRX(1)), (CCMAT(1497),Z(1)),
     1(CCMAT(2993),C(1)), (CCMAT(5251),CR(1))
C
C--------------------------------------------------------------------------
C*****THIS SUBROUTINE CALCULATES THE SEEPAGE VELOCITIES AT EACH GRID****
C*****      INTERFACE,THE LONGITUDINAL AND LATERAL DISPERSION COEFF- ****
C*****      ICIENTS ARE DETERMINED FOR EACH GRID USING A VELOCITY POWER**
C*****      RELATIONSHIP, AND THE COMPONENTS OF THE DISPERSIONTENSOR ARE*
C*****      DETERMINED BY USING THE APPROPRIATE TRANSFORMATIONS.     *****
C*****VX = VELOCITY IN X-DIRECTION.                                   *****
C*****VZ = VELOCITY IN Z-DIRECTION.                                   *****
C*****DIFF = DIFFUSION COEFFICIENT                                    *****
C*****TORT = TORTUOSITY.                                              *****
C*****DIA = MEDIAN GRAIN SIZE DIAMETER.                               *****
C*****VXX =X-VELOCITY AT CENTER OF GRID.                              *****
C*****VZZ = Z-VELOCITY AT CENTER OF GRID.                             *****
C*****DL = LONGITUDINAL DISPERSION COEFFICIENT.                       *****
C*****DT = LATERAL DISPERSION COEFFICIENT.                            *****
C*****RE = REYNOLDS NUMBER.                                           *****
C*****D11,D22,D12 = COMPONENTS OF THE DISPERSION COEFFICIENT TENSOR. ***
C--------------------------------------------------------------------------
C
      DO 10 I=1,NR
      DO 9 J=2,NC
      IF(FK(I,J).EQ.0.0.OR.FK(I,J-1).EQ.0.0) GO TO 8
      DOG=((-2.0)*FK(I,J)*FK(I,J-1))/(DELX*(FK(I,J-1)*POR(I,J)*VIS(I,J)+
     1FK(I,J)*POR(I,J-1)*VIS(I,J-1)))
      VX(I,J)=DOG*((PT(I,J)-PT(I,J-1))+0.5*G*(RHO(I,J)+RHO(I,J-1))*
     1(H(I,J)-H(I,J-1)))
      GO TO 9
    8 VX(I,J)=0.0
    9 CONTINUE
      VX(I,1)=VX(I,2)
      VX(I,IC)=VX(I,NC)
   10 CONTINUE
      DO 20 J=1,NC
      DO 19 I=2,NR
      IF(FK(I,J).EQ.0.0.OR.FK(I-1,J).EQ.0.0) GO TO 18
      DOG=((-2.0)*FK(I,J)*FK(I-1,J))/(DELZ*(FK(I-1,J)*POR(I,J)*VIS(I,J)+
     1FK(I,J)*POR(I-1,J)*VIS(I-1,J)))
      VZ(I,J)=DOG*((PT(I,J)-PT(I-1,J))+0.5*G*(RHO(I,J)+RHO(I-1,J))*
     1(H(I,J)-H(I-1,J)))
      GO TO 19
   18 VZ(I,J)=0.0
   19 CONTINUE
      VZ(1,J)=VZ(2,J)
      VZ(IR,J)=VZ(NR,J)
   20 CONTINUE
      DIFF=0.0
      TORT=0.5
      DIA=0.0965
      DO 30 I=1,NR
      DO 30 J=1,NC
      VXX=VX(I,J)-0.5*(VX(I,J)-VX(I,J+1))
      VZZ=VZ(I,J)-0.5*(VZ(I,J)-VZ(I+1,J))
      VELX=VXX*VXX
      VELZ=VZZ*VZZ
      IF(VELX.EQ.0.0.AND.VELZ.EQ.0.0) GO TO 21
      VEL=SQRT(VELX+VELZ)
      RE=(VEL*DIA*RHO(I,J))/VIS(I,J)
      DL=0.0
      DT=0.0
      D11(I,J)=(DL*VXX*VXX)/(VEL*VEL)+(DT*VZZ*VZZ)/(VEL*VEL)+DIFF*TORT
      D22(I,J)=(DT*VXX*VXX)/(VEL*VEL)+(DL*VZZ*VZZ)/(VEL*VEL)+DIFF*TORT
      D12(I,J)=((DL-DT)*VXX*VZZ)/(VEL*VEL)
      GO TO 25
   21 D11(I,J)=0.0
      D22(I,J)=0.0
      D12(I,J)=0.0
   25 SUMC(I,J)=0.0
      COUNT(I,J)=0.0
      CAVGP(I,J)=CAVG(I,J)
   30 CONTINUE
      RETURN
      END
```

SUBROUTINE DISP

```
      SUBROUTINE DISP (NR,NC,NP1,NP2,NPX,NPZ)
      DIMENSION FK(12,27),POR(12,27),H(12,27),P(12,27),PT(12,27),
     1PP(12,27),POT(12,27),RHO(12,27),VIS(12,27),Q(12,27),CAVG(12,27),
     2CAVGP(12,27),DELC(12,27),SUMC(12,27),COUNT(12,27),D11(12,27),
     3D22(12,27),D12(12,27),VX(12,28),VZ(13,27),CCMAT(5500),X(1496),
     4Z(1496),C(1496),CMATRX(250,21),CR(250),XB1(24),ZB1(24),CB1(24),
     5XB2(24),ZB2(24),CB2(24)
      COMMON DELT,ST,FWTOP,DELX,DELZ,FK,POR,H,P,PT,PP,RHO,VIS,Q,RHOP,
     1CAVG,CAVGP,DELC,G,BETA,ALPHA,GAMMA,RCOMP,SUMC,COUNT,D11,D22,D12,
     2VX,VZ,NWDCNT,XB1,ZB1,CB1,XB2,ZB2,CB2,CCMAT
      EQUIVALENCE (CCMAT(1),POT(1),X(1),CMATRX(1)), (CCMAT(1497),Z(1)),
     1(CCMAT(2993),C(1)), (CCMAT(5251),CR(1))
C
C*************************************************************************
C*****THIS SUBROUTINE CALCULATES THE CHANGE IN CONCENTRATION DUE TO ****
C*****     DISPERSION. CAVG IS THEN CORRECTED FOR THIS DISPERSION EFECT*
C*************************************************************************
C
      MR=NR-1
      MC=NC-1
      DO 47 I=2,MR
      DO 47 J=2,MC
      W=RHO(I,J)/(RHO(I,J)-(ALPHA*CAVG))
      IF(D11(I,J+1).EQ.0.0.OR.D11(I,J).EQ.0.0) GO TO 31
      DCXXA=((2.0*W*POR(I,J+1)*DELT*D11(I,J)*D11(I,J+1))/(DELX*DELX*
     1(POR(I,J)*D11(I,J)+POR(I,J+1)*D11(I,J+1)))))*(CAVG(I,J+1)-CAVG(I,J
     2))
      GO TO 32
   31 DCXXA=0.0
   32 IF(D11(I,J-1).EQ.0.0.OR.D11(I,J).EQ.0.0) GO TO 33
      DCXXB=((2.0*W*POR(I,J-1)*DELT*D11(I,J)*D11(I,J-1))/(DELX*DELX*
     1(POR(I,J)*D11(I,J)+POR(I,J-1)*D11(I,J-1)))))*(CAVG(I,J)-CAVG(I,J-1
     2))
      GO TO 34
   33 DCXXB=0.0
   34 IF(D22(I+1,J).EQ.0.0.OR.D22(I,J).EQ.0.0) GO TO 35
      DCYYC=((2.0*W*POR(I+1,J)*DELT*D22(I,J)*D22(I+1,J))/(DELZ*DELZ*
     1(POR(I,J)*D22(I,J)+POR(I+1,J)*D22(I+1,J)))))*(CAVG(I+1,J)-CAVG(I,J
     2))
      GO TO 36
   35 DCYYC=0.0
   36 IF(D22(I-1,J).EQ.0.0.OR.D22(I,J).EQ.0.0) GO TO 37
      DCYYD=((2.0*W*POR(I-1,J)*DELT*D22(I,J)*D22(I-1,J))/(DELZ*DELZ*
     1(POR(I,J)*D22(I,J)+POR(I-1,J)*D22(I-1,J)))))*(CAVG(I,J)-CAVG(I-1,J
     2))
      GO TO 38
   37 DCYYD=0.0
   38 IF(D12(I,J+1).EQ.0.0.OR.D12(I,J).EQ.0.0) GO TO 39
      DCXYA=((W*POR(I,J+1)*DELT*D12(I,J)*D12(I,J+1))/(2.0*DELX*DELZ*
     1(POR(I,J)*D12(I,J)+POR(I,J+1)*D12(I,J+1)))))*(CAVG(I+1,J)+CAVG(I+1,
     2J+1)-CAVG(I-1,J)-CAVG(I-1,J+1))
      GO TO 40
   39 DCXYA=0.0
   40 IF(D12(I,J-1).EQ.0.0.OR.D12(I,J).EQ.0.0) GO TO 41
      DCXYB=((W*POR(I,J-1)*DELT*D12(I,J)*D12(I,J-1))/(2.0*DELX*DELZ*
     1(POR(I,J)*D12(I,J)+POR(I,J-1)*D12(I,J-1)))))*(CAVG(I+1,J)+CAVG(I+1,
     2J-1)-CAVG(I-1,J)-CAVG(I-1,J-1))
      GO TO 42
   41 DCXYB=0.0
   42 IF(D12(I+1,J).EQ.0.0.OR.D12(I,J).EQ.0.0) GO TO 43
      DCYXC=((W*POR(I+1,J)*DELT*D12(I,J)*D12(I+1,J))/(2.0*DELX*DELZ*
     1(POR(I,J)*D12(I,J)+POR(I+1,J)*D12(I+1,J)))))*(CAVG(I,J+1)+CAVG(I+1,
     2J+1)-CAVG(I+1,J-1)-CAVG(I,J-1))
      GO TO 44
   43 DCYXC=0.0
   44 IF(D12(I-1,J).EQ.0.0.OR.D12(I,J).EQ.0.0) GO TO 45
      DCYXD=((W*POR(I-1,J)*DELT*D12(I,J)*D12(I-1,J))/(2.0*DELX*DELZ*
     1(POR(I,J)*D12(I,J)+POR(I-1,J)*D12(I-1,J)))))*(CAVG(I,J+1)+CAVG(I-1,
     2J+1)-CAVG(I,J-1)-CAVG(I-1,J-1))
      GO TO 46
   45 DCYXD=0.0
   46 DELC(I,J)=DCXXA-DCXXB+DCYYC-DCYYD+DCXYA-DCXYB+DCYXC-DCYXD
   47 CONTINUE
      DO 48 I=1,NR
      DO 48 J=1,NC
      CAVG(I,J)=CAVG(I,J)+DELC(I,J)
   48 CONTINUE
      RETURN
      END
```

SUBROUTINE MOVPT

```
      SUBROUTINE MOVPT (NR,NC,NP1,NP2,NPX,NPZ)
      DIMENSION FK(12,27),POR(12,27),H(12,27),P(12,27),PT(12,27),
     1PP(12,27),POT(12,27),RHO(12,27),VIS(12,27),Q(12,27),CAVG(12,27),
     2CAVGP(12,27),DELC(12,27),SUMC(12,27),COUNT(12,27),D11(12,27),
     3D22(12,27),D12(12,27),VX(12,28),VZ(13,27),CCMAT(5500),X(1496),
     4Z(1496),C(1496),CMATRX(250,21),CR(250),XB1(24),ZB1(24),CB1(24),
     5XB2(24),ZB2(24),CB2(24)
      COMMON DELT,ST,FWTOP,DELX,DELZ,FK,POR,H,P,PT,PP,RHO,VIS,Q,RHOP,
     1CAVG,CAVGP,DELC,G,BETA,ALPHA,GAMMA,RCOMP,SUMC,COUNT,D11,D22,D12,
     2VX,VZ,NWDCNT,XB1,ZB1,CB1,XB2,ZB2,CB2,CCMAT
      EQUIVALENCE (CCMAT(1),POT(1),X(1),CMATRX(1)), (CCMAT(1497),Z(1)),
     1(CCMAT(2993),C(1)), (CCMAT(5251),CR(1))
C
C--*****************************************************************--
C*****THIS SUBROUTINE CORRECTS THE CONCENTRATION OF EACH MOVING POINT***
C*****      FOR THE EFFECTS OF DISPERSION IN THE PREVIOUS TIME STEP *****
C*****      (THIS LOGICALLY SHOULD HAVE BEEN DONE AT THE END OF THE *****
C*****     'PREVIOUS TIME STEP BUT FOR PROGRAMMING EFFICIENCY WAS    *****
C*****      DELAYED). ALSO, THE VELOCITY OF EACH POINT IS DETERMINED ****
C*****      AND THE POINT MOVED ACCORDINGLY. POINTS MOVING OUT OF THE ***
C*****      MODEL ARE LOCATED AND RE-ENTERED AT AN APPROPRIATE INFLOW ***
C*****      BOUNDARY. A RECORD OF SUMC AND COUNT IS MAINTAINED AND CAVG**
C*****      IS RECALCULATED FOR EACH GRID.
C*****VXX,VZZ = VELOCITY COMPONENTS OF MOVING POINT.                  **
C--*****************************************************************--
C
      PX=NPX
      PZ=NPZ
      ALENX=DELX*NC
      ALENZ=DELZ*NR
      ADISX=DELX/PX
      ADISZ=DELZ/PZ
      DO 5 I=1,NP1
      NI1=ZB1(I)/DELZ+1.0
      NI2=XB1(I)/DELX+1.0
      ALL=NI2-1
      VXX=VX(NI1,NI2)-(((XB1(I)-(ALL*DELX))/DELX)*(VX(NI1,NI2)-VX(NI1,
     1NI2+1)))
      IF(VXX.GT.0.0) XB1(I)=XB1(I)+(DELT*VXX)
      NI1=ZB2(I)/DELZ+1.0
      NI2=XB2(I)/DELX+1.0
      ALL=NI2-1
      VXX=VX(NI1,NI2)-(((XB2(I)-(ALL*DELX))/DELX)*(VX(NI1,NI2)-VX(NI1,
     1NI2+1)))
      IF(VXX.LT.0.0) XB2(I)=XB2(I)+(DELT*VXX)
    5 CONTINUE
      NECK=1
      JECK=1
      MECK=0
      LOG=(NP1*NP2)+200
      DO 20 I=1,LOG
      NI1=Z(I)/DELZ+1.0
      NI2=X(I)/DELX+1.0
      IF(NI2.GT.NC) GO TO 100
      AL=NI1-1
      ALL=NI2-1
      C(I)=C(I)+DELC(NI1,NI2)
      VXX=VX(NI1,NI2)-(((X(I)-(ALL*DELX))/DELX)*(VX(NI1,NI2)-VX(NI1,NI2+
     1))))
      VZZ=VZ(NI1,NI2)-(((Z(I)-(AL*DELZ))/DELZ)*(VZ(NI1,NI2)-VZ(NI1+1,NI2
     1)))
      IF(VX(NI1,NI2).EQ.0.0.AND.VXX.LT.0.0) GO TO 40
      GO TO 41
   40 ALL=NI2-1
      DISTA=X(I)-(ALL*DELX)
      DISTB=ABS(DELT*VXX)
      IF(DISTA.GT.DISTB) VXX=(-DISTA+0.01)/DELT
   41 IF(VX(NI1,NI2+1).EQ.0.0.AND.VXX.GT.0.0) GO TO 42
      GO TO 43
   42 ALL=NI2
      DISTA=(ALL*DELX)-X(I)
      DISTB=ABS(DELT*VXX)
      IF(DISTA.GT.DISTB) VXX=(DISTA-0.01)/DELT
   43 IF(VZ(NI1,NI2).EQ.0.0.AND.VZZ.LT.0.0) GO TO 44
      GO TO 45
   44 ALL=NI1-1
      DISTA=Z(I)-(ALL*DELZ)
      DISTB=ABS(DELT*VZZ)
      IF(DISTA.GT.DISTB) VZZ=(-DISTA+0.01)/DELT
   45 IF(VZ(NI1+1,NI2).EQ.0.0.AND.VZZ.GT.0.0) GO TO 46
      GO TO 52
   46 ALL=NI1
      DISTA=(ALL*DELZ)-Z(I)
      DISTB=ABS(DELT*VZZ)
      IF(DISTA.GT.DISTB) VZZ=(DISTA-0.01)/DELT
   52 Z(I)=Z(I)+DELT*VZZ
      X(I)=X(I)+DELT*VXX
  100 IF(X(I).LT.ALENX.AND.Z(I).LT.ALENZ) GO TO 12
      IF(X(I).GE.ALENX) GO TO 80
      GO TO 12
   80 IF(MECK.EQ.2) GO TO 12
      IF(MECK.EQ.1) GO TO 75
   70 IF(XB1(NECK).GE.ADISX) GO TO 72
      JECK=JECK+1
      NECK=NECK+1
      IF(NECK.LE.NP1) GO TO 70
      IF(JECK.GT.NP1) GO TO 74
      JECK=1
      NECK=1
      GO TO 70
   72 XB1(NECK)=XB1(NECK)-ADISX
      X(I)=XB1(NECK)
      Z(I)=ZB1(NECK)
      C(I)=CB1(NECK)
      IF(NECK.LT.NP1) GO TO 11
      NECK=1
      GO TO 12
   74 NECK=1
      JECK=1
      MECK=1
   75 DIST=ALENX-XB2(NECK)
      IF(DIST.GE.ADISX) GO TO 76
```

```
      JECK=JECK+1
      NECK=NECK+1
      IF(NECK.LE.NP1) GO TO 75
      IF(JECK.GT.NP1) GO TO 77
      JECK=1
      NECK=1
      GO TO 75
   76 XB2(JECK)=XB2(NECK)+ADISX
      X(I)=XB2(NECK)
      Z(I)=ZB2(NECK)
      C(I)=CB2(NECK)
      IF(NECK.LT.NP1) GO TO 11
      NECK=1
      GO TO 12
   77 NECK=1
      JECK=1
      MECK=2
      GO TO 12
   11 NECK=NECK+1
   12 NI1=Z(I)/DELZ+1.0
      NI2=X(I)/DELX+1.0
      IF(NI2.GT.NC) GO TO 20
      IF(NI2.EQ.NC) C(I)=0.10
      SUMC(NI1,NI2)=SUMC(NI1,NI2)+C(I)
      COUNT(NI1,NI2)=COUNT(NI1,NI2)+1.0
   20 CONTINUE
      DO 30 I=1,NR
      DO 30 J=1,NC
      IF(COUNT(I,J).EQ.0.0) COUNT(I,J)=1.0
   30 CAVG(I,J)=SUMC(I,J)/COUNT(I,J)
      RETURN
      END
```

SUBROUTINE MBAL

```
      SUBROUTINE MBAL (NR,NC,NA,NB,STOR1,ADD1,STORP,ADDP,SQSO,SQTO,TIME)
      DIMENSION FK(12,27),POR(12,27),H(12,27),P(12,27),PT(12,27),
     1PP(12,27),POT(12,27),RHO(12,27),VIS(12,27),Q(12,27),CAVG(12,27),
     2CAVGP(12,27),DELC(12,27),SUMC(12,27),COUNT(12,27),D11(12,27),
     3D22(12,27),D12(12,27),VX(12,28),VZ(13,27),CCMAT(5500),X(1496),
     4Z(1496),C(1496),CMATRX(250,21),CR(250),XB1(24),ZB1(24),CB1(24),
     5XB2(24),ZB2(24),CB2(24)
      COMMON DELT,ST,FWTOP,DELX,DELZ,FK,POR,H,P,PT,PP,RHO,VIS,Q,RHOP,
     1CAVG,CAVGP,DELC,G,BETA,ALPHA,GAMMA,RCOMP,SUMC,COUNT,D11,D22,D12,
     2VX,VZ,VWHOUT,XB1,ZB1,CB1,XB2,ZB2,CB2,CCMAT
      EQUIVALENCE (CCMAT(1),POT(1),X(1),CMATRX(1)), (CCMAT(1497),Z(1)),
     1(CCMAT(2993),C(1)), (CCMAT(5251),CR(1))
C
C-----------------------------------------------------------------------
C*****THIS SUBROUTINE COMPUTES THE MASS BALANCE FOR THE SOLUTE AND  ****
C*****      THE TRACER.                                              *****
C-----------------------------------------------------------------------
C
      CALL STORAG (NR,NC,NA,NB,STOR,ADD)
      QTO=0.0
      QSO=0.0
      VOLU=0.0
      IR=NR-1
      IC=NC-1
      DO 47 I=2,IR
      Q1=DELZ*VX(I,2)*((FK(I,1)*POR(I,2)*VIS(I,2)+FK(I,2)*POR(I,1)*VIS(
     11,1))/(FK(I,1)*VIS(I,2)+FK(I,2)*VIS(I,1)))
      VOLU=VOLU+Q1
      Q2=DELZ*VX(I,NC)*((FK(I,IC)*POR(I,NC)*VIS(I,NC)+FK(I,NC)*POR(I,IC)
     1*VIS(I,IC))/(FK(I,IC)*VIS(I,NC)+FK(I,NC)*VIS(I,IC)))
      IF(Q1.GT.0.0) QSO=DELT*Q1*RHO(I,1)+QSO
      IF(Q2.LT.0.0) QSO=-DELT*Q2*RHO(I,NC)+QSO
      IF(Q1.LT.0.0) QSO=DELT*Q1*RHO(I,2)+QSO
      IF(Q2.GT.0.0) QSO=-DELT*Q2*RHO(I,IC)+QSO
      IF(Q1.GT.0.0) QTO=QTO+DELT*Q1*CAVG(I,1)
      IF(Q2.LT.0.0) QTO=QTO-DELT*Q2*CAVG(I,NC)
      IF(Q1.LT.0.0) QTO=QTO+DELT*Q1*CAVG(I,2)
   47 IF(Q2.GT.0.0) QTO=QTO-DELT*Q2*CAVG(I,IC)
      CORAL=QSO-STOR+STORP
      CTRAL=QTO-ADD+ADDP
      SQSO=SQSO+QSO
      SQTO=SQTO+QTO
      SCRAL=SQSO-STOR+STOR1
      STRAL=SQTO-ADD+ADD1
      STORP=STOR
      ADDP=ADD
      WRITE (6,222) CORAL,SQRAL,CTRAL,STRAL,TIME
  222 FORMAT(1H ,8X,7HCORAL =,E10.3,8X,7HSQRAL =,E10.3,8X,7HCTRAL =,E10.
     13,8X,7HSTRAL =,E10.3,8X,6HTIME =,E15.6  )
      PT(1,1)=((0.0733/VOLU)*(PT(1,1)-PT(1,NC)))+PT(1,NC)
      P(1,1)=100000.0+PT(1,1)
      DO 66 I=2,NR
      PT(I,1)=PT(I-1,1)+(RHO(I,1)*G*DELZ)
      P(I,1)=PT(I,1)+100000.0
   66 CONTINUE
      RETURN
      END
```

APPENDIX H

LIST OF SYMBOLS USED IN THIS STUDY

Symbol	Definition	Units
A_n	Fourier coefficients	---
[A]	Square coefficient matrix	---
a	Coefficient in stability analysis equal to $\frac{\psi\Delta x_1}{2}$	---
b	Width of injected tracer along input boundary	L
b	Coefficient in stability analysis equal to $\frac{\zeta\Delta x_2}{2}$	---
C	Mass concentration of tracer	FT^2L^{-4}
C_o	Reference concentration	FT^2L^{-4}
C_{max}	Maximum concentration	FT^2L^{-4}
C_F	Formation compressibility factor	L^2F^{-1}
C_p	Mass concentration of tracer in produced fluid	FT^2L^{-4}
$\hat{C}$	Concentration of tracer in fluid element	FT^2L^{-4}
$\mathring{C}$	Deviation of concentration at a point from cross-sectional average	FT^2L^{-4}
D_p	Dispersion coefficient	L^2T^{-1}
D^*_{ij}	Total dispersion coefficient	L^2T^{-1}
D	Effective diffusion coefficient	L^2T^{-1}
D_d	Molecular diffusion coefficient	L^2T^{-1}
D_{ij}	Dispersion coefficient, a second rank tensor	L^2T^{-1}
D_L	Longitudinal dispersion coefficient	L^2T^{-1}
D_T	Transverse (or lateral) dispersion coefficient	L^2T^{-1}
d	Pore size parameter	L
d	Coefficient in stability analysis equal to $\frac{\gamma\Delta x_3}{2}$	---
d*	Aquifer thickness	L
$E^{\bar{S}}_{\bar{P},\bar{Q},\bar{R}}$	Error at node of grid $(\bar{P},\bar{Q},\bar{R})$ at time level $\bar{S}\Delta t$	---
$E^{\pm}_{x_i x_i}$	Coefficients for finite difference scheme and defined by Eqs. D-19	---
E or E(t)	Error between numerical and analytical solutions	---
$F^{\pm}_{x_i x_j}$	Coefficients for finite difference scheme and defined by Eqs. D-19	---
F_1	Even function of Peclet number	---

Symbol	Definition	Units
F_2	Even function of Reynolds number	---
$G^{\pm}_{x_i x_j}$	Coefficients for finite difference scheme and defined by Eqs. D-19	---
g	Gravitational acceleration	LT^{-2}
$H^{\pm}_{x_i x_j}$	Coefficients for finite difference scheme and defined by Eqs. D-19	---
h^*	Piezometric head	L
h	Elevation above datum	L
i,j,k	Subscript used to denote row and columns of finite difference grid	---
ij	Subscript used to denote tensor where i and $j = 1,2,3$	---
J_1^*,J_2^*,J_3^*	Tracer mass flux components averaged over cross section of volume element (relative to pore area)	FTL^{-3}
J_1,J_2,J_3	Diffusive mass flux components in fluid element	FTL^{-3}
K	Hydraulic conductivity	LT^{-1}
k_r	Relative permeability to fluid	---
k_{x_i}	Permeability in x_i-direction	L^2
L	Number of grids in x_3-direction	---
L	Length of sea-water wedge	L
ℓ_1,ℓ_2,ℓ_3	Length in x_1-, x_2-, and x_3-directions	L
M	Total mass flow rate	$FL^{-1}T$
M	Number of grids in x_2-direction	---
M_{VE}	Mass of volume element	$FL^{-1}T^2$
M_p	Mass flow rate of source or sink	$FL^{-1}T$
M_t	Mass flow rate of tracer	$FL^{-1}T$
M_{tVE}	Tracer mass in volume element	$FL^{-1}T^2$
M_{tp}	Tracer mass flow rate of source or sink	$FL^{-1}T$
m	Number of rows in matrix	---
$N^{\pm}_{x_i}$	Coefficients calculated for the finite difference scheme and defined in Eqs. C-7	---
N	Number of grids in x_1-direction	---
n	Number of columns in matrix	---
P	Fluid pressure	FL^{-2}
P_o	Reference pressure	FL^{-2}
$[P]$	Column vector	---
Q	Rate of fluid production	L^3T^{-1}
$\tilde{q}$	Fresh-water flow rate per unit width of ocean front	L^2T^{-1}

Symbol	Definition	Units
q	Volume flux	LT^{-1}
$\mathbb{R}$	Reynolds number	---
r	Radius	L
[rhs]	Column vector	---
S	Saturation of fluid	---
T	Temperature	---
T	Tortuosity	---
T_{ij}	Tortuosity factor, a second rank tensor	---
$\hat{T}_{ij}$	Tortuosity on microscopic scale, a second rank tensor	---
$\mathring{T}_{ij}$	Deviation of tortuosity at a point from cross-sectional average	---
t	Time	T
t+1	New time level	T
t-1	Previous time level	T
t+Δ	Time level between t and t+1	T
V_1, V_2, V_3	Seepage velocity components (flow per unit pore area)	LT^{-1}
V_p	Seepage velocity of production fluid	LT^{-1}
V	Magnitude of velocity vector	LT^{-1}
$\hat{V}$	Velocity of fluid element	LT^{-1}
$\hat{V}_t$	Velocity of tracer in fluid element	LT^{-1}
$\mathring{V}_1, \mathring{V}_2, \mathring{V}_3$	Deviation of velocity at a point from cross-sectional average	LT^{-1}
$V_{1_\ell}, V_{2_\ell}, V_{3_\ell}$	Velocity components of ℓth moving point	LT^{-1}
x_1, x_2, x_3	Cartesian coordinates	L
x'_1, x'_2, x'_3	Rotated cartesian coordinates	L
$x_{1_\ell}, x_{2_\ell}, x_{3_\ell}$	Coordinates of ℓth moving point	L
y	Thickness of fresh-water flow	L
α	Factor relating concentration and density	---
β	Fluid compressibility	L^2F^{-1}
$\Delta x'_1, \Delta x'_2, \Delta x'_3$	Grid dimensions in rotated coordinates	L
$\Delta x_1, \Delta x_2, \Delta x_3$	Dimensions of volume element	L
$\Delta A_1, \Delta A_2, \Delta A_3$	Cross-sectional area of volume element perpendicular to x_1, x_2, and x_3 directions (i.e., $\Delta A_1 = \Delta x_2 \Delta x_3$)	L^2
$\Delta\overline{V}$	Volume of volume element ($\Delta\overline{V} = \Delta x_1 \Delta x_2 \Delta x_3$)	L^3
$\Delta h^{\pm}_{x_i}$	Coefficient in finite difference equation defined in Eq. C-7	---

Symbol	Definition	Units
Δt	Time increment	T
Δt_o	Time increment in previous time step	T
$\Delta\rho$	Difference in density, $\rho_s-\rho_f$	FT^2L^{-4}
ε_1	Longitudinal dispersivity	L
ε_2	Lateral dispersivity	L
ε_{ijmn}	Coefficient of dispersivity, a fourth rank tensor	L
σ	Length of tortuous tube	L
ξ	Shortest distance between ends of tortuous tube	L
ξ	Amplification factor in stability analysis	---
ξ	Height of ocean above top of aquifer	L
$\rho^{\pm}_{x_i}$	Coefficient for finite difference equation defined in Eq. C-7	---
ρ	Fluid density	FT^2L^{-4}
ρ_o	Reference density	FT^2L^{-4}
ρ_f	Fresh water density	FT^2L^{-4}
ρ_s	Salt water density	FT^2L^{-4}
ρ_p	Density of produced fluid	FT^2L^{-4}
ϕ	Porosity	---
ϕ_o	Reference porosity	---
μ	Viscosity	FTL^{-2}
μ_o	Reference viscosity	FTL^{-2}
ν	Kinematic viscosity	L^2T^{-1}
δ_{ij}	Kronecker delta	---
λ	Factor relating viscosity and concentration	---
τ	Capillary tube coefficient	---
ω	Factor defined by $\rho/(\rho-\alpha C)$	---
ψ_n	Coefficient equal to $n\pi/N\Delta x_1$	---
ζ_n	Coefficient equal to $n\pi/M\Delta x_2$	---
γ_n	Coefficient equal to $n\pi/L\Delta x_3$	---
Φ	Potential function	---
Ψ	Stream function	---
erf	Error function	---
erfc	Complimentary error function	---

Key Words: Dispersion, Water Quality, Numerical Simulation, Ground Water

Abstract: A flow equation for a mixture of miscible fluids was derived by combining the law of conservation of mass, Darcy's law, and an equation of state describing the pressure-volume-temperature-concentration relationship. The result is an equation involving two dependent variables, pressure and concentration. A relationship for determining concentration was derived by expressing a continuity equation for the dispersed tracer. An implicit numerical technique was used to solve the flow equation for pressure and the method of characteristics with a tensor transformation was used to solve the convective-dispersion equation. The results from the flow equation were used in solving the convective-dispersion equation and the results from the convective-dispersion equation were then used to resolve the flow equation. The computer simulator successfully solved the longitudinal dispersion problem and the longitudinal and lateral dispersion problem. Using the tensor transformation, problems of longitudinal and lateral dispersion were successfully solved in a rotated co-ordinate system. The computer simulator was used to solve the salt-water intrusion problem. The numerical results for the fresh water head in the aquifer closely matched those obtained analytically.

Reference: Reddell, Donald L. and Daniel K. Sunada, Colorado State University, Hydrology Paper No. 41(June 1970) "Numerical Simulation of Dispersion in Groundwater Aquifers."

Key Words: Dispersion, Water Quality, Numerical Simulation, Ground Water

Abstract: A flow equation for a mixture of miscible fluids was derived by combining the law of conservation of mass, Darcy's law, and an equation of state describing the pressure-volume-temperature-concentration relationship. The result is an equation involving two dependent variables, pressure and concentration. A relationship for determining concentration was derived by expressing a continuity equation for the dispersed tracer. An implicit numerical technique was used to solve the flow equation for pressure and the method of characteristics with a tensor transformation was used to solve the convective-dispersion equation. The results from the flow equation were used in solving the convective-dispersion equation and the results from the convective-dispersion equation were then used to resolve the flow equation. The computer simulator successfully solved the longitudinal dispersion problem and the longitudinal and lateral dispersion problem. Using the tensor transformation, problems of longitudinal and lateral dispersion were successfully solved in a rotated co-ordinate system. The computer simulator was used to solve the salt-water intrusion problem. The numerical results for the fresh water head in the aquifer closely matched those obtained analytically.

Reference: Reddell, Donald L. and Daniel K. Sunada, Colorado State University, Hydrology Paper No. 41(June 1970) "Numerical Simulation of Dispersion in Groundwater Aquifers."

Key Words: Dispersion, Water Quality, Numerical Simulation, Ground Water

Abstract: A flow equation for a mixture of miscible fluids was derived by combining the law of conservation of mass, Darcy's law, and an equation of state describing the pressure-volume-temperature-concentration relationship. The result is an equation involving two dependent variables, pressure and concentration. A relationship for determining concentration was derived by expressing a continuity equation for the dispersed tracer. An implicit numerical technique was used to solve the flow equation for pressure and the method of characteristics with a tensor transformation was used to solve the convective-dispersion equation. The results from the flow equation were used in solving the convective-dispersion equation and the results from the convective-dispersion equation were then used to resolve the flow equation. The computer simulator successfully solved the longitudinal dispersion problem and the longitudinal and lateral dispersion problem. Using the tensor transformation, problems of longitudinal and lateral dispersion were successfully solved in a rotated co-ordinate system. The computer simulator was used to solve the salt-water intrusion problem. The numerical results for the fresh water head in the aquifer closely matched those obtained analytically.

Reference: Reddell, Donald L. and Daniel K. Sunada, Colorado State University, Hydrology Paper No. 41(June 1970) "Numerical Simulation of Dispersion in Groundwater Aquifers."

Key Words: Dispersion, Water Quality, Numerical Simulation, Ground Water

Abstract: A flow equation for a mixture of miscible fluids was derived by combining the law of conservation of mass, Darcy's law, and an equation of state describing the pressure-volume-temperature-concentration relationship. The result is an equation involving two dependent variables, pressure and concentration. A relationship for determining concentration was derived by expressing a continuity equation for the dispersed tracer. An implicit numerical technique was used to solve the flow equation for pressure and the method of characteristics with a tensor transformation was used to solve the convective-dispersion equation. The results from the flow equation were used in solving the convective-dispersion equation and the results from the convective-dispersion equation were then used to resolve the flow equation. The computer simulator successfully solved the longitudinal dispersion problem and the longitudinal and lateral dispersion problem. Using the tensor transformation, problems of longitudinal and lateral dispersion were successfully solved in a rotated co-ordinate system. The computer simulator was used to solve the salt-water intrusion problem. The numerical results for the fresh water head in the aquifer closely matched those obtained analytically.

Reference: Reddell, Donald L. and Daniel K. Sunada, Colorado State University, Hydrology Paper No. 41(June 1970) "Numerical Simulation of Dispersion in Groundwater Aquifers."

PREVIOUSLY PUBLISHED PAPERS

Colorado State University Hydrology Papers

No. 26 "The Investigation of Relationship Between Hydrologic Time Series and Sun Spot Numbers," by Ignacio Rodriguez-Iturbe and Vujica Yevjevich, April 1968.

No. 27 "Diffusion of Entrapped Gas From Porous Media," by Kenneth M. Adam and Arthur T. Corey, April 1968.

No. 28 "Sampling Bacteria in a Mountain Stream," by Samuel H. Kunkle and James R. Meimann, March 1968.

No. 29 "Estimating Design Floods from Extreme Rainfall," by Frederick C. Bell, July 1968.

No. 30 "Conservation of Ground Water by Gravel Mulches," by A. T. Corey and W. D. Kemper, May 1968.

No. 31 "Effects of Truncation on Dependence in Hydrologic Time Series," by Rezaul Karim Bhuiya and Vujica Yevjevich, November 1968.

No. 32 "Properties of Non-Homogeneous Hydrologic Series," by V. Yevjevich and R. I. Jeng, April 1969.

No. 33 "Runs of Precipitation Series," by Jose Llamas and M. M. Siddiqui, May 1969.

No. 34 "Statistical Discrimination of Change in Daily Runoff," by Andre J. Dumas and Hubert J. Morel-Seytoux, August 1969.

No. 35 "Stochastic Process of Precipitation," by P. Todorovic and V. Yevjevich, September 1969.

No. 36 "Suitability of the Upper Colorado River Basin for Precipitation Management," by Hiroshi Nakamichi and Hubert J. Morel-Seytoux, October 1969.

No. 37 "Regional Discrimination of Change in Runoff," by Viboon Nimmannit and Hubert J. Morel-Seytoux, November 1969.

No. 38 "Evaluation of the Effect of Impoundment on Water Quality in Cheney Reservoir," by J. C. Ward and S. Karaki, March 1970.

No. 39 "The Kinematic Cascade as a Hydrologic Model," by David F. Kibler and David A. Woolhiser, February 1970.

No. 40 "Application of Run-Lengths to Hydrologic Series," by Jaime Saldarriaga and Vujica Yevjevich, April 1970.